Surface Design for Flank Milling

by

Chenggang Li

A thesis
presented to the University of Waterloo
in fulfillment of the
thesis requirement for the degree of
Doctor of Philosophy
in
Mechanical Engineering

Waterloo, Ontario, Canada, 2007

AUTHOR'S DECLARATION

I hereby declare that I am the sole author of this thesis. This is a true copy of the thesis, including any required final revisions, as accepted by my examiners.

I understand that my thesis may be made electronically available to the public.

Abstract

In this dissertation, a numerical method to design a curved surface for accurately flank milling with a general tool of revolution is presented. Instead of using the ruled surface as the design surface, the flank millable surface can better match the machined surface generated by flank milling techniques, and provide an effective tool to the designer to control the properties and the specifications of the design surface.

A method using the least squares surface fitting to design the flank millable surface is first discussed. Grazing points on the envelope of the moving tool modeled by the grazing surface are used as the sample points and a NURBS surface is used to approximate the given grazing surface. The deviation between the grazing surface and the NURBS surface can be controlled by increasing the number of the control points. The computation process for this method is costly in time and effort.

In engineering design, there is a need for fast and effortless methods to simplify the flank millable surface design procedure. A technique to approximate the grazing curve with NURBS at each tool position is developed. Based on the characteristics of the grazing surface and the geometries of the cutting tool, these NURBS representations at a few different tool positions, namely at the start, interior and end, are lofted to generate a NURBS surface. This NURBS surface represents the grazing surface and is treated as the design surface. Simulation results show that this design surface can accurately match the machined surface. The accuracy of the surface can be controlled by adding control points to the control net of the NURBS surface.

A machining test on a 5-axis machine was done to verify the proposed flank millable surface design method. The machined surface was checked on a CMM and the obtained results were compared with the designed flank millable surface. The comparison results show that the machined surface closely matches the design surface. The proposed flank millable surface design method can be accurately used in the surface design.

Acknowledgements

I would like to thank my supervisors, Professor Sanjeev Bedi and Professor Stephen Mann, for their support, enthusiasm and guidance. I don't think I can finish my research in three years without their great patience and help. Their intelligent ideals and suggestions directed me through the period of my study, and I have learned and grown so much in this time.

I also would like to thank all my friends and colleagues for their unselfish supports. I think this thesis is not my individual project. It is a collection of many peoples' suggestions, efforts and ideals.

Finally I would like to thank my wife for her love, patience and support during my study; thank my son Anyang and my daughter Dorothy for their encouragement and understanding; thank my parents, brothers and sisters for their love and support. I cannot get this achievement without you. I love you all.

To my wife Yan bin

and children

Anyang, and Dorothy

To the memory of my father, Zhi zhong Li

and

To the memory of my grandmother, Feng yun Li

Table of Contents

List of Figures

List of Tables

Chapter 1
Introduction

Computer Numerical Control (CNC) machining is a widely used machining technique in today's manufacturing industry. In the CNC machining, the motion of the machine tool is controlled by its CNC unit. The Numerical Control commands are generated by a Computer Aided Manufacturing (CAM) system and are transferred to the CNC unit. The machined part is cut based on the input commands (or tool paths). Compared to traditional machining techniques, the use of the computer makes the machining process more accurate and efficient. Meanwhile, the user based control panel provides versatile tools to users to control the CNC unit and display instant data and information about the machine, and the tool library in the CNC unit gives a flexible option to the programmer to select the cutting tools in his/her tool path generation. The application of CNC techniques greatly supports the development of manufacturing engineering.

In 5-axis CNC machining, curved surfaces are the main target surfaces to be machined. Different cutting tool positioning methods have been developed. Flank milling is one of the important techniques among these methods and is broadly used in current manufacturing industry. In flank milling, the side of the cutter machines the surface, removing the stock in front of it. Compared to other machining methods, flank milling can offer higher machining efficiency, higher material removing rate, and provide a better surface finish. Flank milling is used in the machining of turbine blades, fan impellers and other engineering objects of interest in today's economy. As a consequence, research in flank milling has flourished in the past decade. Researchers' workings on improving flank milling have developed different tool

positioning techniques. In general, these techniques can be categorized into three classes, namely, the direct tool positioning methods, the step by step tool positioning methods and the improved tool positioning methods.

In the direct tool positioning method, the cylindrical cutting tool is used to machine a ruled surface and the tool is positioned tangentially to the given surface at one point on the ruled line either in the middle or end (or near the end) while the tool axis is parallel to the same ruled line. Alternatively, the tool is positioned to directly touch two points on the ruled line. The position of the cutting tool is decided by offsetting it by a distance R (tool radii) at each touching point along the surface normal direction. Methods that belong to this class include the early method [12, 13], Rubio et al.'s method [12], Stute et al.'s method [1], and Liu's method [2]. The error defined as the difference between the machined surface and the desired surface in this class is high, but the cutting tool is easy to position and the computation time for tool positioning is low.

The step by step tool positioning method is an improvement over the direct tool positioning method. In this class, the cutting tool is first positioned on the given surface with one of the direct tool positioning methods and then the tool is lifted a little and/or twisted a little to reduce the error between the machined surface and the desired surface. Methods developed by Rehsteiner et al. [14], Bohez et al. [3], Chiou [15], Tsay and Her [4], and Bedi et al. [9-11] belong to this class. In comparison to the direct tool positioning methods, the step by step tool positioning methods result in a machined surface that is close to the desired surface, but the computation time of these methods is long.

The improved tool positioning method is a combination of the techniques used in the two classes described above. In this method, the cutting tool is positioned on the given surface so that it touches at three contact points as shown in Fig. 1-1. A machined surface can be generated with many tool positions, each of which has three contact points (two on the guiding curves $T(u)$ and $B(u)$, and one on the rule). Three contact points at any tool position can be obtained directly by solving seven transcendental equations based on the given geometrical conditions [5]. The error between the machined surface and the desired surface is small in this type of tool positioning method. Redonnet et al.'s method [5] and Monies et al.'s method [6-7] belong to this class. This class of methods results in high accuracy machined surfaces. However, it requires the solution of seven transcendental equations at each tool position, which makes it computationally cumbersome.

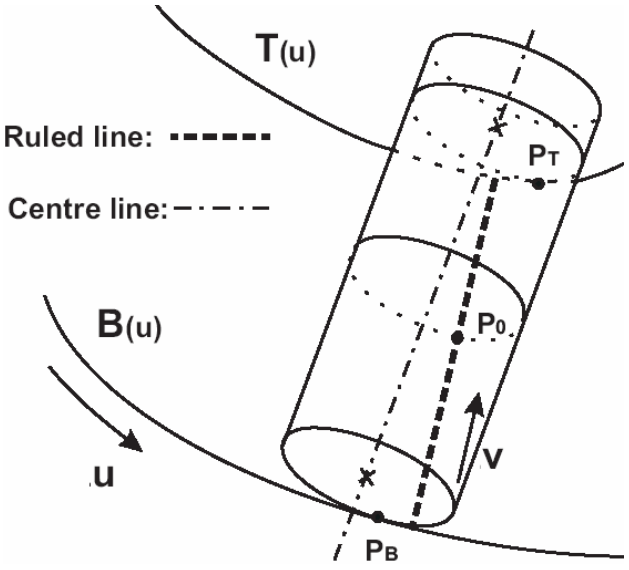

Figure 1-1 A cylindrical tool with the improved tool positioning method: P_T and P_B are two contact points on the guiding curves $T(u)$ and $B(u)$. P_0 is another contact point on the rule.

Recently, methods developed by Gong et al. [16] and Chu et al. [17] used different approaches to position the cutting tool. In Gong et al.'s method [16], the deviation at the extreme point between the given ruled surface and the grazing (machined) surface is proposed to be equal to the maximum deviation between the offset surface of the ruled surface and the tool axis trajectory surface (which is also a ruled surface.). The cutting tool is twisted so that the maximum deviation between the tool axis trajectory surface and the offset surface can be minimized at each tool position. Consequently, the tool path can be generated. To further reduce the deviation between the tool axis trajectory surface and the offset surface, they suggested sampling the offset surface with points and using the least squares surface fitting method to find a B-spline surface that closely matches these sample points. The resulting B-spline surface is used as the tool axis trajectory surface. Even though the authors mentioned that the generated surface before and after optimization can all get minimum surface errors, there is no relation between the methods before and after optimization. Further, the authors didn't explain how to project each sample point onto the tool axis trajectory surface to obtain the parameters of the sample points. In Chu et al.'s method [17], they suggested using developable Bézier patches along two guiding curves to approach the given ruled surface. Each patch is a ruled surface and the tangent lines of the ends of each rule (along the patch guiding curve directions) on the patch are coplanar with the rule itself. The tool path of the patch can easily be generated using the early tool positioning method [12, 13]. Each patch has its own tool path. Combining the tool paths from the different patches in sequence, the tool path for the given ruled surface can be constructed and the designed ruled surface can be milled.

All these methods described above focus on ruled surfaces and attempt to use different techniques to reduce the deviation between the machined surface and the given surface. Although it is widely recognized that flank milling produces curved surfaces, no one has attempted to design free form surfaces that can be flank milled. Some researchers in academics [3, 18] and industry [19] have tried to use flank milling techniques to machine free form surfaces. In their methods, they first divide the target surface into multiple ruled surfaces, and then machine these ruled surfaces in pieces with one of the above techniques. Obviously, there are spatial limitations to this method and it results in longer tool paths.

One of the key applications of flank milling is machining of impellers. Engineers design the impeller surfaces to extract power from fluid flowing over them. They use sophisticated aerodynamic analysis to improve the efficiency and performance of the impeller. However, to machine the impellers, these surfaces are approximated with ruled surfaces even though a curved surface is better for efficiency or produced at large cost with point machining techniques. If a curved surface that can be flank milled directly can be designed, it can be used to design surfaces and optimize efficiency and thus will be of great benefit not only for manufacturing but also for application engineering. With such a surface design technique, engineers would be able to design impellers and optimize their performance without worrying about compromises during machining. A method to achieve this is a big challenge in surface design and machining. In this thesis, this challenge is probed and solutions are presented. First, the surfaces that can be machined with the flank milling method are identified, and then a method to design such surfaces is developed and tested.

1.1 Basis of the Idea

In previous work, the surface that can be produced by flank milling has been evaluated. As the flank milling cutter moves in 3D space, its position and orientation change and the envelope surface produced by this movement, also referred to as a grazing surface, is evaluated with discrete grazing points. Bedi et al. [9] suggested a cross product method to calculate the envelope surface for a cylindrical tool, and Mann et al. [20] generalized this method and applied it to tools with a general surface of revolution. Li et al. [11] and Menzel et al. [10] applied this method to the conical tool and cylindrical tool to simulate the machined surface and used it to optimize each tool position. Li et al. [21] also used this method to study the surface error. Lartigue et al. [22] presented a similar method to determine an envelope surface in their surface deformation analysis. Senatore et al. [23] used a similar method to define the grazing points and envelope surface. They also geometrically proved that, at each tool position, the contact points (between cutter and guiding curves, cutter and rule) are on the envelope surface. All these techniques use discrete points to simulate the grazing surface (or the envelope surface). Furthermore, they use the grazing surface to approximate the machined surface. The grazing surface is a model of the envelope surface and has no obvious NURBS representation. If a NURBS approximation can be developed, a designer could use it to define curved surfaces in engineering objects and in subsequent analysis and optimization processes. This would also simplify the manufacture of these surfaces and improve the product accuracy.

1.2 The Goal

The focus of this study is to develop a method to represent the machined surface with a NURBS representation so that the surface can be generated accurately by flank milling techniques. The surface fitting method should be general enough to be used by engineers to design impellers, blades and other engineering parts geometrically.

The key idea behind this proposal is to develop a method that provides accuracy control in approximating the grazing surface with a NURBS definition. The surface method is based on the properties of guiding curves and the cutter, for example a cylindrical cutter. At any tool position, the corresponding grazing curve lies on the cylindrical tool surface and can be represented by a NURBS curve. This curve can be constructed with three or four control points with their corresponding weights (as shown in Fig. 1-2). As the three or four control points are moved along guiding curves, a surface close to the grazing surface is generated. The method presented in this thesis ensures that the control points move along the guiding curves in a manner that retains their grazing curve character, while generating the surface. This method is based on the property of guiding curves.

The guiding curves along the feed direction (as shown in Fig.1-2) control the characteristics of the final machined surface and the guiding curves themselves lie on the machined surface. Thus the control points of the approximate surface along the feed direction on the boundaries can be assumed to be the same as the control points of the guiding curves (say the number is N). The control points in the middle row or rows between the two boundary curves are computed using the technique described in the following chapters. The approximate NURBS surface can be constructed using these three by N or four by N

control points and is evaluated by measuring the error between it and the machined surface. If the maximum error is not within the specified tolerance, more control points can be added along the tool axis direction or the feed direction. With the increased number of control points, the maximum deviation between the approximate surface and the machined surface can be reduced to any specified tolerance.

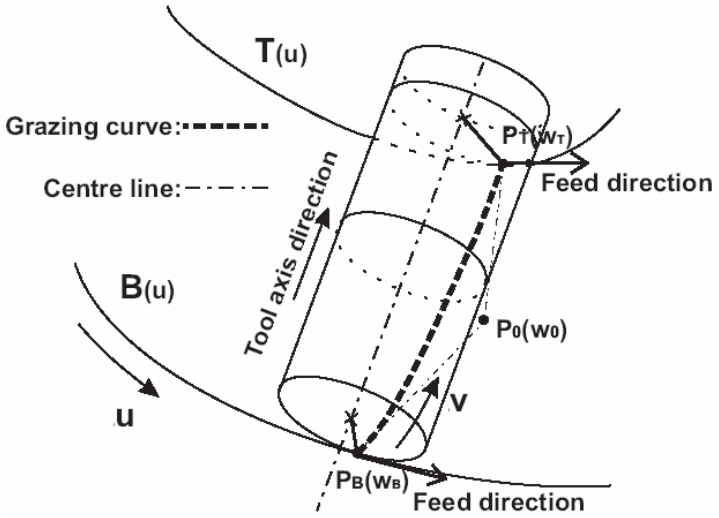

Figure 1-2 The cylindrical tool and guiding curves: $T(u)$ and $B(u)$ are two guiding curves. P_T, P_0 and P_B are three control points of a grazing curve. w_T, w_0 and w_B are their corresponding weights. The tool moves along feed directions.

1.3 Thesis Organization

In the following chapters, the proposed method is investigated and studied. In Chapter 2, background on flank milling is reviewed. The tool positioning method used in the proposed solution, Bedi et al.'s method, and the method of computing the grazing surface (the swept surface) are given. The error measurement methods are discussed and the parametric error measurement method used in the remaining study is identified. Background material about Bézier and B-spline curves and surfaces are also presented. The least squares is a well known

surface fitting method. This method will be probed in Chapter 3. Chapter 4 presents the strategy of modeling the grazing surface with NURBS using cylindrical tools. The basic theory of the method is introduced and the properties of the method are discussed. Examples are also given to demonstrate the proposed method. In Chapter 5, a surface design method that improves the accuracy of the surface is discussed. The use of NUBS (Non-Uniform B-spline) in defining the flank millable surfaces is introduced and its properties are discussed. The flank millable surface design technique can also be used with tools of other shapes. Chapter 6 generalizes the proposed method given in Chapters 4 and 5, which can be used to design the flank millable surface with any general shaped tools. Chapter 7 presents the experimental verification of the proposed flank millable surface design methods with a machining test. The result shows that the machined surface can closely match the developed flank millable surface. To demonstrate the proposed methods in actual engineering application, a procedure to design an impeller with a proposed flank millable surface design method is given in this chapter. Finally, Chapter 8 presents the conclusion of this thesis and future research opportunities. Areas of potential works are also discussed.

Seven different methods for generating flank millable surfaces are discussed in this dissertation with the variation being in the type of tool and the type of surface generated. For easy to trace flank millable surfaces and cutting tools that will be discussed, Table 1-1 provides an overview of which method is discussed in which chapter and the distribution of these methods that will be addressed in this thesis.

	Cutting Tool					
	Cylinder		Cone		General	
	NURBS	NUBS	NURBS	NUBS	NURBS	NUBS
Chapter 3		*		×		×
Chapter 4	*					
Chapter 5		*				
Chapter 6.1			*	*		
Chapter 6.1					*	*

Table 1-1 Chapters with surfaces that will be discussed. * means discussed in chapter. × means method could be used for these tools but isn't discussed in this dissertation.

Chapter 2
Background of Surface Design for Flank Milling

Different tool positioning methods result in different tool locations and orientations for machining the same surface. Thus, a surface designed for flank milling will apply to a specific method of tool positioning. In this work, surface design methods are developed for designing a surface that can be machined with the flank milling method presented by Bedi et al. [9-11]. This tool positioning method is fundamental to the developed flank millable surface and is thus introduced in this chapter for completeness. In addition to the tool positioning method, the surface design technique also depends on the shape of the grazing surface produced by a moving tool. Thus, a technique used to calculate the grazing surface is presented in this chapter for the same reason. Other concepts used in this thesis including the surface error measurement method, Bézier and B-spline curves and surfaces, are also reviewed in this chapter.

2.1 Flank Milling of Ruled Surfaces

Flank Milling has evolved as a method of manufacturing used in traditional 3-axis machining. The advantages of flank milling in 3-axis machining are that the effective contact area between the given surface and the cutting tool is a straight line and a good surface finish can be achieved. These advantages have attracted manufacturing engineers who have extended this method to 5-axis machining and developed different tool positioning techniques. 5-axis based flank milling techniques were initially used to machine the curved

surfaces composed of straight lines. This type of surface is called a ruled surface. In the late 80s, a method to machine ruled surfaces with a flank milling technique was proposed. In this method, the cutting tool contacts one end of the rule at every tool position and the axis of tool is positioned to be parallel to the rule [12, 24] as shown in Fig. 2-1. The tool path generated with this method is used to machine ruled surfaces. Measurement of the surface error has shown that this type of machined surface overcuts the desired ruled surface. The reason for this is that at each tool position, the target ruled line lies on the tool surface, but the tool itself will overcut in the vicinity of the ruled line due to the varying nature of the curvature of the grazing surface. The maximum overcut is located at the guiding rail on the opposite side of the contact point used to offset the tool axis.

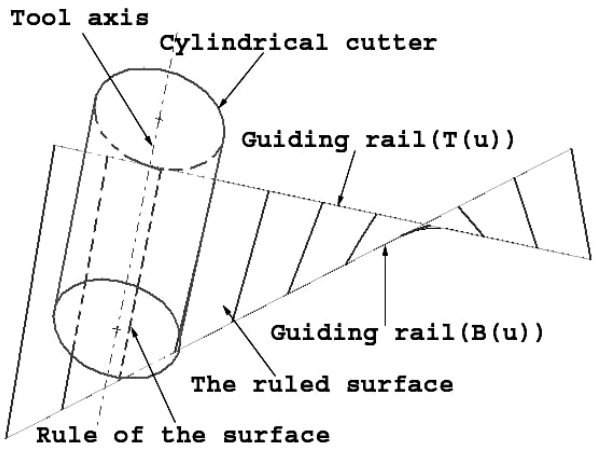

Figure 2-1 Position of the cylindrical tool and the ruled surface.

2.1.1 Rubio et al.'s Method

To reduce the maximum deviation, Rubio et al. [12] suggested that this maximum deviation can be distributed at both ends of the rule by setting the contact point at the middle of the

rule. The tool axis in this method is parallel to the target rule at each tool position. With this method, the maximum deviation is reduced to half of the original one and is equally distributed at both ends of the rule.

2.1.2 Stute's Method

Even though the maximum deviation is reduced, further investigation of the surface error showed that the effective contact area between the machined surface and the design surface at each tool position is a curve and not a straight line as in traditional flank milling of 3-axis machining. Therefore, Stute et al. [1] suggested that it is not necessary to force the tool axis to be parallel to the rule at each tool position. The cylindrical tool can be positioned on the ruled surface by offsetting it with a distance of radii R (cylindrical cutter) along the ruled surface normal direction at two points located at the ends of the rule. Using this method, the tool axis can be defined and the tool path generated. In this method, the maximum deviation at each tool position occurs at the middle of the rule. Liu [2] gave a similar solution and improved this method. He moved the two points of contact on the rule to lie at the quarter and three quarter positions. This reduced the maximum deviation significantly. The computational results from Liu's method supported Liu's suggestion.

2.1.3 Bedi et al.'s Method

Based on the above study, other researchers developed different tool positioning methods that reduce the maximum deviation between the given rule and the grazing curve. Most of these methods suggested that the two contact points can be moved along the rule or/and twisted along the feed direction to reduce the maximum deviation. This includes methods due

to Rehsteiner et al. [14], Bohez et al.[3], Tsay and Her [4]. A representative method of this type is due to Bedi et al. [9-11]. In Bedi et al.'s method, the cutting tool (for example, a flat end mill modeled as a cylinder) is initially positioned to contact two guiding curves. The two contact points (located at the ends of the rule) have the same parametric value along the guiding curves. The authors showed that by moving the contact points toward the middle of the rule, the maximum error between the rule and the grazing curve can be reduced. This maximum error can be further reduced by twisting the tool around the surface normal. Fig. 2-2 shows these steps. The results from the simulation study and the machining test successfully demonstrated the error reduction ability of this tool positioning method.

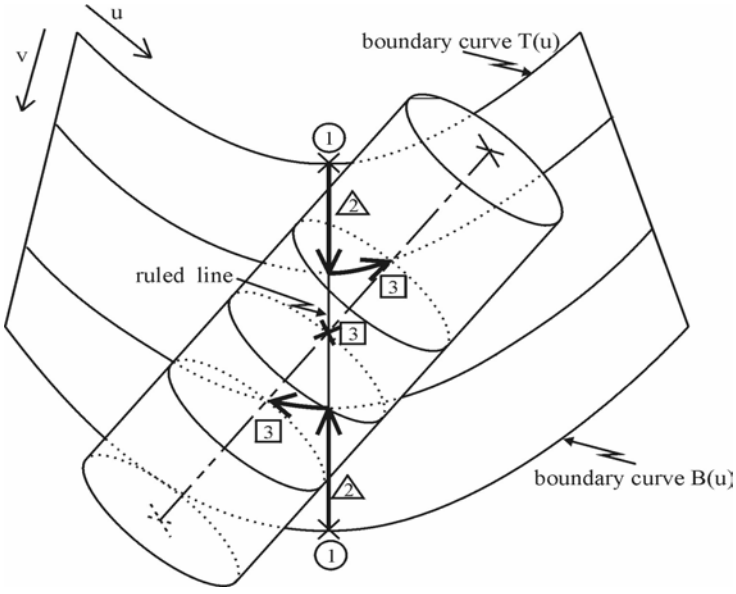

Figure 2-2 Positioning a cylindrical tool on a ruled surface with Bedi et al.'s method

2.1.4 Redonnet et al.'s Method

Redonnet et al. [5] and Monies et al. [6-7] also developed a similar method. In their method, they suggested that the smallest maximum deviation between the rule and the grazing curve should be decided by three contact points between the cutting tool and the given ruled

surface. Where as in other methods, like Bedi et al.'s method, these points are found by lifting and/or twisting the cutting tool, they suggested a direct method of positioning the cutting tool on the given ruled surface at three points. One point is on the desired ruled line and others are on the two guiding curves. The tool is tangent to the guiding curves at the two contact points. Using geometrical relationships between the ruled surface and the cutting tool, seven transcendental equations are obtained. The tool position is obtained by solving these equations. The maximum deviation is checked by Monies et al. and this deviation is close to the result from Bedi et al.'s method.

2.1.5 Summary of Flank Milling of Ruled Surfaces

All the methods described above focus on ruled surfaces. No research related to the machining of general surfaces using flank milling is described in literature. Until recently, the equations and the shape of the grazing curve and surface produced by a moving tool required a significant amount of calculation. However, due to the swept surface method developed by Bedi et al. [9], it has become easy to determine the shape of the grazing curve and surface. Since the shape of the swept surface is doubly curved, it begs the question why not design doubly curved surfaces that can be flank milled exactly. The ability to design surfaces that can be flank milled accurately will help in design of impellers, blades and other engineering parts with optimized shapes and performance. Thus, in this research, I will focus on this issue. Bedi et al.'s tool positioning method will be used and is introduced in detail in the next section.

2.2 Positioning a Machining Tool on the Surface

Based on Bedi et al.'s technique [9], a cylindrical cutter with radii R, for example, is positioned on a given surface $S(u,v)$ as shown in Fig. 2-3.

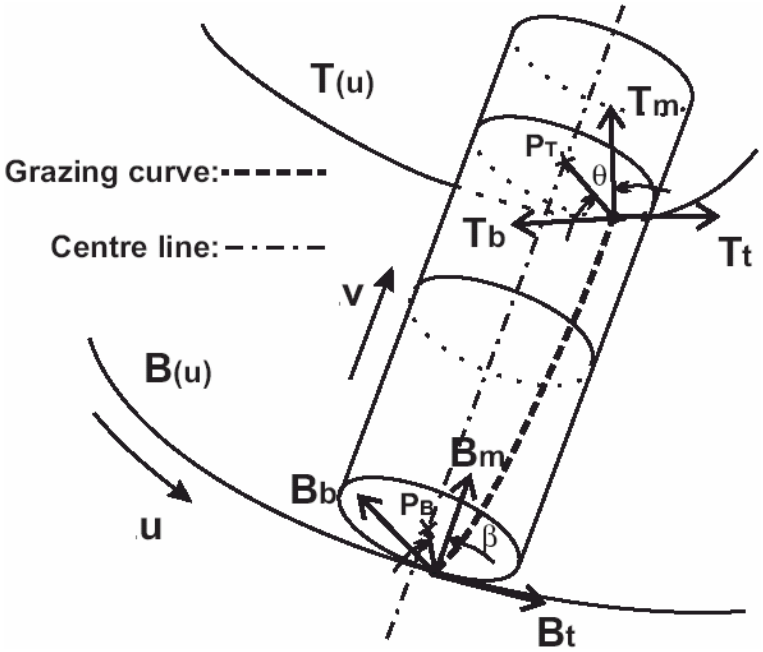

Figure 2-3 Cutter rolling on two rails

$T(u)$ and $B(u)$ are two boundary curves of the surface $S(u,v)$. These curves are treated as two guiding curves. The cutter runs along the guiding curves. The contact points between the cutter and the guiding curves share common tangent lines. The stock in front of the cutter is machined away. The two contact points on the guiding curves are identified by the same u parameter value. Fig. 2-3 shows one tool at a particular position at parameter value u. The two contact points are $T(u)$ and $B(u)$. Two local coordinate systems, the Frenet Frames [25], are set up at each contact point. T_t and B_t are the tangent vectors, T_m and B_m are the main normal vectors, T_b and B_b are the binomial vectors. The cutter moves along T_t at

contact point $T(u)$ and the cutter moves along B_t at contact point $B(u)$. Depending on the geometrical relationship between the cylindrical cutter and the guiding rails, mathematical equations can be developed [9] and are given below:

$$P_T - T(u) = R\cos(\theta)T_m(u) + R\sin(\theta)T_b(u), \tag{2.1}$$

$$P_B - B(u) = R\cos(\beta)B_m(u) + R\sin(\beta)B_b(u), \tag{2.2}$$

$$(P_T - P_B)(\cos(\theta)T_m(u) + \sin(\theta)T_b(u)) = 0, \tag{2.3}$$

$$(P_T - P_B)(\cos(\beta)B_m(u) + \sin(\beta)B_b(u)) = 0. \tag{2.4}$$

Solving equations (2.1), (2.2), (2.3) and (2.4), P_T and P_B can be obtained. This gives the cutter position at parameter value u.

If other types of cutting tools, for example, conical tools, are used, the tool radius R will be a function of the tool geometry. Under this condition, an extra equation for the tool radius needs to be considered to solve the above equations. For more details, see [11].

2.3 Swept Surface

After a tool position is defined, the grazing curve at each tool position can be derived using the cross product method given in [9], which is presented here for completeness.

As shown in Fig. 2-3, if the velocity at point P_T is V_T and at point P_B is V_B, then the velocity between P_B and P_T along tool axis direction can be linearly interpolated and is given by

$$V = V_B(1-v) + V_T v, \qquad 0 \le v \le 1. \tag{2.5}$$

V_T is the first derivative of the guiding curve $T(u)$ at the top contact point (the parameter value u). It is the moving trend of the cutting tool at this point. For solid body of the cutting tool, the velocity of this point should be the same with P_T that is the center of the circular slice of the tool passing through the top contact point.

Similarly, V_B can be determined by the first derivative of the guiding curve $B(u)$ at the bottom contact point.

The coordinate between P_B and P_T along the tool axis direction can also be linearly interpolated and is given by

$$P = P_B(1-v) + P_T v, \qquad 0 \le v \le 1. \tag{2.6}$$

The grazing curve between T and B is calculated as

$$G = P + \frac{V * T_{axis}}{|V * T_{axis}|} R, \tag{2.7}$$

where T_{axis} is the cutter axis direction.

Using equation (2.7), a continuous grazing curve can be obtained. For simplicity, only a series of discrete grazing points are generated to represent the grazing curve.

If the cutting tool is a conical tool or other tool of revolution, the radius R will be the function of the tool geometry and needs to be combined with the equation (2.7) to get the grazing curve.

By connecting consecutive grazing curves along the u direction into a mesh, a swept surface (or a grazing surface) can be generated. This surface is also composed of discrete

points. This method gives us the ability to generate accurately the surface produced by a tool in flank milling. In engineering applications, a NURBS equation would be more helpful and acceptable especially when the target surface needs to be connected to other NURBS surfaces around it. Thus, to define a surface that can be flank milled will be of significance in today's engineering applications.

2.4 The Surface Error Measurement

There are a variety of tool positioning methods that are used for flank milling. All these methods are used to produce surfaces that approximate ruled surfaces. To compare these methods and identify the improvement that result from the various methods, an error analysis technique is required to compare the machined surface and the designed surface. In the literature, different error measurement methods are used and there are no commentaries on the quality of any of these methods. In a previous work, these methods [21] were analyzed and studied.

There are four types of error metrics used in the literature. These are the radial method, the parametric method, the tangent plane method and the closest point method. The parametric method is an easy method to compute the surface error, but the accuracy of the error is low. The radial method can get a better result than the parametric method. The tangent plane method and the closest point method can give the best estimation of the surface error in the known surface error measurement methods. But both of them require longer computation time. For more details of these methods, refer to [21].

Although these developed methods are designed for comparing the machined surface and the designed surface, they can also be used to measure the difference between the grazing surface (or the grazing curve) and the approximate NURBS surface (or the approximate NURBS curve) in surface design. If the grazing surface and the approximate surface are very close, the two surfaces will nearly coincide and the errors from the different error measurement methods described above should be close or the same. In this work, the approximating NURBS surface and the grazing surface are usually very close. So, for ease of computation, the parametric method is almost the appropriate surface error measurement metrics. However, for some of the surface design methods that will be discussed in this dissertation, the parametric error method is not accurate enough. Therefore, a modified parametric error measurement method will be used in this research to better reflect the surface error variation.

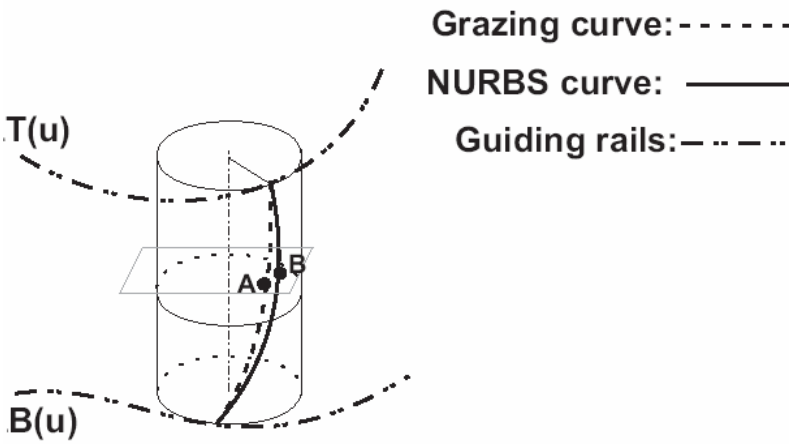

Figure 2-4 A modified parametric error measurement method

Fig. 2-4 illustrates the modified parametric error measurement method. At each specific tool position, a grazing curve is calculated and plotted as the dash line. A NURBS curve is used to approximate the grazing curve. A plane that is perpendicular to the tool axis can be created. The two curves intersect the plane with two points, A and B. The distance between the A and the B is used as the approximating error at the grazing point A. In this dissertation, this modified error measurement method will be referred as *the reparameterized parametric method* and is the error measurement method used it in this research.

2.5 Bézier Curves and Surfaces

Bézier and B-spline curves and surfaces are the mathematical basis of this thesis and are reviewed in this section. For more details, see [25, 26].

2.5.1 Bézier Curves

A parametric *Bézier curve* is defined by

$$B(t) = \sum_{i=0}^{n} P_i B_i^n(t), \tag{2.8}$$

where P_i are points in space known as *control points*, and $B_i^t(t) = \binom{n}{i}(1-t)^{n-i}t^i$ are the Bernstein polynomials, which form a basis for degree n polynomials. The parameter t is a real number in the domain. As t goes from 0 to 1, a curve is traced starting at point P_0 and ending at point P_n. An example of a cubic Bézier curve is shown in Fig.2-5.

An affine combination is a linear combination of points whose coefficients sum to 1; e.g., $aP_0 + bP_1$ is an affine combination of P_0 and P_1 if $a+b=1$. Note that the degree n Bernstein

polynomials sum to 1, so a Bézier curve, which is a sum of points weighted by Bernstein basis functions, is an affine combination of its control points.

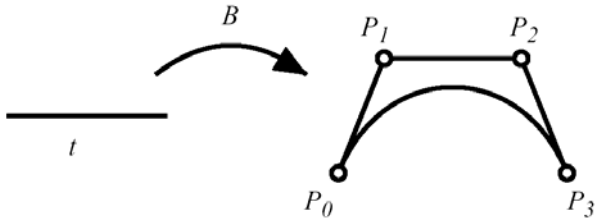

Figure 2-5 A cubic Bézier curve

A Bézier curve can be evaluated using repeated affine combinations via de Casteljau's algorithm as follows. Let $P_i^0 = P_i$. Then to evaluate $B(t)$ at $t = \bar{t}$, we compute $P_i^1 = (1-\bar{t})P_i^0 + \bar{t}P_{i+1}^0$ for $i = 0, \cdots, n-1$. Repeat this step for $j = 2, \cdots, n$,

$$P_i^j = (1-\bar{t})P_i^{j-1} + \bar{t}P_{i+1}^{j+1} \tag{2.9}$$

and $i = 0, \cdots, n-j$. This gives $B(\bar{t}) = P_0^n$. See Fig. 2-6 for a geometrical depiction of the formulation. The solid point lies on the Bézier curve.

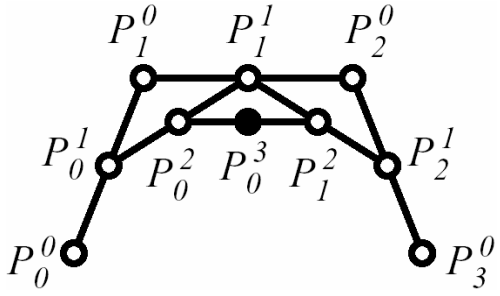

Figure 2-6 de Casteljau evaluation of Bézier curve

2.5.2 Tensor-product Bézier surfaces

A tensor-product Bézier surface is defined by

$$S(u,v) = \sum_{i=0}^{n}\sum_{j=0}^{m} P_{i,j} B_i^n(u) B_j^m(v), \tag{2.10}$$

where the $P_{i,j}$ are the control points for the surface and $B_i^n(u)$ and $B_j^m(v)$ are Bernstein polynomials. As u and v are varied over the [0,1]×[0,1] domain, a surface patch is traced out. An example of a bi-cubic tensor-product Bézier patch is shown in Fig. 2-7.

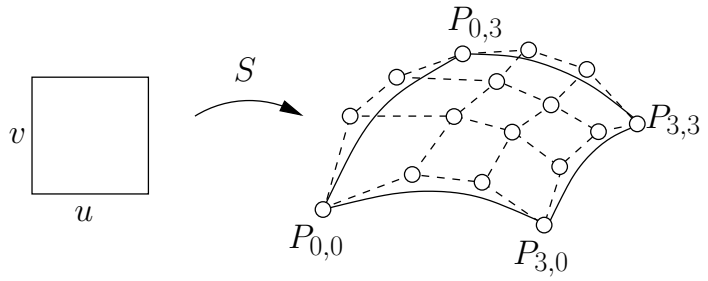

Figure 2-7 A tensor-product Bézier patch

2.6 B-spline Curves and Surfaces

Even though the Bézier definition can be used to model curves and surfaces, there are two common difficulties in geometrical design. First, if more control points are needed to define the curves or surfaces, high degree curves or surfaces will be generated. However, a high degree will cause the computation process to be inefficient and the resulting curves or surfaces may be numerically unstable. Second, if the geometry of a curve or a surface is of high complexity, a high degree Bézier curve or surface will be required to fit them. Moving any control point to improve the fit will produce changes everywhere along the curve or the

surface. The control is very sensitive and not sufficiently local. To overcome these problems, B-spline curves or surfaces need to be used.

2.6.1 B-spline Curves

A B-spline curve is defined by

$$C(t) = \sum_{i=0}^{n} N_{i,p}(t) P_i \,, \tag{2.11}$$

where P_i are control points in space, and p is the degree of the curve. n is the number of control points that are used to define the B-spline curve $C(t)$. $N_{i,p}(t)$ is *i*th B-spline basis function and is defined as

$$N_{i,0}(t) = \begin{cases} 1 & if \quad t_i \le t < t_{i+1} \\ 0 & otherwise \end{cases},$$

$$N_{i,p}(t) = \frac{t - t_i}{t_{i+p} - t_i} N_{i,p-1}(t) + \frac{t_{i+p+1} - t}{t_{i+p+1} - t_{i+1}} N_{i+1,p-1}(t) \,,$$

where $\{t_0, \cdots, t_{n+p}\}$ is a non-decreasing sequence of real numbers known as *knots*. The sequence is referred to as a knot vector, say U. There is no closed form for the B-spline basis functions. The knots t_i are break points on the curve. They separate the curve into *p*th degree polynomial curve segments. The number of times a knot occurs is known as its *multiplicity*. If a knot has multiplicity p, the knot is said to have *full multiplicity*. For a full end knot multiplicity curve, the knot vector U is defined as $U = \left\{ \underbrace{0, \cdots, 0}_{p+1}, t_0, \cdots t_{n-p-1}, \underbrace{1, \cdots, 1}_{p+1} \right\}$.

The parameter t is also a real number. As t varies from 0 to 1, a curve is mapped out from P_0 to P_n. An example of a quadratic B-spline curve is shown in Fig. 2-8. The knot vector of this curve is $U = \{0,0,0,t_0,t_1,t_2,1,1,1\}$.

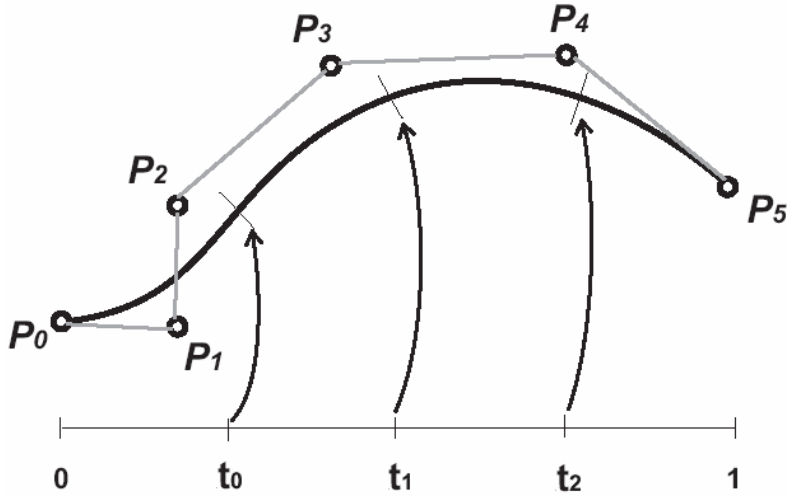

Figure 2-8 A quadratic B-spline curve

There are some important properties for a full end knot multiplicity B-spline curve:

- If $n = p$, then $U = \{0,\cdots,0,1,\cdots,1\}$ and $C(t)$ is a Bézier curve.
- A B-spline curve in general is a sequence of degree p polynomial curves that meet with C^{p-1} continuity.
- Moving control point P_i only changes $C(t)$ in the interval $[t_i, t_{i+p+1})$.
- The curve $C(t)$ is held in the convex hull of its control polygon.
- The control polygon represents a piecewise linear approximation of a curve. The accuracy of the approximation can be refined by knot insertion or degree elevation.

- There is de Casteljau style evaluation algorithm known as the de Boor algorithm.

For more details on properties and calculating a B-spline curve, see [25, 26].

2.6.2 B-spline Surfaces

A B-spline surface is given by

$$S(u,v)=\sum_{i=0}^{n}\sum_{j=0}^{m}N_{i,p}(u)N_{j,q}(v)P_{i,j}\ , \tag{2.12}$$

where the $P_{i,j}$ are control points for the surface and the $N_{i,p}$, $N_{j,q}$ are B-spline basis functions. The parameters u and v are real numbers. As u and v are varied over the $[0,1]\times[0,1]$ domain, a B-spline surface is traced out. The knot vectors in both the u and v directions are defined as $U=\left\{\underbrace{0,\cdots,0}_{p+1},u_0,\cdots u_{n-p-1},\underbrace{1,\cdots,1}_{p+1}\right\}$ and $V=\left\{\underbrace{0,\cdots,0}_{q+1},v_0,\cdots v_{m-q-1},\underbrace{1,\cdots,1}_{q+1}\right\}$. p and q are the degrees of the B-spline surface in the u and v directions. For a given (u,v) value, if it is outside the domain $[u_i,u_{i+p+1}]\times[v_j,v_{j+q+1}]$, $N_{i,p}(u)N_{j,q}(v)=0$. Moving $P_{i,j}$ only affects the surface inside the domain.

Equation (2.12) can be re-written as

$$S(u,v)=\sum_{i=0}^{n}N_{i,p}(u)\left(\sum_{j=0}^{m}N_{j,q}(v)P_{i,j}\right)$$

$$=\sum_{i=0}^{n}N_{i,p}(u)C_i(\bar{v})\,.$$

$\bar{v}$ is a specified value in the parameter v direction and the $C_i(\bar{v})$ is a point of a B-spline curve along the parameter u direction. The surface $S(u,v)$ can be supposed to be generated by interpolating several $C_i(\bar{v})$ curves at different parameter $\bar{v}$ values. In this thesis, the idea of constructing a surface to interpolate a sequence of curves is used to generate the flank millable surface.

For more details on properties and calculating a B-spline surface, see [25, 26].

2.7 Rational Curves and Surfaces

A rational curve or surface is the ratio of two polynomials. A rational Bézier curve is defined as

$$B(t) = \sum_{i=0}^{n} P_i w_i B_i^n(t) \Big/ \sum_{i=0}^{n} w_i B_i^n(t), \tag{2.13}$$

and a rational B-spline curve is defined as

$$C(t) = \sum_{i=0}^{n} N_{i,p}(t) P_i w_i \Big/ \sum_{i=0}^{n} N_{i,p}(t) w_i, \tag{2.14}$$

where w_i are the weights (scalar values) of each control point, $B_i^n(t)$ are the Bézier basis functions and $N_{i,p}(t)$ are the B-spline basis functions.

Similarly, a rational Bézier surface is defined as

$$S(u,v) = \sum_{i=0}^{n}\sum_{j=0}^{m} P_{i,j} w_{i,j} B_i^n(u) B_j^m(v) \Big/ \sum_{i=0}^{n}\sum_{j=0}^{m} w_{i,j} B_i^n(u) B_j^m(v), \tag{2.15}$$

and a rational B-spline surface is defined as

$$S(u,v) = \sum_{i=0}^{n}\sum_{j=0}^{m} N_{i,p}(u)N_{j,q}(v)P_{i,j}w_{i,j} \Big/ \sum_{i=0}^{n}\sum_{j=0}^{m} N_{i,p}(u)N_{j,q}(v)w_{i,j} \,, \qquad (2.16)$$

where $w_{i,j}$ are the weights of each control point.

Chapter 3
Flank Milling Surface Design with the Least Squares Approach

In flank milling, the machined surface can be closely represented by the grazing surface that is composed of a bundle of discrete grazing points. The method given in the section 2.3 can be used to compute the discrete grazing points. To express this surface with NUBS for engineering applications, a surface fitting method needs to be developed. A well known method for approximating a set of points is the least squares surface fitting method. This method will be probed first in this research.

3.1 Math Background

The least squares technique is a mathematical method to fit a curve or a surface to a given set of sample points such that the square of the deviation between the fitted and sample points is minimized. The fitted curve or surface does not necessarily pass through each sample point. In this application, the goal is to identify a NUBS surface that approximates the sample points to within engineering tolerance. A NUBS surface has many variables that include: knots, order of B-spline and control points. In the current application, the knot vectors and the order of the surface are given by the user and the control points are determined through the least squares formulation presented below.

3.1.1 Fitting a Curve to Point Data

Assume that a set of discrete points $\{Q_l\}$, $l = 0,1,2,\cdots,k$, are given. A p^{th} degree non-rational B-spline curve is used to approximate these points. The parameter of each sample point uu ($uu \in [0,1]$) is chosen either using the equal spacing method, the chord length method, the centripetal method (see Appendix A). The user can choose the knot vector or use the following knots, from Piegl [26]:

$$u_0 = u_1 = \cdots = u_p = 0,$$

$$u_{m-p} = u_{m-p+1} = \cdots = u_m = 1,$$

$$d = \frac{m+1}{n-p+1}, \quad i = \text{int}(jd), \qquad \alpha = jd - i,$$

$$u_{j+p} = (1-\alpha)\cdot uu_{i-1} + \alpha \cdot uu_i,$$

$$j = 1,2,\cdots,n-p, \tag{3.1}$$

where m is the number of knots counted from 0 in the knot vector and n (also counted from 0) is the number of control points defined by the user. Therefore, the knot vector of the interpolation curve is defined as

$$U = \{u_0, u_1, \cdots, u_{m-1}, u_m\}.$$

As described in Chapter 2, a NUBS curve is defined as

$$Q_l = \sum_{i=0}^{n} N_{i,p} P_i. \tag{3.2}$$

This equation can be written in matrix form as

$$Q = NP, \tag{3.3}$$

where $Q = \begin{bmatrix} Q_0 \\ Q_1 \\ \vdots \\ Q_l \end{bmatrix}$, $P = \begin{bmatrix} P_0 \\ P_1 \\ \vdots \\ P_n \end{bmatrix}$, $N = \begin{bmatrix} N_{0,p}(uu_0) & N_{1,p}(uu_0) & \cdots & N_{n,p}(uu_0) \\ N_{0,p}(uu_1) & N_{1,p}(uu_1) & \cdots & N_{n,p}(uu_1) \\ \vdots & \vdots & \ddots & \vdots \\ N_{0,p}(uu_l) & N_{1,p}(uu_l) & \cdots & N_{n,p}(uu_l) \end{bmatrix}$.

Solving equation (3.3), the control points for the least squares approximating curve can be determined as follows:

$$P = (N^T N)^{-1} N^T Q. \tag{3.4}$$

Using the results from equation (3.4), the p^{th} degree NUBS curve that approximates the sample points can be produced.

3.1.2 Fitting a Surface to Point Data

Suppose a set of discrete points $\{Q_{k,l}\}$, as shown in Fig. 3-1, are given, $k = 0,1,\cdots,r$ and $l = 0,1,\cdots,s$. A $(p,q)^{th}$ degree non-rational B-spline surface with $(m+1)\times(n+1)$ control points can be used to approximate these discrete points. Two parameters, u and v, are used to describe the approximating surface. In Fig. 3-1, u varies along the column direction (parameter l) from 0 to s. Similarly, v varies along the row direction (parameter k) from 0 to r.

The parameter corresponding to each sample point $uu_{k,l}$ $(uu_{k,l} \in [0,1])$ along u direction is calculated using either the equal spacing method, the chord length method, the centripetal method [26]. The parameter $\overline{uu_l}$ for each column is given by

$$\overline{uu_l} = \frac{1}{r+1}\sum_{k=0}^{r} uu_{k,l}\ , \tag{3.5}$$

where $l = 0,1,\cdots,s$.

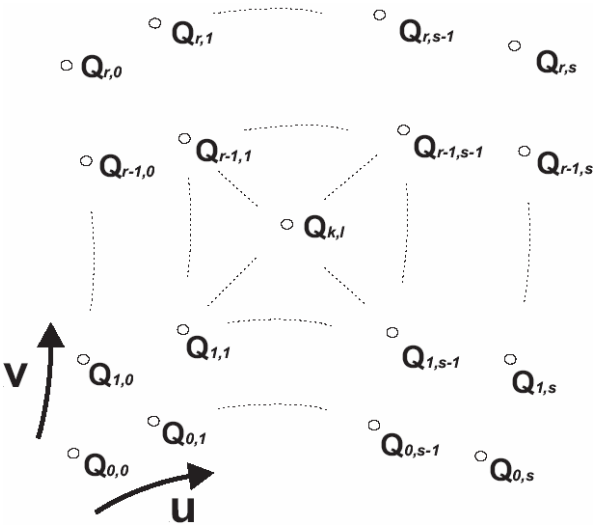

Figure 3-1 Discrete sample points and their position

Similarly, the parameter for each sample point $vv_{k,l}$ ($vv_{k,l} \in [0,1]$) along the v direction is calculated and the parameter $\overline{vv_k}$ for each row is given by

$$\overline{vv_k} = \frac{1}{s+1}\sum_{l=0}^{s} vv_{k,l}\ , \tag{3.6}$$

where $k = 0,1,\cdots,r$.

After the parameter of each sample point is defined, the knot vectors along two parameter directions (u and v directions) need to be determined. As the parameter value of each sample point must be unique, the knot vectors in the two directions are decided by using the

sample points along any row and column (simply treats sample points of the row or the column as the sample points of a curve). The technique to decide the knot vector of a curve described in the section 3.1.1 can be used to define the knot vectors of the surface. For more details on selecting the knot vector, see [25, 26].

Using equation (3.1), the knot vector of the approximating surface along the u direction is decided and is given by

$$U = \{u_0, u_1, \cdots, u_{n+p}, u_{n+p+1}\}.$$

Similarly, the knot vector of the approximating surface along the v direction can also be obtained and is given by

$$V = \{v_0, v_1, \cdots, v_{m+q}, v_{m+q+1}\}.$$

With the least squares approach [25], a non-rational B-spline equation can be obtained by manipulating the following,

$$Q = N_v P N_u^{\ T}, \tag{3.7}$$

where N_v and N_u are matrixes of the B-spline basis functions. P is the matrix of control points and Q is the matrix of given sample points.

$$Q = \begin{bmatrix} Q_{r,0} & Q_{r,1} & \cdots & Q_{r,s} \\ \vdots & \vdots & \ddots & \vdots \\ Q_{1,0} & Q_{1,1} & \cdots & Q_{1,s} \\ Q_{0,0} & Q_{0,1} & \cdots & Q_{0,s} \end{bmatrix}, \qquad N_v = \begin{bmatrix} N_{0,q}(\overline{vv_r}) & N_{1,q}(\overline{vv_r}) & \vdots & N_{m,q}(\overline{vv_r}) \\ \vdots & \vdots & \ddots & \vdots \\ N_{0,q}(\overline{vv_1}) & N_{1,q}(\overline{vv_1}) & \cdots & N_{m,q}(\overline{vv_1}) \\ N_{0,q}(\overline{vv_0}) & N_{1,q}(\overline{vv_0}) & \cdots & N_{m,q}(\overline{vv_0}) \end{bmatrix},$$

$$P = \begin{bmatrix} P_{m,0} & P_{m,1} & \cdots & P_{m,n} \\ \vdots & \vdots & \ddots & \vdots \\ P_{1,0} & P_{1,1} & \cdots & P_{1,n} \\ P_{0,0} & P_{0,1} & \cdots & P_{0,n} \end{bmatrix}, \qquad N_u = \begin{bmatrix} N_{0,p}(\overline{uu_s}) & N_{1,p}(\overline{uu_s}) & \cdots & N_{n,p}(\overline{uu_s}) \\ \vdots & \vdots & \ddots & \vdots \\ N_{0,p}(\overline{uu_1}) & N_{1,p}(\overline{uu_1}) & \cdots & N_{n,p}(\overline{uu_1}) \\ N_{0,p}(\overline{uu_0}) & N_{1,p}(\overline{uu_0}) & \cdots & N_{n,p}(\overline{uu_0}) \end{bmatrix}.$$

Solving equation (3.7), the control points of the least squares approximating NUBS surface can be obtained using

$$P = (N_v{}^T N_v)^{-1} N_v{}^T Q (N_u (N_u{}^T N_u)^{-1}) . \tag{3.8}$$

Using the results from equation (3.8), the $(p,q)^{th}$ degree NUBS approximating surface can be generated to approximate the sample points. Changing the parameterization, the degree, the number of control points or the knot vector will result in a different surface. These parameters can be used to find a surface suited for a particular application.

After the approximating NUBS surface is built, the developed surface error measurement method can be used to estimate the approximating surface error. If the error exceeds the user defined tolerance, more control points can be used to generate the approximating surface. The computation steps are the same as before. The degrees of the surface can be kept the same or changed. This computation process is repeated until the surface error is controlled and brought in the range the user desires.

3.2 Surface Design with the Least Squares Method

The machined surface generated by the flank milling technique can be described with a NUBS using the method given in the last section. To generate the machined surface, a grazing surface comprised of grazing points is required. Different tool positioning methods

generate different machined surfaces. Consequently, different grazing surfaces can be obtained with different tool positioning methods. In this research, the Bedi et al.'s tool positioning method given in section 2.2 is used to produce the machined surface and the method given in section 2.3 is used to calculate each grazing point on the grazing surface.

After the grazing points are obtained, they can be used as the sample points and the least squares method can be used to find a NUBS surface to fit these grazing points. To apply the least squares method, the degrees and the number of control points of the approximating surface along two parameter directions (u and v) need to be decided first. The degree and the number of control points along the guiding curves direction (u direction) are important factors that control the characteristic of the final machined surface, thus the degree of the approximating surface along u direction is selected to be the same as the degree of the guiding curves. Alternatively, the degree can be selected to be degree 2 or 3, as lower degree surfaces do not exhibit unwanted oscillations and can make it much easier to design good fitting surfaces [25, 26]. The number of control points along the guiding curve direction can initially be the same as the number of control points of the guiding curves. Of course, more control points can be added in this direction if desired.

The degree along the parameter v direction (the tool axis direction) is initially set to 2 or 3 for the same reasons explained above. The numbers of control points along the v direction are primarily set to 3 or 4.

After the degrees and the number of control points have been selected, the position of each control point is calculated using the method described in the section 3.1. Consequently, the

approximating NUBS surface can be generated. The error between the approximating surface and the given grazing points can be measured. If the maximum error exceeds the user defined tolerance, more control points can be added along the two parameter directions. Degrees of the surface can also be changed depending on error analysis and simulation results. With an increased the number of control points, the error between the approximating NUBS surface and the grazing surface can be effectively controlled.

In the section 3.1, the parametric value of each sample point ($\overline{uu}$, $\overline{vv}$) is given by equations (3.5) and (3.6). An alternative method to get this parametric value is to use the parametric value of each grazing point directly. When the grazing surface is calculated with equations (2.5), (2.6) and (2.7), each grazing point corresponds to a certain parametric value (u, v). This parametric value more closely reflects the grazing point's location than the average value from equations (3.5) and (3.6). Thus, for simplicity, the parametric value of each grazing points is taken to be the value from equations (3.5) and (3.6). For this reason, $uu = u$, $vv = v$ at each grazing point.

The knot vectors of the approximating NUBS surface can use unit knot vectors in both of the u and the v directions in place of the knot vectors obtained from equation (3.1). The main concern in equation (3.1) is to ensure that each knot span at least contains one uu or vv so that the knot vector truly reflects the sample points' distribution on the given surface. For the parametric value of each grazing point (u and v), equal space between two consecutive tool positions is normally used. Thus, a unit knot vector can guarantee that the number of grazing points at each knot span is equal and it also promises the knot vector itself reflects

the grazing points' distribution exactly. Therefore, the unit knot vectors can be used instead of knot vectors from equation (3.1).

After these changes, the computation process is greatly simplified. The resulting surface may be different and the difference between the two surface parameter setting methods will be analyzed in the next section.

3.3 Examples

Examples that apply the proposed method are given in this section. Two guiding curves are given and the control points of these curves are listed in Table 3-1. A cylindrical cutter is used to machine the surface and the radius of the cylindrical cutter is $R = 5$. The degree of the guiding curves is two. The knot vectors of the two curves are both $[0,0,0,1,1,1]$.

	T_0	T_1	T_2	B_0	B_1	B_2
x	75	30	0	60	30	15
y	15	30	60	0	30	75
z	-5	-5	-5	-45	-45	-45
w **(weight)**	1	1	1	1	1	1

Table 3-1 Control points for guiding curves [mm]

A NUBS surface that can be exactly flank milled is designed. Bedi et al.'s tool positioning method is used in this design and the grazing points on the grazing surface are calculated by

equation (2.7). Using these grazing points and the surface fitting method described above, the desired surface can be obtained.

First, the method described in the section 3.1 is used to design this surface. The degree of the surface in both the u and v directions is selected to be two and a three by three polygon of control points is initially selected to generate this NUBS surface. The parametric value of each sample point (grazing points) is given by equations (3.5) and (3.6) and the knot vectors along the u and v directions are calculated using equation (3.1). Using equation (3.8), control points of the approximating NUBS surface can be decided. After selecting these, the NUBS surface is constructed. The error between the approximating surface and the grazing points is calculated and the result is plotted in Fig. 3-2 below. The deviation between the approximating surface and the grazing points on the machined surface is in the range [0, 0.076]. The maximum surface error is close to 0.076.

The alternative way described in the section 3.2 is next used to design the same surface. The degree of the surface in both the u and the v directions is kept as two and the number of control points of the approximating surface are selected to be three by three. The parametric value of each sample point as used in the grazing point calculations of equations 2.5, 2.6 and 2.7 are used along with unit knot vectors in both u and v directions. The approximating NUBS surface is designed. The surface error is measured and plotted in Fig. 3-3 below.

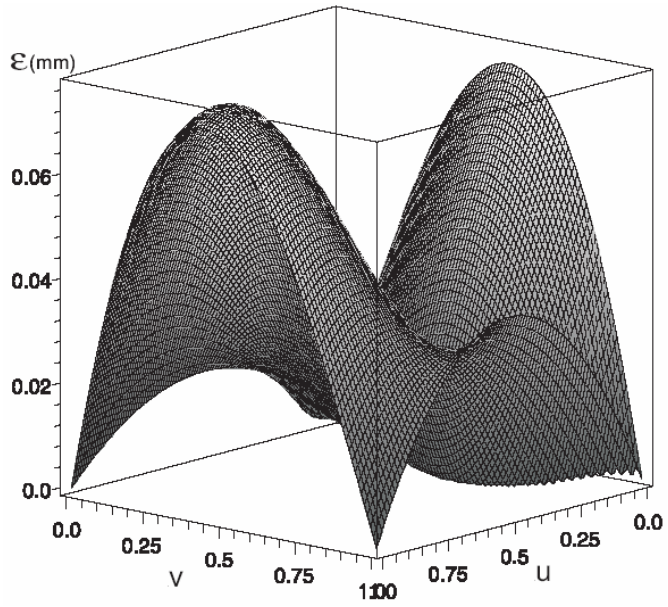

Figure 3-2 Error distribution of the approximating NUBS surface

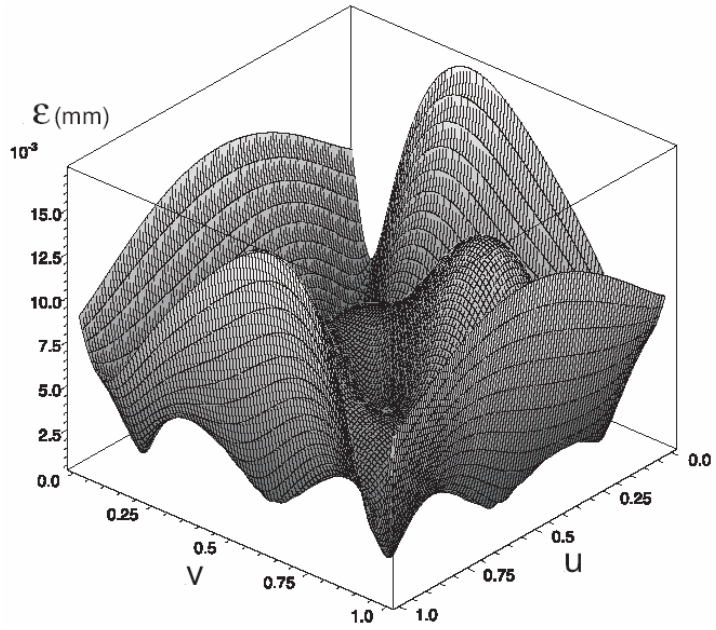

Figure 3-3 Error distribution of the 3 by 3 NUBS surface for unit surface knot vector

The deviation between the approximating surface and the grazing points is in the range [0, 0.0172]. The maximum surface error is less then 0.0172. Compared to Fig. 3-2, the maximum surface error reduces from 0.076 to 0.0172. The approximating NUBS surface with unit knot vectors and inheriting parametric value (for each sample points) generate small surface error. Thus, unit knot vectors and parametric values inherited from the grazing point calculations are used for each sample point for the remaining examples.

If the maximum surface error, 0.0172, still exceeds user defined tolerance, more control points can be added to reduce this maximum surface error. To demonstrate the process of surface error control, the number of control points is increased from three by three to various values up to four (the v direction) by five (the u direction). The degree of the approximating surface is kept as two along both parameter (u and v) directions. The approximating NUBS surfaces can be built using the least squares method given before. These surface errors are calculated and final results are listed in Table 3-2. The numbers of sample points were also varied from thirty by thirty to one hundred by one hundred to check the trend of the surface error change.

From this table, it can be seen that the change in the surface error as we increase the control points from three by three to three by four, three by five is not significant. However, the change is notable from three by three to four by three, three by four to four by four and three by five to four by five. Even the variation from four by three to four by four and four by five is drastically. This result also suggests that the number of control points in u and v directions affect each other. Sometimes, only an increase in the control points in one

direction can not significantly reduce the maximum surface error. Both of the u and the v directions need to be considered.

S.Ps / C.Ps	30×30	50×50	70×70	100×100
3×3	0.016	0.0166	0.017	0.0172
3×4	0.013	0.0135	0.0138	0.014
3×5	0.0134	0.014	0.0142	0.0143
4×3	0.0108	0.0113	0.0114	0.0116
4×4	0.0045	0.0048	0.0049	0.00505
4×5	0.0025	0.00245	0.0025	0.00255

Table 3-2 the number of control points vs. the maximum surface error [mm]. S.Ps: Sample Points. C.Ps: Control Points.

We may also notice that the maximum surface errors at certain numbers of control points under different number of sample points do not change significantly. Probably, in this example, thirty by thirty sample points can satisfy the simulation requirements. The reason for this phenomenon is that the machined surface is simple and the curvature variation is small. Less evenly distributed sample points can assure the accuracy of the design surface. If a big, complex and curvature changing surface needs to be designed, the thirty by thirty number of sample point surface, obviously, will not meet the design requirements. More sample points are needed and can give a higher accuracy surface then the less number of sample points. For sure, the accuracy of the surface will not change significantly when the number of sample points goes above a certain value. However, with more sample points, the computation time is longer. This will be discussed in the next section. Thus, to balance

choosing the total number of sample points is an important issue in the least squares surface fitting method.

3.4 Discussion

Using grazing points on a grazing surface, the machined surface can be approximated by a NUBS surface with the least squares approach. The accuracy of this surface is influenced by the distribution of the grazing points, the degree and the number of control points of the surface.

The distribution of the grazing points plays an important role in the least squares surface fitting method. High density of grazing point patches on the grazing surface will make the approximating surface match these patches well and impose the accuracy of the surface match. For flank milling surface design, the design surface needs to closely match the machined surface, thus, the grazing points should be evenly scattered along the grazing surface. With more grazing points, the computation time increases. For reason of demonstration, a table of sample points vs. time for the example given in the section 3.3 is shown in Table 3-2 (even though thirty by thirty number of sample points can satisfy the accuracy requirement). The computer used in this example was a Pentium 4 CPU 3.06GHz with 1.00 GB of RAM. The software used for calculation was Maple, a symbolic algebra package. Of course, other software like C++ can also be used. However, the trend of the variation will be the same.

S.Ps / C.Ps	30×30	50×50	70×70	100×100
3×3	28.9s	88.5s	202.2s	562.1s
3×4	32.1s	93.1s	214.1s	585.5s
4×5	45.2s	154.5s	374.2s	1054.9s

Table 3-3 the number of sample points vs. the computation time. S.Ps: Sample Points. C.Ps: Control Points.

The degrees and the number of control points of the approximating surface also significantly affect the surface design. Properly selecting the degrees and the number of control points are important in the least squares approach. Normally, a good guess at these numbers is required initially, then, control points can be added or deleted as desired in different parameter directions or alternatively the degrees of the approximating surface can be changed to make the surface fit the grazing points closely. More control points and low degree values will result in good surface fits.

Clearly, a high accuracy surface can be produced if sufficient and evenly distributed grazing points are given, proper degree of the surface is selected, and adequate control polygons are used. To achieve this target requires a large mesh of sample points and a long computation time. Thus, another easy to handle flank milling surface design method that simplifies the computation process is needed.

Chapter 4
Flank Millable Surface Design with Cylindrical Tools

To find an alternative and easy method to design the flank millable surface, the characteristics and geometries of the cutting tool and the given guiding curves need to be considered. To interpret this surface design method, we start from cylindrical tools and then extend the proposed method to any tools of revolution.

The idea behind the proposed technique for approximating a grazing surface is to select a few representative grazing curves and construct a surface that is close to these grazing curves. If enough grazing curves are used and they are close to one another, then the resulting surface should be a good approximation to the swept surface.

Each grazing curve is modeled using a NURBS representation (e.g., in Fig. 4-6 the control points $P_{0,0}$, $P_{1,0}$, $P_{2,0}$ are the NURBS representation for one grazing curve). Since we are working with a cylindrical tool, the projection of one grazing curve into a plane perpendicular to the tool axis direction will be a circular arc. To approximate this grazing curve, start with a NURBS representation of this circular arc, and then move the control points off the plane to approximate the grazing curve itself. A sequence of NURBS approximations to the grazing curves are used for several tool positions as the tool is moved along two guiding curves ($T(u)$ and $B(u)$ in Fig. 4-6). By increasing the number of control points along both the guiding curve and tool axis directions, better representations of grazing

curves can be defined and a better NURBS approximation of the grazing surface can be obtained. The details of this method are presented below.

4.1 Approximating a Grazing Curve

The grazing curve is the contact between the grazing surface and the cutting tool. Thus it lies on the cylindrical tool surface. This grazing curve is shown in Fig. 4-2 as a dashed line. P_0 is at the bottom and lies on the guiding curve $B(u)$ and similarly P_2 is on the top guiding curve $T(u)$. For simplicity, the coordinate system is set up at the bottom of the cylinder centre with the Z axis lying along the cylinder axis. P_0 and P_2 have the same parameter value u along the guiding curves and are known. The grazing curve with the end points P_0 and P_2 is projected onto the xy - plane (P_0^p and P_2^p correspond to P_0 and P_2) and the projection is a 2D circular arc, $P_0^p \overset{\frown}{P_2^p}$. This 2D arc can be represented exactly by a quadratic NURBS curve [25, 26] with three weighted control points P_0^p, P_1^p and P_2^p. The X and Y coordinates of P_0^p and P_2^p are known; however, P_1^p needs to be calculated. Fig. 4-1 below shows this relationship graphically.

P_1^p is calculated from the intersection of the two tangent lines passing through P_0^p and P_2^p. If α is the angle of the arc $P_0^p \overset{\frown}{P_2^p}$, then the weights w_0, w_1 and w_2 at points P_0^p, P_1^p and P_2^p are [25, 26]:

$$w_0 = w_2 = 1, \quad w_1 = \cos(\alpha/2).$$

w_1 is positive if $\alpha < \pi$. Otherwise, it is negative.

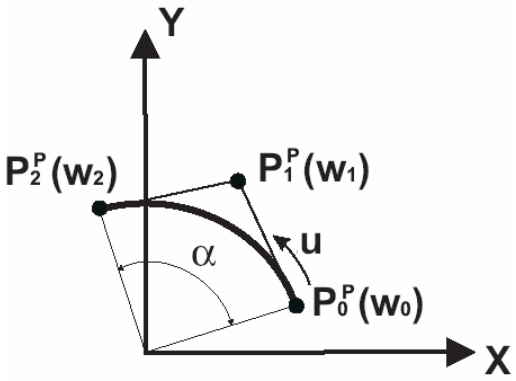

Figure 4-1 Arc with its control points

The arc $\overset{\frown}{P_0^p P_2^p}$ can be represented exactly as a NURBS curve $C^p(u)$ with control points P_0^p, P_1^p and P_2^p in the form given below.

$$C^p(u) = \frac{(1-u)^2 w_0 P_0^p + 2u(1-u) w_1 P_1^p + u^2 w_2 P_2^p}{(1-u)^2 w_0 + 2u(1-u) w_1 + u^2 w_2} \quad . \tag{4.1}$$

4.1.1 Modeling the Grazing Curve

Once the arc has been defined as a 2D NURBS curve, its control points can be stretched along the tool axis direction by moving P_0^p to P_0, P_2^p to P_2 and P_1^p to P_1, where P_1 needs to be decided. This changes the 2D NURBS curve to a 3D NURBS curve and is given by

$$C(u) = \frac{(1-u)^2 w_0 P_0 + 2u(1-u) w_1 P_1 + u^2 w_2 P_2}{(1-u)^2 w_0 + 2u(1-u) w_1 + u^2 w_2} . \tag{4.2}$$

The X and Y coordinates of P_1 are the same as P_1^p. The Z coordinates of P_1 must be properly selected to make the 3D NURBS curve closely match the grazing curve at this tool position.

The grazing curve is a function of the magnitude and direction of the velocities V_T and V_B as shown in equations (2.5), (2.6) and (2.7). Since the Z coordinate of P_1 must be determined by measuring the deviation from the grazing curve, it becomes a function of V_T and V_B. A convenient assumption would be to assume $|V_T| = |V_B|$. This will put P_1 in the middle of P_0 and P_2. The impact of this assumption on the error is studied in following section.

Fig. 4-2 shows this relationship graphically. The Z coordinates of P_0 and P_2 are 0 and h and P_0 and P_2 pass through the contact points $B(u)$ and $T(u)$ respectively.

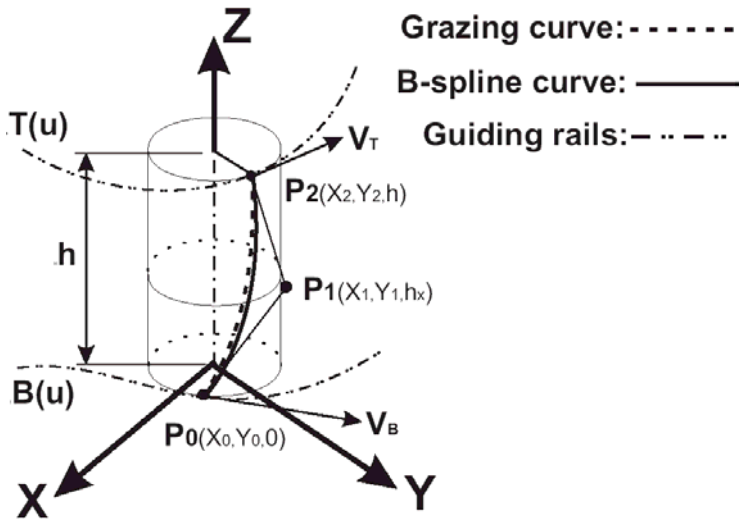

Figure 4-2 Grazing curve and its control points on the cylindrical surface

4.1.2 Error in Grazing Curve ($|V_T| = |V_B|$)

If the Z coordinate of point P_1 is set to half of the effective contact length h ($h_x = h/2$, h is measured along the tool axis direction between points P_0 and P_2), then the curve generated by equation (4.2) can be used to check the deviation of the grazing curve. To test the deviation, a simple case is set up. In this test, the parameters of the cylindrical cutter and control points used are:

$$P_0[R\cos(\pi/6), R\sin(\pi/6), 0],\quad P_1[\frac{R\cos(\pi/4)}{\cos(\pi/12)}, \frac{R\sin(\pi/4)}{\cos(\pi/12)}, h/2],$$

$$P_2[R\cos(\pi/3), R\sin(\pi/3), h],$$

$$V_B[-R\sin(\pi/6), R\cos(\pi/6), 0],\ V_T[-R\sin(\pi/3), R\cos(\pi/3), 0],$$

$$w_0 = 1,\ w_1 = \cos(\pi/12),\ w_2 = 1,\ R = 10,\ h = 45,$$

where the X and Y coordinates of point P_1 are obtained using the method described in section 4.1.1; R is the radii of the cylindrical cutter; h is the effective contact length along the axis of the cylindrical cutter; V_B and V_T are velocities at points P_0 and P_2, their directions are along tangent line directions of each circle and their magnitudes are true velocities; w_0, w_1 and w_2 are the weights of points P_0, P_1 and P_2.

Using equations (2.5), (2.6), (2.7) and (5.2), the grazing curve and the approximate NURBS curve can be obtained. The deviation between the two curves is calculated and is shown in Fig. 4-3. The errors at $v = 0$, $v = 0.5$ and $v = 1$ are zero. The shape of the error curve is symmetric and the maximum error is smaller than 0.035.

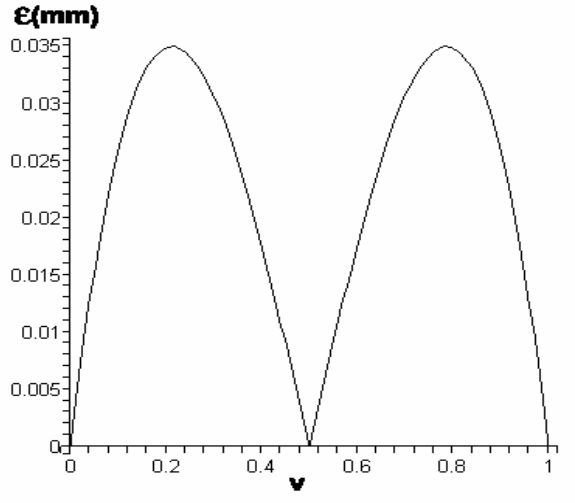

Figure 4-3 Deviation along the grazing curve if $|V_B| = |V_T|$

A close study of this error shows that the deviation between the NURBS curve and the grazing curve depends on the angle α between V_B and V_T which lie in the plane perpendicular to the tool axis, the radius of the cylindrical cutter, etc. The contact length (L) between the cutter and machined surface measured along the tool axis direction, however, has little influence on it. Different parametric combinations were considered and the resulting maximum deviations are listed in Tables 4-1, 4-2 and 4-3. From these tables, it can be seen that the influence of the angle α measured between V_B and V_T and the radii of the cutter are significant. The larger the angle α, the larger the deviation; the bigger the radius, the higher the deviation (the deviation varies linearly in the tool radius). The contact length has almost no influence on the deviation. To effectively control the deviation, more control points can be used and the curve tolerance requirement (the permitted error between the desired curve and the grazing curve) can be satisfied. In general, three control points satisfy most engineering applications for $\alpha < 30^0$ and $R < 30$.

$L(mm)$	25	45	65	85	105	150
$\varepsilon(mm)$	0.03493	0.03493	0.03493	0.03493	0.03493	0.03493

Table 4-1 Error for varying L ($\alpha = 30^0$, $R = 10$)

α	10^0	20^0	30^0	40^0	50^0	70^0	90^0
$\varepsilon(mm)$	0.001281	0.0103	0.0349	0.0835	0.165	0.467	1.033

Table 4-2 Error for varying α ($L = 45$, $R = 10$)

$R(mm)$	5	10	20	30	40	50
$\varepsilon(mm)$	0.0175	0.0349	0.0698	0.105	0.140	0.175

Table 4-3 Error for varying R ($L = 45$, $\alpha = 30^0$)

4.1.3 Modeling a Grazing Curve ($|V_T| \neq |V_B|$)

In a general situation, the magnitudes of velocities are unlikely to be equal. The magnitude of V_B (or V_T) depends on the geometry of the guiding curves and the cutting tool. Different velocity magnitudes of V_B and V_T influence the velocity distribution along tool axis, and as a result effect the shape of the grazing curve. If the Z coordinate (h_x) of the middle control point P_1 is kept as $h_x = h/2$, then the deviation between the given grazing curve and the approximate NURBS curve will increase. This is shown by considering the same example as before but the magnitude of V_T is bigger than V_B ($|V_T|/|V_B| = 1.07$). The maximum deviation is shown in Fig. 4-4 and is much bigger than the maximum deviation in Fig. 4-3.

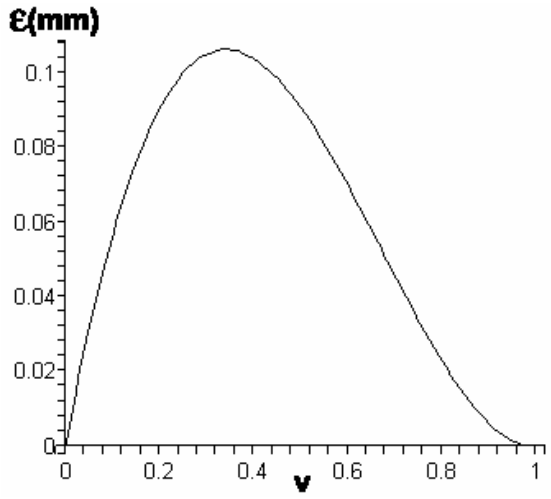

Figure 4-4 Deviation along the grazing curve if $|V_T| \neq |V_B|$

To reduce the maximum deviation along the grazing curve, the control point P_1 is moved from the middle along the tool axis direction toward the point with the smaller velocity magnitude. By re-stretching the motion of P_1 to the tool axis direction, we ensure that our approximation of the grazing curve will always lie on the surface of the cylindrical tool. The length of movement depends on the difference of the two magnitudes. The bigger the difference, the longer the movement. A study of the influence of this movement on the maximum error showed that if the ratio between the two magnitudes is less than $k = 1.35$ ($k = |V_B|/|V_T| \leq 1.35$ or $k = |V_T|/|V_B| \leq 1.35$), then the movement is less than or equal to $(k-1)*h/2$. For the above example, P_1 is moved toward P_0 by 1.55 along the tool axis. The resulting deviation between the grazing curve and the approximation NURBS curve is significantly reduced as shown in Fig. 4-5.

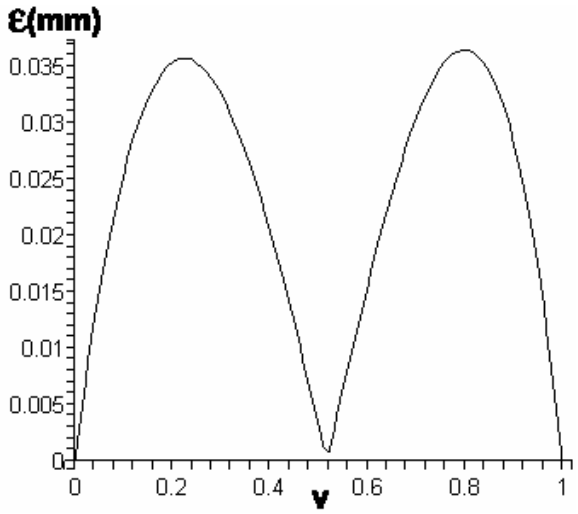

Figure 4-5 Deviation after P_1 position shifting

If the ratio k is bigger than 1.35, moving the point P_1 does not effectively reduce the maximum deviation. In this case, four or more control points are needed to approximate the grazing curve.

Generally, there are two methods that can be used to increase control points along the tool axis direction, knot insertion and degree elevation [25, 26]. Among these two methods, degree elevation has less flexibility in surface design [25, 26]. Thus, for simplicity, knot insertion is used to increase the control points along the tool axis direction.

If four of more control points are used, their locations along the axis of the tool are uncertain. These points are moved along the tool axis in a direction that reduces the deviation between the grazing curve and the approximate curve. Normally, four control points will satisfy requirements of normal engineering applications and produce surfaces that approximate the desired surface well.

4.2 Modeling a Surface

In the NURBS representation of the grazing curve, the outer control points move along two guiding curves $T(u)$ and $B(u)$ as explained in section 2.2. To build a NURBS surface representation of the swept surface, $T(u)$ and $B(u)$ make up the two boundaries of the NURBS surface. To do so, the two guiding curves, $T(u)$ and $B(u)$, must be constructed with the same number of control points. If the number of control points and the knot vectors are different for $T(u)$ and $B(u)$, then the method requires that additional control points be added to either or both $T(u)$ and $B(u)$ to ensure they have the same number of control points and knots.

Since $T(u)$ and $B(u)$ are the boundary curves of the grazing surface, the number of control points in the approximate NURBS surface along the generating lines should be equal to or greater than the number of control points in $T(u)$ (or $B(u)$).

Let the number of control points used to define $T(u)$ and $B(u)$ be three. Consider the case when the ratio of velocity magnitudes ($|V_B|/|V_T|$ or $|V_T|/|V_B|$) is less than 1.35, the angle α is less than 30^0 and tool radii is less than $30\,\text{mm}$. Based on these conditions and the discussion in the last section, the number of control points in the approximating NURBS surface along the guiding curve direction (u) are selected to be three. Since each grazing curve is approximated by a 3-control point-NURBS-curve, three control points are used to define the approximating NURBS surface along the tool axis direction (v). A 3 by 3 NURBS surface can be created to approximate the grazing surface. The control points of this surface

along with their weights are calculated using the technique given below. This new surface is comprised of a 3 by 3 grid of control point as shown in Fig. 4-6.

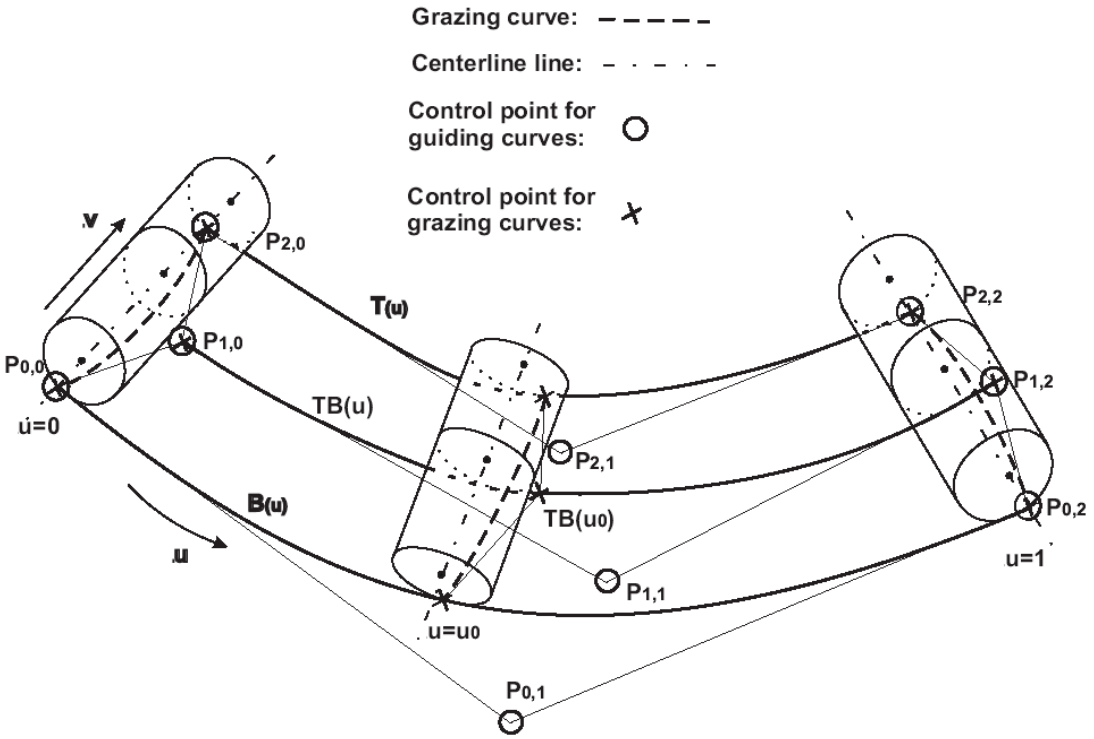

Figure 4-6 Control points for the approximate surface

The Fig. 4-6 shows the tool rolling along quadratic guiding curves $T(u)$ and $B(u)$. The grazing curves at the start ($u=0$), the end ($u=1$) and the interior position ($u=u_0$) are shown as dashed lines. Each of these curves is approximated by a NURBS curve with three control points. The control points at $u=0$ and $u=1$ form the boundary of the control polygon of the approximate NURBS surface along the v direction; control points of the guiding curves form the boundary control points of the NURBS surface along the u direction. This leaves only one control point, $P_{1,1}$, undefined. The weights of the various

control points also need to be determined. If the guiding curves $T(u)$ and $B(u)$ have n control points, then the number of undefined $P_{1,i}$ will be $n-2$.

4.2.1 Definition of NURBS Surface

A NURBS surface is defined as (see section 2.7)

$$S(u,v)=\frac{\sum_{i=0}^{n}\sum_{j=0}^{m}N_{i,p}(v)N_{j,q}(u)w_{i,j}P_{i,j}}{\sum_{i=0}^{n}\sum_{j=0}^{m}N_{i,p}(v)N_{j,q}(u)w_{i,j}},\ 0\le u,v\le 1. \tag{4.3}$$

For a bi-quadratic surface with three by three control points as shown in Fig. 4-6, equation (4.3) can be rewritten as

$$S(u,v)=\frac{\sum_{i=0}^{2}\sum_{j=0}^{2}N_{i,2}(v)N_{j,2}(u)w_{i,j}P_{i,j}}{\sum_{i=0}^{2}\sum_{j=0}^{2}N_{i,2}(v)N_{j,2}(u)w_{i,j}}$$

$$=\frac{N_{0,2}(v)\sum_{j=0}^{2}N_{j,2}(u)w_{0,j}P_{0,j}+N_{1,2}(v)\sum_{j=0}^{2}N_{j,2}(u)w_{1,j}P_{1,j}+N_{2,2}(v)\sum_{j=0}^{2}N_{j,2}(u)w_{2,j}P_{2,j}}{N_{0,2}(v)\sum_{j=0}^{2}N_{j,2}(u)w_{0,j}+N_{1,2}(v)\sum_{j=0}^{2}N_{j,2}(u)w_{1,j}+N_{2,2}(v)\sum_{j=0}^{2}N_{j,2}(u)w_{2,j}}$$

$$=\frac{(1-v)^2B^w(u)+2v(1-v)TB^w(u)+v^2T^w(u)}{(1-v)^2w_B(u)+2v(1-v)w_{TB}(u)+v^2w_T(u)}, \tag{4.4}$$

where

$$T^w(u)=(1-u)^2w_{2,0}P_{2,0}+2u(1-u)w_{2,1}P_{2,1}+u^2w_{2,2}P_{2,2}, \tag{4.5}$$

$$TB^w(u) = (1-u)^2 w_{1,0} P_{1,0} + 2u(1-u) w_{1,1} P_{1,1} + u^2 w_{1,2} P_{1,2}, \quad (4.6)$$

$$B^w(u) = (1-u)^2 w_{0,0} P_{0,0} + 2u(1-u) w_{0,1} P_{0,1} + u^2 w_{0,2} P_{0,2}, \quad (4.7)$$

$$w_T(u) = (1-u)^2 w_{2,0} + 2u(1-u) w_{2,1} + u^2 w_{2,2}, \quad (4.8)$$

$$w_{TB}(u) = (1-u)^2 w_{1,0} + 2u(1-u) w_{1,1} + u^2 w_{1,2}, \quad (4.9)$$

$$w_B(u) = (1-u)^2 w_{0,0} + 2u(1-u) w_{0,1} + u^2 w_{0,2}. \quad (4.10)$$

In equation (4.4), each specific u value represents a grazing curve. This grazing curve is approximated by a NURBS curve with three control points $T^w(u)$, $TB^w(u)$ and $B^w(u)$. $T^w(u)$ is the homogeneous coordinates of $T(u)$. It can be written as

$$T^w(u) = T(u) \cdot w_T(u),$$

where $w_T(u)$ is its corresponding weight.

Similarly, $TB^w(u) = TB(u) \cdot w_{TB}(u)$, $B^w(u) = B(u) \cdot w_B(u)$.

For polynomial guiding curves, the weights of control points $w_{2,0}$, $w_{2,1}$, $w_{2,2}$, $w_{0,0}$, $w_{0,1}$ and $w_{0,2}$ are equal to one. Equation (4.4) can be rewritten as

$$S(u,v) = \frac{(1-v)^2 B(u) + 2v(1-v) TB^w(u) + v^2 T(u)}{(1-v)^2 + 2v(1-v) w_{TB} + v^2}, \quad (4.11)$$

where

$$T(u) = (1-u)^2 P_{2,0} + 2u(1-u) P_{2,1} + u^2 P_{2,2}, \quad (4.12)$$

$$B(u) = (1-u)^2 P_{0,0} + 2u(1-u)P_{0,1} + u^2 P_{0,2}\,. \qquad (4.13)$$

At $u = 0$, equation (4.11) simplifies to the grazing curve at the start point of the guiding curves. Since the equation of the grazing curve and its NURBS curve approximation (see section 4.1) are known, two unknowns, $P_{1,0}$ and $w_{1,0}$, can be determined.

Similarly, at $u = 1$, equation (4.11) simplifies to the grazing curve at the end of the grazing surface. Equating it to the approximate NURBS surface results in $P_{1,2}$ and $w_{1,2}$.

The remaining two unknowns, $P_{1,1}$ and $w_{1,1}$, can also be calculated correspondingly; however, in this case, the grazing curve at $u = u_0$ is used.

Three methods can be used to select u_0, namely the unique step method, the chord length and the centripetal method [26]. In the unique step method, $u_0 = 0.5$. In the chord length method or the centripetal method, the value of u_0 is decided by the distribution of control points of each guiding curve. The ratio between the chord length of middle control point and the total chord length is used to calculate u_0 (see Appendix A).

If the control points of the two boundary curves are evenly distributed, the unique step method is selected. Otherwise, the chord length method or the centripetal method is used. Once u_0 is decided, w_{TB} can be set to $w_{TB} = \cos\alpha_3 / 2,$ where α_3 is the angle between $B(u_0)$ and $T(u_0)$ measured in the plane normal to the cylinder axis. Equations (4.11), (4.9) and (4.6) can be solved for $w_{1,1}$ and $P_{1,1}$.

If the guiding curves have more than three control points, additional grazing curves at $u = u_i$ may be required. Each grazing curve is used to determine two unknown coefficients.

For rational B-spline guiding curves, the weights of their corresponding control points are not 1. Similar technique can be applied to compute each interior control point and its weight using equations 4.4 through 4.10.

4.2.2 Re-evaluation of Weight

Even though $w_{1,1}$ and $P_{1,1}$ can be calculated by equations (4.6), (4.9) and (4.11), the weights and control points used in the equations will not result in a good approximating NURBS surface because $w_{1,0}$, $w_{1,2}$ and w_{TB} are obtained by considering the grazing surface shape along the tool axis direction (the v direction) and the shape of the grazing surface along the feed direction (the u direction) is not considered. This results in surface error between the approximate surface and the grazing surface. Thus, to effectively control the surface error, the weight selection should reflect the change in shape of the grazing surface not only along the tool axis direction, but also along the feed direction. More control points can be added along the feed direction to reduce this error. With an increase in the number of the control points along the feed direction, the error of the approximating NURBS surface can be effectively controlled. This will be discussed in section 4.4. Another solution is to determine the weight of the middle control point in a way that takes into account the surface variation along the guiding curves. An average weight can be used to roughly reflect the surface shape variation along the feed direction. Hence, the weight of the middle control point is set to the average weight of all the interior control points as shown below:

$$w^* = (w_{1,0} + w^{TB} + w_{1,2})/3,$$

$$\overline{w}_{1,0} = \overline{w}_{1,1} = \overline{w}_{1,2} = w^{TB} = w^* , \qquad (4.14)$$

where $w_{1,0}$, w^{TB} and $w_{1,2}$ are corresponding interior control point weight of each grazing curve at three tool positions and $\overline{w}_{1,0}$, $\overline{w}_{1,1}$ and $\overline{w}_{1,2}$ are the weights of interior control points of the approximating NURBS surface. When a NURBS surface is created using this method, it results in a smaller maximum surface error as compared to the surface with variable weights $w_{1,0}$, w^{TB} and $w_{1,2}$. We are unsure to why averaging gives smaller error, but we mention this since it gives better results. This will be discussed in sections 4.4.2.1 and 4.4.2.2.

Substituting the result of equation (4.14) into equation (4.6), $P_{1,1}$ is determined. Once all the unknowns are solved, equation (4.11) gives the approximating NURBS surface.

4.2.3 Generalization of Surface Modeling

The guiding curves $T(u)$ and $B(u)$ can have more than three control points. Suppose that the guiding curves $T(u)$ and $B(u)$ are two NURBS curves of degree p, then the degree of the approximating NURBS surface along the feed direction can be selected to be p as well. The number of control points along the feed direction is $n+1$, where $n \geq p$. The control points of the NURBS surface in the tool axis direction is still three. If there are $n+1$ control points along the guiding curve direction, then $n+1$ tool positions are used to determine the NURBS surface.

At each of these tool position, the grazing curves are developed and the NURBS approximation to these curves are used to calculate the weights k_0, k_1, k_2, ..., k_n at the interior control points. While the weights k_0, k_1, k_2, ..., k_n can be directly used, it was again found that averaging the weights gives better results. The equations to compute these weights are given below.

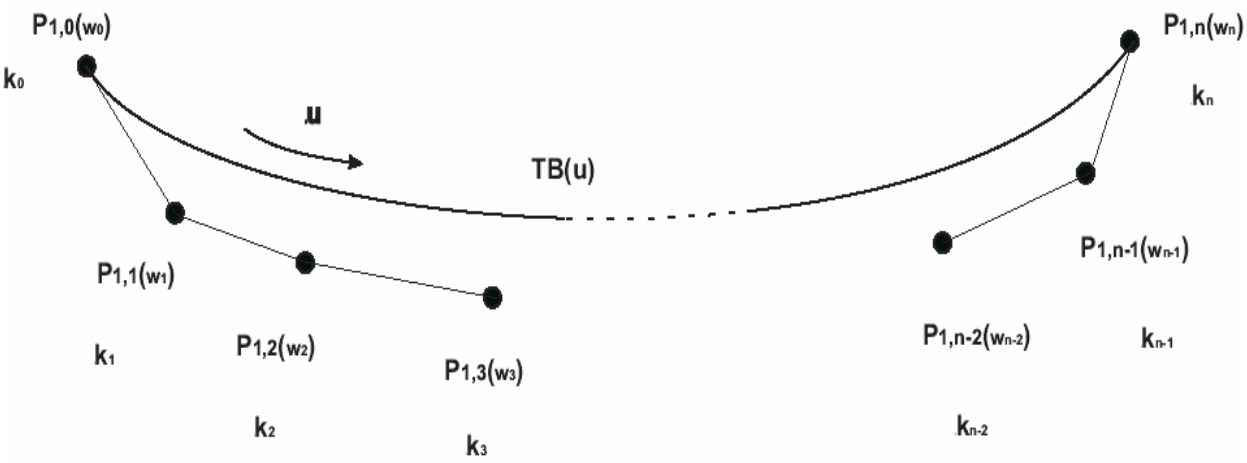

Figure 4-7 Weight distribution along $TB(u)$

$$w_i = \frac{(k_i + k_{i+1} + \cdots + k_{i+p}) + (k_0 + k_1 + \cdots + k_p)}{2(p+1)}, \qquad \text{if } 0 \le i \le p.$$

$$w_i = \frac{(k_i + k_{i+1} + \cdots + k_{i+p}) + (k_{i-p} + k_{i-p+1} + \cdots + k_i)}{2(p+1)}, \qquad \text{if } p+1 \le i \le n-p-1.$$

$$w_i = \frac{(k_{n-p} + k_{n-p+1} + \cdots + k_n) + (k_{i-p} + k_{i-p+1} + \cdots + k_i)}{2(p+1)}, \qquad \text{if } n-p \le i \le n. \qquad (4.15)$$

With these weights, NURBS equations of the grazing curves in terms of the unknown control points [25, 26] can be obtained as

$$TB(u_1) = \frac{\sum_{i=0}^{n} N_{i,p}(u_1) P_{1,i} w_i}{\sum_{i=0}^{n} N_{i,p}(u_1) w_i},$$

$$TB(u_2) = \frac{\sum_{i=0}^{n} N_{i,p}(u_2) P_{1,i} w_i}{\sum_{i=0}^{n} N_{i,p}(u_2) w_i},$$

$$\vdots$$

$$TB(u_{n-1}) = \frac{\sum_{i=0}^{n} N_{i,p}(u_{n-1}) P_{1,i} w_i}{\sum_{i=0}^{n} N_{i,p}(u_{n-1}) w_i}. \qquad (4.16)$$

These equations can be solved for the interior control points ($P_{1,i}$, $i = 1, \cdots, n-1$) of the approximate NURBS surface. With these control points and their corresponding weights, the approximate surface is completely defined.

After the surface is defined, the deviation between the actual grazing surface and the approximate NURBS surface can be evaluated. Control points of the NURBS surface can be increased along the u and/or the v direction if the surface error is more than the specified tolerance. The knot insertion method can be used to increase control points in the u and/or the v direction. With more control points, the surface deviation can be lowered but more unknowns need to be calculated. The calculation procedures, however, are the same as above.

4.3 Flow Chart for Surface Design

To explain the basic concept of surface design for flank milling, a flow chart that describes the whole design procedure is given in Fig. 4-8. This chart can also be used to implement the surface design process.

The design starts with two user specified guiding curves and their control points. The cutting tool is also selected by the user at the onset of design. Depending on the relationship among the grazing surface, the cutting tool and the guiding curves, the number of control points and the knot vector of the approximate NURBS surface can initially be determined. Consequently, the average weight of interior control points can be calculated.

In the proposed method, the position of the interior control point is initially set to the middle of each effective tool contact length at all specified tool positions. The positions of these interior control points are then optimized to reduce the error over the whole design surface. After optimization, all control points of the flank millable surface are known and this flank millable surface can be built. The error that would result when this surface is machined is checked next. If the maximum surface error exceeds the specified tolerance, more control points can be added to the control polygon of the surface and this process is iterated until the surface error reaches the required tolerance.

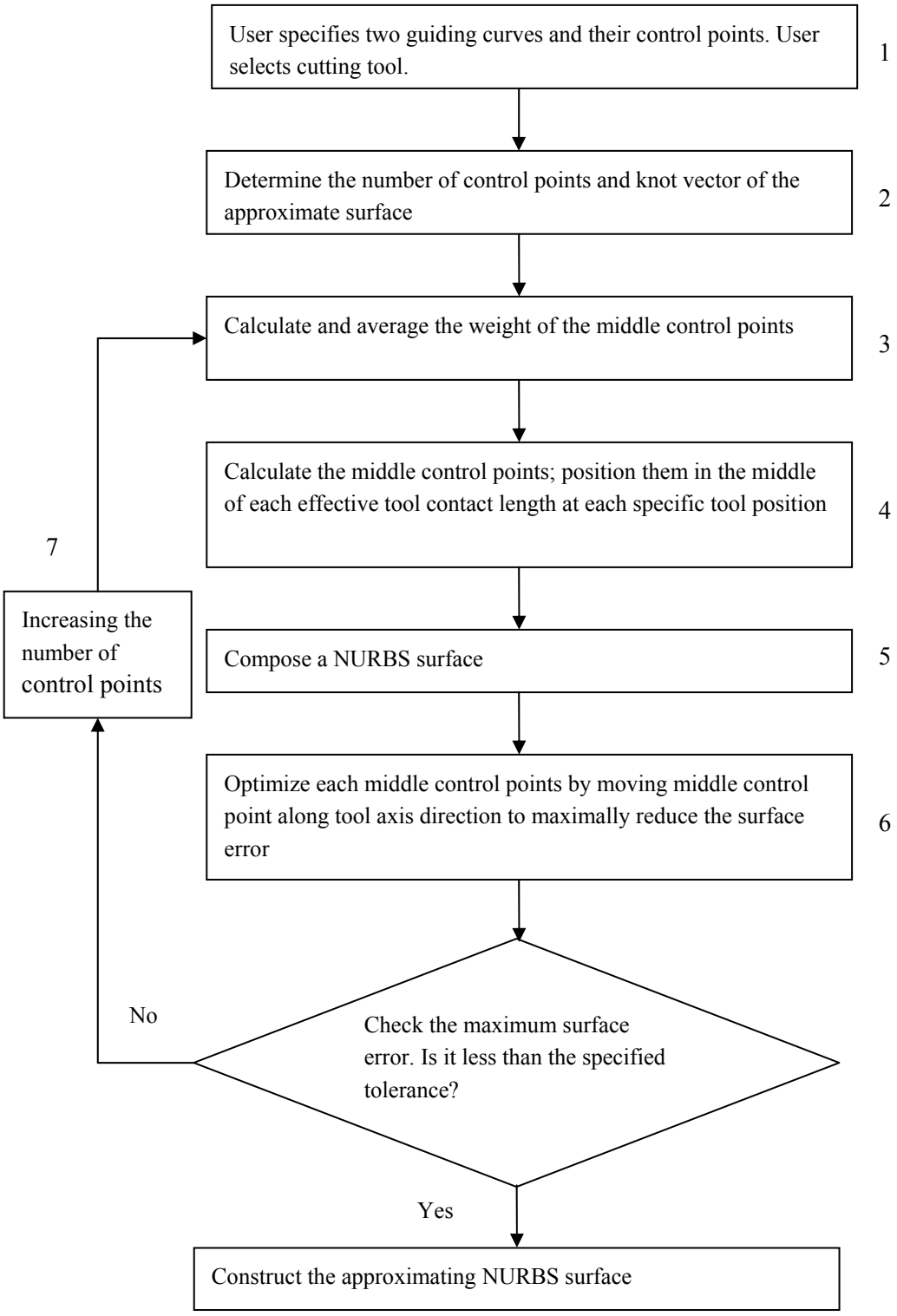

Figure 4-8 The flow chart of implementation

4.4 Accuracy Control for Surface Design

In this section, the technique of designing a surface for flank milling is demonstrated with examples and the method to control the surface error in the design of the flank millable surface is also studied. The results are presented below. The results are explained by referring to the flow chart shown in Fig. 4-8. Blocks in the chart are numbered to simplify this discussion.

In the flow chart, the step to optimize the middle control points along the tool axis direction is performed as part of generation of the approximating NURBS surface. This is different from the method given in section 4.2. In the section 4.2, the optimization of the middle control point is performed before the flank millable surface is constructed in step 5. As the middle control point for each tool position is optimized separately, the influence from other grazing curves is not considered. A study of the effect of optimizing the location of the middle control points on the overall surface error was done. The study shows that reducing the maximum error between the grazing curve and the approximating NURBS curve does not necessarily reduce the maximum surface error between the flank millable surface and the grazing surface. In Fig. 4-9, as the middle control point of the first approximating curve changes, the maximum error between the approximating NURBS curve and the grazing curve reduces, but the maximum error between the flank millable surface and the grazing surface starts to increase after some time. To avoid this, a new method to optimize the middle control point is employed. In this new method, the middle control points of all selected grazing curves are moved together as the surface error is optimized. The middle control points are thus located to optimize for minimal surface error.

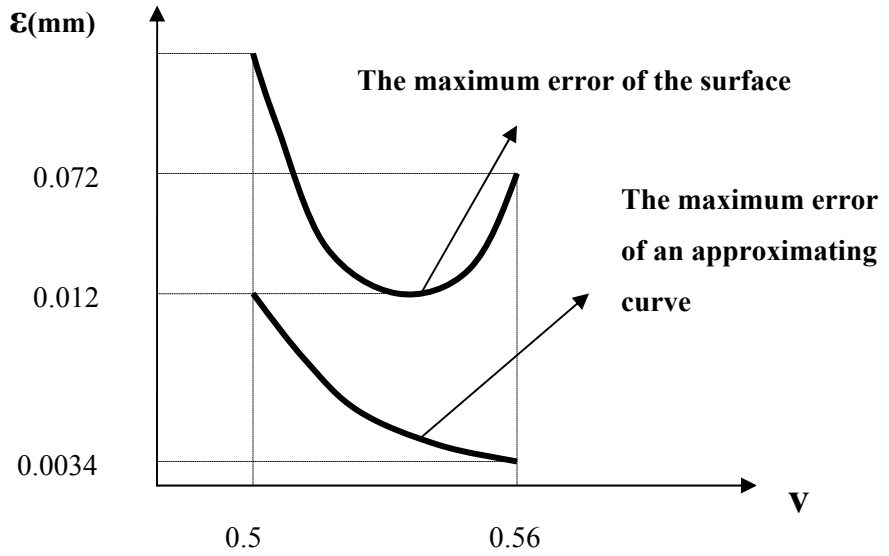

Figure 4-9 The maximum error of the grazing curve & the grazing surface as middle control point moved along tool axis direction to reduce the grazing curve error.

4.4.1 Surface Design for Flank Milling

The design of a surface that can be flank milled begins with two guiding curves, $T(u)$ and $B(u)$. In our example, the two quadratic curves represent the top and the bottom curves of an impeller or a blade surface (or any free form surface of an engineering part). The same example given in section 3.3 is used. The control points for the curves are tabulated in Table 3-1. The degree of both the curves is 2. The knot vector of the two curves is $[0,0,0,1,1,1]$.

A NURBS surface that can be accurately flank milled is designed. A cylindrical cutter of radius $R = 5$ is used and Bedi et al.'s tool positioning method [9] is adopted to position the cutter and consequently to generate the tool path. The resulting machined surface is calculated using the swept surface method. The grazing surface and the guiding curves are plotted in Fig. 4-10.

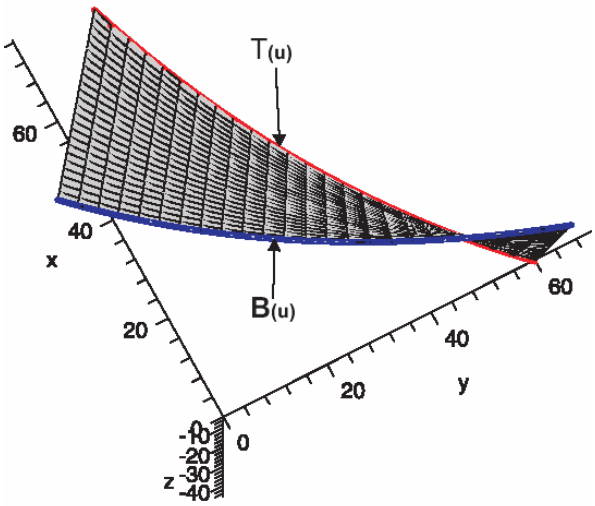

Figure 4-10 The grazing surface and guiding curves

The first step in designing the NURBS surface is to select the number of control points of the surface and its knot vector. The control points and knot vector are selected by user. Since the guiding curves lie on the machined surface and the numbers of control point defining the guiding curve in this example are three, the numbers of control point of the design surface along the guiding curve direction can initially be selected to be three. The knot vector of the surface along the guiding curve direction is the same as the guiding curve, i.e., [0,0,0,1,1,1]. These parameters can be corrected based on the surface error analysis later. If the maximum surface error is larger than the specific tolerance, more control points can be added. Of course, the knot vector of the surface will also change.

In the second step, the tangent vectors of $T(u)$ and $B(u)$, that represent the direction of motion of the tool at these points, are investigated by plotting the angle α, which is the angle between the tangent vectors of $T(u)$ and $B(u)$ measured in the plane perpendicular to the cutting tool axis. The angle α and the ratio of the magnitudes of these tangents 'k' are

plotted as shown in Fig. 4-11 and Fig. 4-12. The angle α varies from 24^0 to 28.1^0, the ratio k changes from 0.89 to 1.12. Since the magnitude does not change radically, three control points will be used to model the approximating surface along the tool axis direction. Experiments with different surfaces have shown that if the ratio k is bigger than 1.35 (or smaller than 0.74) or the angle α is bigger than 30 degree, then more control points should be used in the tool axis direction. If the surface needs to be redefined as a result of error analysis, additional knots can be added using knot insertion as described in [25, 26] and more control points can be added along the tool axis direction.

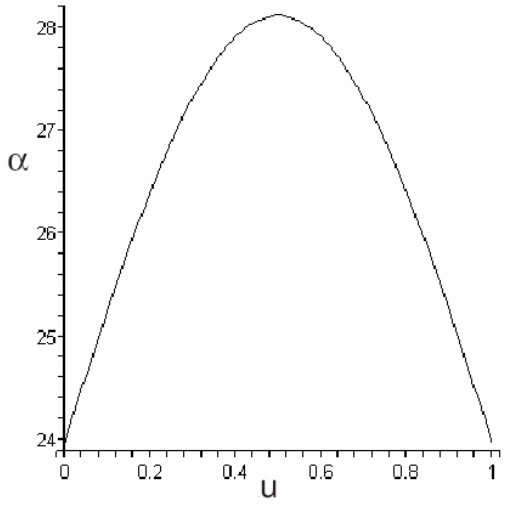

Figure 4-11 The variation of angle α along the feed direction.

In the third step, a 3 by 3 bi-quadratic NURBS surface is constructed using the proposed surface design method. The procedure to build this surface is demonstrated in the next section.

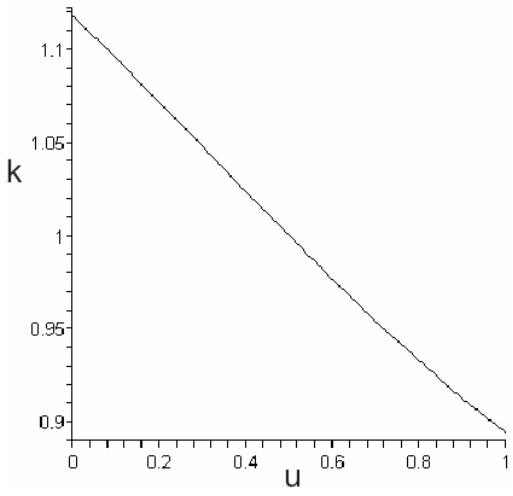

Figure 4-12 The variation of the ratio k along the feed direction.

4.4.2 Three by Three Approximate NURBS Surface

Blocks 3 to 6 in Fig. 4-8 are used in this section. The control points and weights of the generating curves are directly assigned to the corresponding control points of the surface. This leaves three of the middle control points, namely $P_{1,0}$, $P_{1,1}$ and $P_{1,2}$, and their corresponding weights undetermined (see Fig. 4-6). The middle control points and weights are defined with the method discussed in section 4.2. Three tool positions, $u = 0$, $u = u_0$ and $u = 1$, are used to decide these parameters. In the current example, $u_0 = 0.5$. At each specified tool position, a grazing curve is calculated, and then a NURBS curve is used to approximate this grazing curve. The middle control points of the NURBS curves are optimized together by moving their locations simultaneously to reduce the approximate NURBS surface error as explained in section 4.1. The middle control points of the NURBS curve at tool positions $u = 0$ and $u = 1$ are directly added to the control polygon of the

surface. The remaining control point $P_{1,1}$ is calculated as described in section 4.2. The weights of these middle control points were determined when the grazing curves were calculated. These weights are averaged and re-assigned to the middle control points. After all control points and weights are obtained, a 3 by 3 NURBS surface is generated. The deviation between the grazing surface and the designed NURBS surface is calculated. The result is shown in Fig. 4-13.

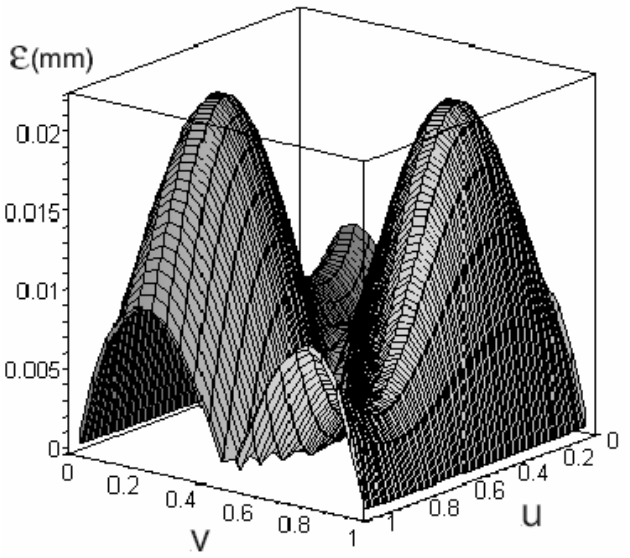

Figure 4-13 Deviation between the grazing surface and the NURBS surface

The deviation between the grazing surface and the approximate surface is in the range [0, 0.022]. The maximum error is less than 0.022.

In generating this surface, the velocity at the top and the bottom were assumed to be given by the derivatives of $T(u)$ and $B(u)$. Similarly, the weights of the middle control points were averaged. The effect of these assumption (or steps) is explored next before the method of improving surface error is presented.

4.4.2.1 Surface Model for Fixing Middle Control Point ($v = 0.5$)

The selection of the middle control points is based on the ratio of the velocity magnitudes at $T(u)$ and $B(u)$. For simplification, this ratio can be neglected and the middle control point (along $TB(u)$, see Fig. 4-6) is forced to lie at $v = 0.5$, the middle of the effective contact length along the tool axis. This will simplify the procedure and speed up the computations significantly. But this changes the NURBS surface. Following the flow chart steps 1 to 5 (Fig. 4-8), the flank millable surface is reconstructed and the deviation is again measured and the result is plotted in Fig. 4-14.

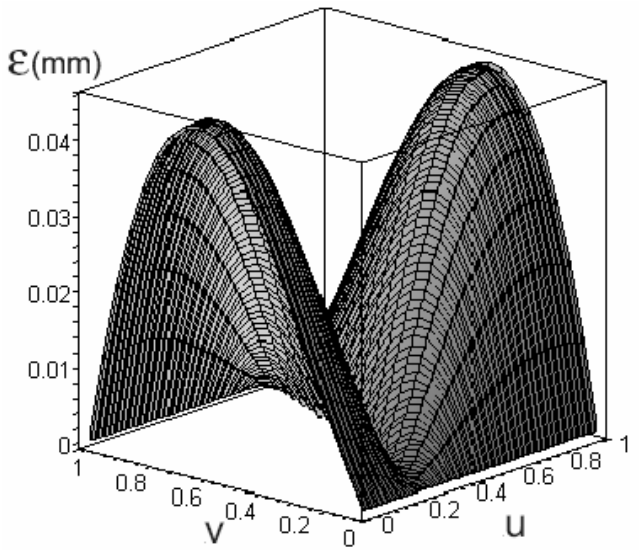

Figure 4-14 Deviation between the grazing surface and the NURBS surface with a fixed middle control point

The deviation between the grazing surface and the approximate surface is in the range [0, 0.045]. The maximum deviation is close to 0.045. Compared to Fig. 4-13, the maximum deviation has increased, but the surface design procedure is simpler. The middle control points are obtained easily. This deviation may be acceptable in some engineering situation

especially when the ratio of velocity magnitudes (between two contact points on $T(u)$ and $B(u)$) is close to 1 and further improvement can be achieved by insertion of knots or degree elevation as described later. If the ratio of magnitudes is equal to 1, Fig. 4-13 and Fig. 4-14 will give similar results.

4.4.2.2 Effect of Varying Weight on Surface Model

The results obtained above use the average weight for each middle control point of the NURBS surface. If separate weights are used for each middle control point as described in section 4.2.1, it follows the path 1, 2, 4, 5 and 6 in the flow chart in Fig. 4-8 and a different surface can be obtained. The error of this surface is plotted in Fig. 4-15.

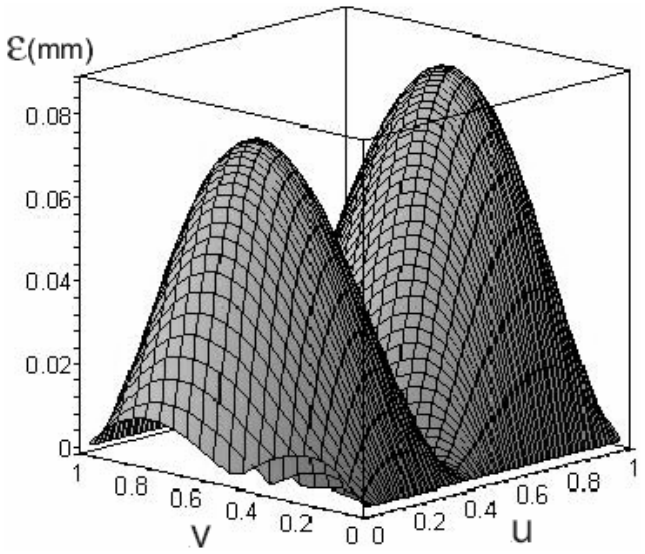

Figure 4-15 Deviation between the grazing surface and the NURBS surface with separate weight of each middle control point.

The deviation between the grazing surface and the approximate surface is in the range [0, 0.088]. The maximum deviation is close to 0.088. Compared to Fig. 4-13, this gives a larger

deviation. The separate weight of each middle control point results in a highest surface error in all the cases tried by authors. Thus, using weights that are the average of the weights from the NURBS grazing curves are recommended.

4.4.3 Flank Millable Surface with more Control Points

As discussed before, the deviation between the grazing surface and the flank millable surface will decrease if the control points along the generating curve direction (u) and/or along the tool axis direction (v) are increased. To illustrate this, additional control points are added to the surface generated in the example above.

4.4.3.1 Increasing Control Points in the u (or v) Direction

In this case study, the numbers of control points along v or the tool axis are kept the same. The control points in u direction or along the guiding curves are increased from three to four and then to five. Knot insertion [25, 26] is used to increase the number of control points. The degree of the NURBS surface is kept the same, i.e., two. The control points of the two guiding curves ($T(u)$ and $B(u)$) are first increased, then, the remaining control points and weights along the middle are decided. For four control points, the knot vector becomes $[0,0,0,\frac{1}{2},1,1,1]$ and four tool positions, at $u=0$, $u=0.33$, $u=0.66$ and $u=1$, are used to calculate the middle control points and weights. For the case of five control points, the knot vector becomes $[0,0,0,0.\frac{1}{3},\frac{2}{3},1,1,1]$ and five tool positions, $u=0$, $u=0.25$, $u=0.5$ $u=0.75$, and $u=1$, are used to calculated the middle control points and weights. Using the

technique developed above, the approximating NURBS surfaces are created and the maximum surface deviations are calculated and listed in Table 4-4.

The maximum deviation for a 3×4 NURBS surface is 0.0195 and for a 3×5 NURBS surface is 0.0165. Compared to the 3×3 NURBS surface, the maximum surface error has reduced from 0.022 to 0.0195 and 0.0165 as the numbers of control points increased from three to four and five along the guiding curve direction. With an increase in the number of control points in the u direction, the maximum surface error decreases.

Similarly, one can increase the number of control points in the v direction and keep the number of control points in the u direction the same. The number of control points is increased from three to four and the knot vector is changed to $[0,0,0,\frac{1}{2},1,1,1]$ in the v direction. A quadratic NURBS surface is created and the maximum surface error is calculated and also tabulated in Table 4-4.

The maximum error for the 4×3 NURBS surface is around 0.0152, smaller than the maximum error 0.022 from 3×3 approximating NURBS surface. In general, the maximum surface error decreases with the number of control points increased in the v direction.

4.4.3.2 Increasing Control Points in the u and the v Directions

The control points can also be simultaneously increased in both u and v directions to further reduce the deviation between the grazing surface and the NURBS surface. Using the same example, the control points along the v direction (or the tool axis direction) are increased from three to four, while at the same time, the control points along the u direction (or the

guiding curve direction) are also increased from three to four and then to five. The degree of the NURBS surface in both of u and v directions are kept the same as before. The knot vector changes from [0,0,0,1,1,1] to $[0,0,0,\frac{1}{2},1,1,1]$ along the v direction, and from [0,0,0,1,1,1] to $[0,0,0,\frac{1}{2},1,1,1]$ along the u direction as the control points are increased to four and to $[0,0,0,\frac{1}{3},\frac{2}{3},1,1,1]$ when the control points are increased to five. Four tool positions at $u=0$, $u=0.33$, $u=0.66$ and $u=1$ for 4×4 surface (or five tool positions at $u=0$, $u=0.25$, $u=0.5$, $u=0.75$ and $u=1$ for the 4×5 surface) are used to calculate the middle control points and weights. The maximum surface error is checked and plotted in Table 4-4.

The maximum surface error for the 4×4 surface is around 0.0087 and for the 4×5 surface is around 0.0065. Compared to the 3×3 NURBS surface, the maximum deviation has reduced from 0.022 to 0.0087 and 0.0065 as the numbers of control points has increased from three by three to four by four and four by five respectively.

C.Ps($v\times u$)	3×3	3×4	3×5	4×3	4×4	4×5
ε_{max}	0.022	0.0195	0.0165	0.0152	0.0087	0.0065

Table 4-4 Errors for different NURBS surface. C.Ps: Control Points.

From this Table 4-4, it can also be seen that the maximum surface errors are reduced insignificantly as the numbers of control points are only increased in the u direction from 3×3 to 3×4 and 3×5. However, the maximum surface errors are reduced drastically when the numbers of control points are increased in both of u and v directions. It suggests that

both of u and v directions need to be considered when the control points are added to the control net of the surface. Sometimes, only adding control points in one direction can not significantly reduce the maximum surface error.

4.5 More Examples

The proposed method was also tried on two more examples of different surfaces as demonstrated below. The deviation of the surface in both examples can be effectively controlled by changing the number of control points and the knot vector. The guiding curves used in surface design are shown in Fig. 4-16(a) and Fig. 4-17(a) as bold lines. The error distribution calculated with the method described earlier is given in Fig. 4-16(b) and Fig. 4-17(b) for the respective surfaces. Accuracy of the surface can be achieved in each case with increase in control points.

4.6 Comparison with the Least Squares Method

In this chapter, the method for design of a flank millable surface that approximates a grazing surface has been developed. Although the accuracy of the approximation can be improved by knot insertion, it is still necessary to compare the presented method with the established Least Squares technique, which guarantees the best fit.

Table 4-5 gives a comparison of the error of the two methods for approximating the same surface. (The data come from section 3.3 and section 4.4.3.)

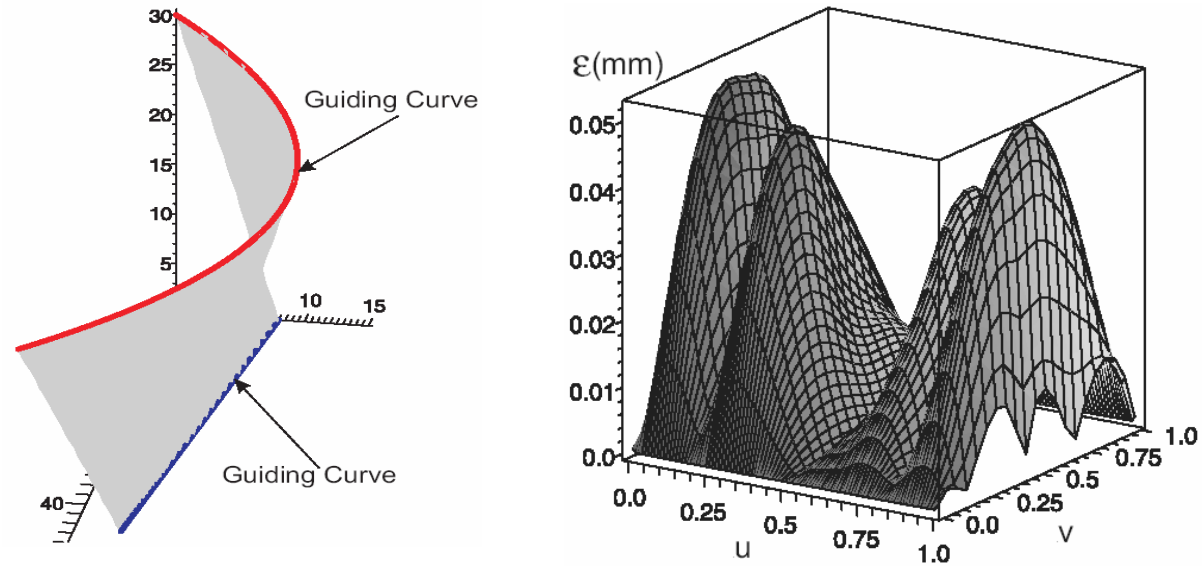

(a) **(b)**

Figure 4-16 The surface designed using the proposed method and its surface error
(a) The designed surface and its guiding curves. (b) the surface error distribution.

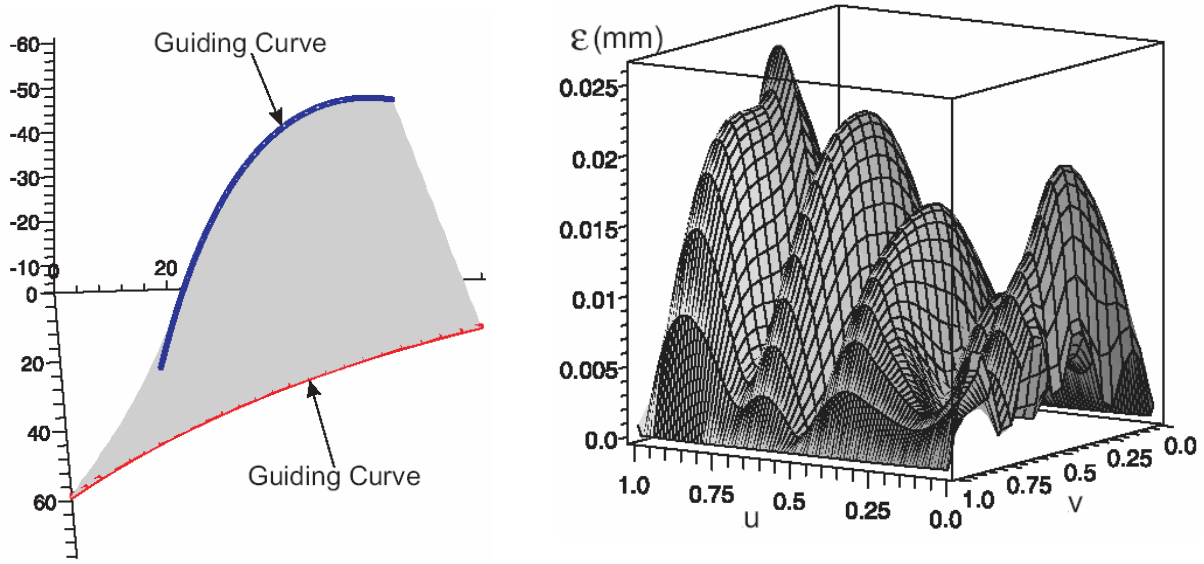

(a) **(b)**

Figure 4-17 The surface designed using the proposed method and its surface error
(a) The designed surface and its guiding curves. (b) The surface error distribution.

C.Ps / Methods	3×3	3×4	3×5	4×3	4×4	4×5
L.S	0.016	0.013	0.0134	0.0108	0.0045	0.0025
P.M	0.022	0.0195	0.0165	0.0152	0.0087	0.0065

Table 4-5 The maximum error [mm] in the flank millable surfaces generated using different number of control points. C.Ps: Control Points. L.S: Least Squares. P.M: Proposed Method

From this table, it can be seen that the maximum errors from the two surface fitting methods are of the same order of magnitude. The Least Squares Method can offer a higher accuracy surface for the same number of control points, etc., but the error is dependent on the selection of the knot vector, the parametric value of each sample point, the number of sample points and their distribution. Furthermore, the computation process is complex. A large number of sample points result in a long computation time. On the other hand, the surface error from the proposed method is not influenced by the variation of the number of sample points. The knot vector of the surface is the same as the knot vector of the guiding curves. The parametric value of each sample point is known. Only a few tool positions are used to define the approximating surface. The computation process is simple and computation time is short and the flank millable surface error can be controlled by increasing the number of control points of the surface.

For comparison, the runtime of the Least Squares method addressed in Chapter 3 and the method presented in this chapter are compared in Table 4-6. As before, the computer used in the example was a Pentium 4 CPU 3.06GHz with 1.00GB of RAM. The software used was Maple.

	L.S				P.M
S.Ps / C.Ps	30×30	50×50	70×70	100×100	4×20~6×20
3×3	28.9s	88.5s	202.2s	562.1s	67.8s
3×4	32.1s	93.1s	214.1s	585.5s	68.9s
4×5	45.2s	154.5s	374.2s	1054.9s	96.6s

Table 4-6 Runtime comparision. C.Ps: Control Points. L.S: Least Squares. P.M: Proposed Method. S.P: Sample Points.

The runtime is seriously affected by the number of sample points for the least squares method. Of course, the runtime is also affected by the quality of the code, the complexity of the mathematical models, etc. For a simple design surface, like this example, both of the least squares and the proposed method can provide a reasonable runtime. However, for a complex design surface, a large number of sample points should be used to represent the target surface and the runtime will be an important factor for engineering applications. From this point of view, the proposed method can offer a more economic runtime than the least squares method.

4.7 Discussion

The proposed flank millable surface design method is based on a few grazing curves and the surface can be built by lofting these grazing curves along the guiding curves direction. Thus, the position of each selected grazing curve also influences the developed flank millable surface. Even though the equal step method or the centripetal method can help to select the target grazing curves, they are just roughly estimated. Slightly moving each interior grazing curve can further reduce the surface error.

The method itself is tested with polynomial guiding curves. It can also be applied to the rational B-Spline guiding curves. More control points need to be added along the guiding curve direction to control the error between the designed surface and the machined surface. Alternatively, the rational guiding curves can first be approximated with polynomial curves and then be used to design the surface for flank milling.

Even though the proposed method is demonstrated with Bedi et al.'s tool positioning method, it can still be applied to other developed flank milling tool positioning methods.

In the proposed method, each selected grazing curve is expressed with a NURBS curve. For NUBS (Non-Uniform B-spline) guiding curves, NURBS representation grazing curves will still result in a NURBS surface. Normally, NUBS guiding curves expect to generate a NUBS flank millable surface. Furthermore, the selection of the average weight affects the surface generation. Thus, further improvement of this method is still necessary and is presented in the next chapter.

Chapter 5
NUBS Based Method for Surface Design with Cylindrical Tools

To complete the proposed method developed in Chapter 4, a method to use the same or more number of unit weigh interior control points to represent each grazing curve and consequently to generate the flank millable surface is proposed.

5.1 NUBS based Surface Design for Flank Milling

In the previous method, the contact curve between the cutting tool and the machined surface, the grazing curve, is morphed into the NURBS curve at each tool position as the tool is moved along the boundary or guiding curves. The collection of these morphed grazing curves generates the surface. Each of them is expressed with three weighted control points that are generated by stretching three weighted control points of each 2-D NURBS arc along the cutting tool axis direction. The 2-D arc is the projection of a grazing curve in a plane perpendicular to the cutting tool axis and can be exactly defined by a NURBS curve with three weighted control points. The weight of each control point of the grazing curve is inherited from the weight of the control point of its corresponding 2-D arc. The weights of interior control points represent the variation along the grazing curve direction only and cannot be used directly in the surface polygon. The average weight is used for each interior control point of the surface. If a method of representing the grazing curve without weights

can be developed, then the weights of the interior control points of the design surface can also be eliminated. To eliminate the weight of each control point, two ways are proposed.

5.1.1 Arc Modeling with Three Unit Weight Control Points

The first way to eliminate the weight is to force the weight of each control point is equal to 1. As shown in Fig. 4-1, $\overset{\frown}{P_0^p P_2^p}$ is a 2-D arc defined by a NURBS curve with three weighted points $P_0^p(w_0)$, $P_1^p(w_1)$ and $P_2^p(w_2)$ [25, 26], where w_0, w_1, w_2 are weights. The NURBS representation of the arc is given by the equation (4.1).

If the weight of the middle control point (w_1) is set to 1, then the equation (4.1) becomes

$$C^p(u) = (1-u)^2 P_0^p + 2u(1-u)P_1^p + u^2 P_2^p . \qquad (5.1)$$

This curve is a Bézier curve and it will deviate from the circular arc. The accuracy of this 2-D arc is investigated before it is used in design of surfaces for flank milling applications.

If the coordinates of the three control points of the 2-D arc are

$$P_0^p[R,0], \quad P_1^p[R, R\tan(\alpha)], \quad P_2^p[R\cos(\alpha), R\sin(\alpha)],$$

then the deviation between the exact arc (equation (4.1)) and its simplified form (equation (5.1)) can be calculated based on the parametrical error measurement metric [21], and is given by

$$\varepsilon = R - \sqrt{x^2 + y^2} \ , \qquad (5.2)$$

where R is the radius of the arc and (x, y) is a point obtained from equation (5.1).

Using equation (5.2), the maximum error can be calculated as α is changed from 0^0 to 70^0. The result is shown in Table 5-1.

α	5^0	10^0	20^0	25^0	30^0	50^0	70^0
ε / R	4.53×10^{-7}	7.2×10^{-6}	1.17×10^{-4}	2.88×10^{-4}	6×10^{-4}	4.84×10^{-3}	0.02

Table 5-1 Curve error for varying α .

From this table, it can be seen that the difference between the Bézier representation of the arc and the arc itself varies with α. The larger the value of α, the larger the maximum error of the arc. If $R \le 25$ and $\alpha \le 25^0$, the maximum error will be less than 7.2×10^{-3} which is acceptable for many engineering applications. In the design of impellers and blades, the angle α is usually less than 25^0 which indicates that the NURBS curve with three unit weight control points (i.e., a NUBS curve) is adequate for defining these surfaces for flank milling. If high accuracy is required or $R > 25$ or $\alpha > 25^0$, the curve with three unit weight control points can not be used and three weighted control points or more non-weighted control points need to be used to design the arc. A NURBS arc with three weighted control points has already been developed in Chapter 4; a NURBS arc with more non-weighted control points will be discussed in the following section.

The possible application to use the three unit weight control point to define the 2-D arc and surface will be demonstrated in the end of section 5.2.1.

5.1.2 Arc Model with Four Unit Weight Control Points

To accurately represent an arc on a circle with Bézier curves and/or NUBS curves, different methods have been developed [27, 28]. The method used in this research is the Dokken et al.'s circle approximation method [28]. As Fig. 5-1 shows, $\overset{\frown}{P_0^p P_3^p}$ is a 2-D arc and Dokken et al. suggested that this arc can be approximated by a Bézier curve with four control points, P_0^p to P_3^p. $P_0^p P_1^p$ and $P_3^p P_2^p$ are two tangential lines of the arc at points P_0^p and P_3^p with $| P_0^p P_1^p | = | P_3^p P_2^p | = L = \frac{4}{3} R \tan(\frac{\alpha}{4})$, where R is the radius of the arc. A cubic Bézier curve with these four control points can be generated and is given by

$$C^p(u) = (1-u)^3 P_0^p + 3u(1-u)^2 P_1^p + 3u^2(1-u) P_2^p + u^3 P_3^p . \qquad (5.3)$$

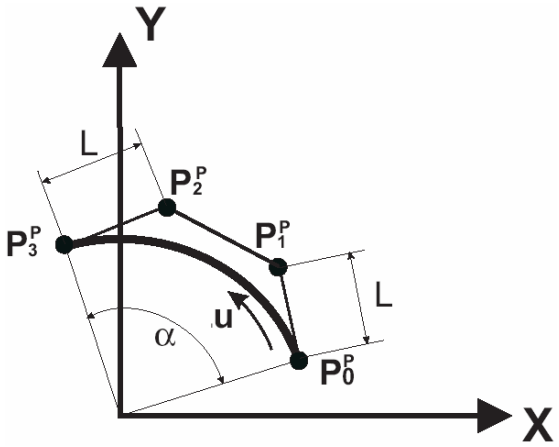

Figure 5-1 Arc with four unit weight control points

The arc $\overset{\frown}{P_0^p P_3^p}$ can be closely represented by equation (5.3). The accuracy of this curve is checked using equation (5.2) and the results corresponding to the different values of α are tabulated in Table 5-2.

α	5^0	10^0	25^0	30^0	50^0	70^0	90^0
ε / R	7.95×10^{-12}	5.08×10^{-10}	1.24×10^{-7}	3.7×10^{-7}	7.95×10^{-6}	6×10^{-5}	2.71×10^{-4}

Table 5-2 Error for different α .

From Table 5-2, it can be seen that the difference between the arc and its Bézier approximation under 90^0 is very small and is acceptable for all engineering applications. If α is less then 50^0 and R is less than 30, then the maximum arc error will be less then 2.39×10^{-4} ($=30\times7.95\times10^{-6}$). Thus, in this chapter, four control points with unit weight will be used to define the 2-D arc and subsequently be used to define the grazing curve and the grazing surface (except at the end of section 5.2.1, where using the three point Bézier arc is studied).

5.1.3 Modeling of the Grazing Curve

When a surface is machined, the cutting tool is imagined to roll along two guiding curves. At each tool position, a grazing curve is generated to represent the machined surface. A dashed line shows the grazing curve in Fig. 5-2. In this figure, $T(u)$ and $B(u)$ are two guiding curves. A cylindrical tool is used to machine the surface. A Cartesian coordinate is set up at the bottom center of the cylindrical cutting tool and the grazing curve at parameter value u represented by the dashed curve is generated using the Bedi et al. tool positioning method [9]. This curve can be projected into a plane that is perpendicular to the cutting tool axis (the xy - plane, in this case) and the projection is a 2-D arc that is shown in Fig. 5-1. P_0 and P_3 are two contact points located on the guiding curves $T(u)$ and $B(u)$. Their corresponding

points on the 2-D arc are P_0^p and P_3^p. h is the effective contact length along tool axis direction between the cutting tool and the machined surface.

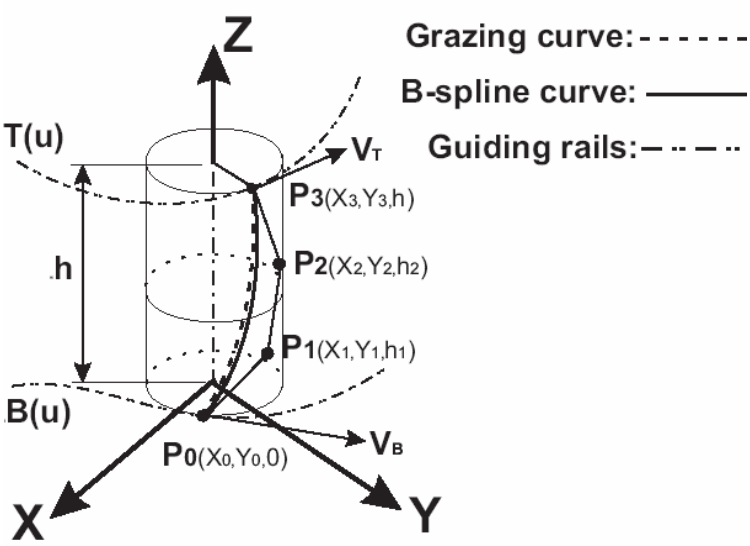

Figure 5-2 Grazing curve and its control points on the cylindrical cutting tool surface

Using the method described in section 5.1.2, this 2-D arc can be approximated by a Bézier curve with four control points. These four points can be moved along tool axis direction (Z direction, in this case) to generate a 3-D Bézier curve to approximate the grazing curve. This curve is given as

$$C(u) = (1-u)^3 P_0 + 3u(1-u)^2 P_1 + 3u^2(1-u)P_2 + u^3 P_3, \qquad (5.4)$$

where P_0 and P_3 are known (P_0^p and P_3^p are set to P_0 and P_3). The z coordinates of P_1 and P_2 (h_1 and h_2) still need to be determined.

P_0^p, P_1^p, P_2^p and P_3^p are not evenly distributed along the arc as shown in the Fig. 5-1 ($|P_1^p P_2^p| \neq L$, $|P_0^p P_1^p| = |P_3^p P_2^p| = L$), which indicates that P_0, P_1, P_2 and P_3 should not be

evenly distributed along the tool axis direction in Fig. 5-2. To determine the z coordinates of P_1 and P_2, h_1 and h_2 are initially set to $h/3$ and $2*h/3$, and then P_1 and P_2 are moved along the tool axis direction separately so that the maximum error between the grazing curve and the approximate curve can be reduced. Examples are used to test this method. Since the grazing curve depends on the velocity V_B and V_T, two cases are considered, namely $|V_T| = |V_B|$ and $|V_T| \neq |V_B|$. The parameters of the cutting tool and control points used in the examples are given below.

$R = 10$, $h = 45$, $\alpha = \pi/6$, $L = 4*\tan(\alpha/4)/3$, $L1 = \sqrt{R^2 + L^2}$, $\alpha 1 = \alpha - \arcsin(L/L1)$,

$P_0[R,0,0]$, $P_1[R,L,h/3]$, $P_2[R*\cos(\alpha 1), R*\sin(\alpha 1), 2*h/3]$, $P_3[R*\cos(\alpha), R*\sin(\alpha), h]$.

If the magnitude of the velocity V_T at point P_3 and the magnitude of the velocity V_B at point P_0 are equal and $V_B : [R,0,0]$, $V_T : [-R*\sin(\alpha), R*\cos(\alpha), 0]$, then the error between the grazing curve and the approximate Bézier curve can be calculated and the results are plotted in Fig. 5-3.

From this figure, it can be seen that the maximum error is around 0.026 when $h_1 = h/3$ and $h_2 = 2*h/3$. The maximum error is reduced significantly from 0.026 to $1.9*10^{-4}$ after P_1 and P_2 are moved along the tool axis direction.

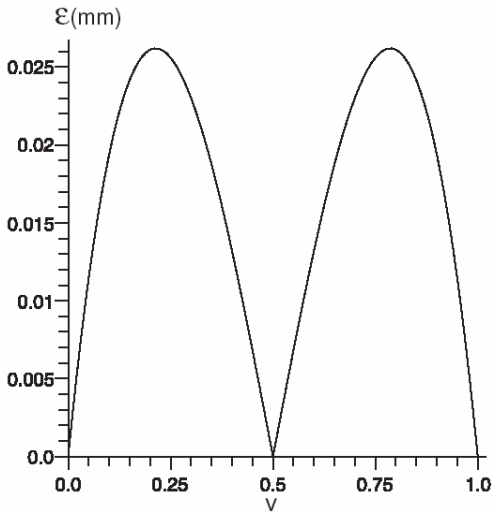

(a)

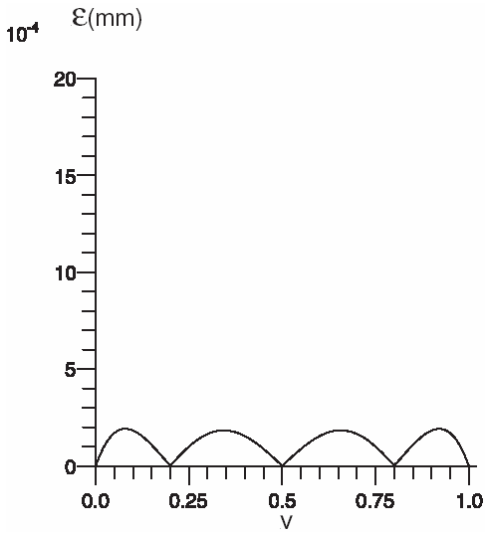

(b)

Figure 5-3 Deviation along the grazing curve for $|V_T| = |V_B|$

(a) Curve error for $h_1 = h/3$ and $h_2 = 2*h/3$. (b) Curve error as P_1 and P_2 are optimized by moving them along the cutting tool axis direction.

In general, the magnitude of the velocity V_T and the magnitude of the velocity V_B are not equal. Under this condition, similar steps can still be used to get the positions of P_1 and P_2. The same example given above is used here to demonstrate the method when the magnitude of V_T is bigger than V_B ($|V_T|/|V_B| = 1.07$). P_1 and P_2 are shifted along the tool axis direction separately and iteratively until the smallest deviation between the grazing curve and the approximating Bézier curve is obtained. The z coordinates of P_1 and P_2 are then defined. Using equation (5.4), the approximate curve is determined. The curve error is calculated and plotted in Fig. 5-4. From this figure, it can be seen that the maximum curve error is less than $8.4*10^{-4}$. The approximate Bézier curve closely matches the given grazing curve.

In both cases, namely $|V_T| = |V_B|$ and $|V_T| \neq |V_B|$, the movement of P_1 and P_2 reduces the approximation error and is therefore adopted as a standard sequence in this method.

If the maximum errors shown in Fig. 5-3 or Fig. 5-4 do not satisfy the user's requirement, more control points can be added. The knot insertion method [25, 26] is used to increase the number of control points along the cutting tool axis direction. With an increased number of control points, the curve error can be reduced to the desired level. Note that knot insertion will change the Bézier curve into a NUBS (Non-Uniform B-spline) curve. Since a Bézier curve is a special case of a NUBS curve, we will use the term NUBS through the rest of this chapter.

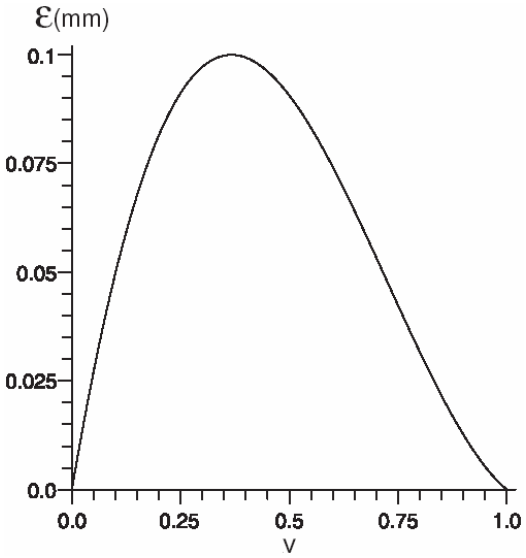

(a)

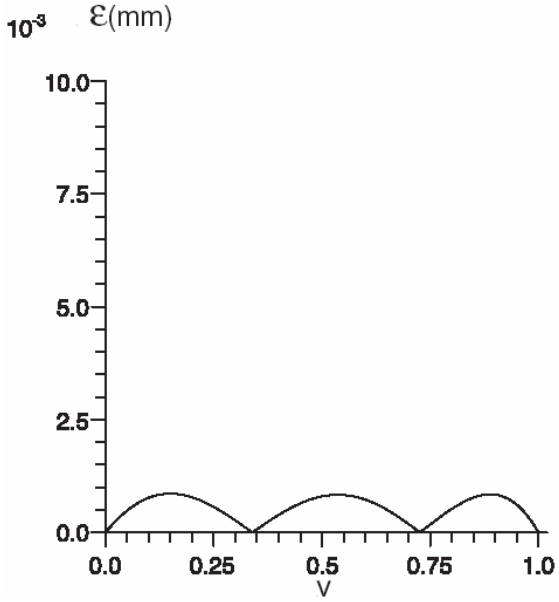

(b)

Figure 5-4 Deviation along the grazing curve for $|V_T| \neq |V_B|$

(a). Curve error for $h_1 = h/3$ and $h_2 = 2*h/3$. (b). Curve error as P_1 and P_2 are optimized by moving them along the cutting tool axis direction.

5.1.4 Modeling of the Grazing Surface

After the grazing curve is defined, the grazing surface can be approximated using the method described in the section 4.2. The machined surface is generated by moving a grazing curve along two guiding curves as shown in Fig. 5-5.

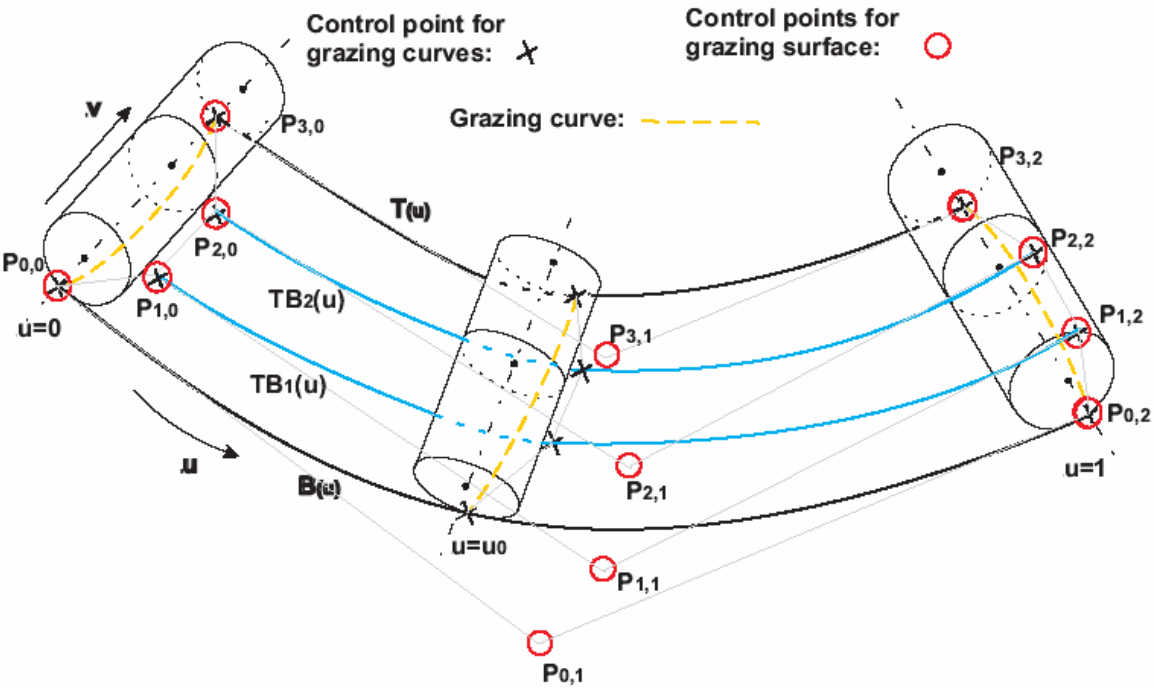

Figure 5-5 Control points for grazing surface

$T(u)$ and $B(u)$ are two NUBS guiding curves. They lie on the machined (or the grazing) surface. The character of these guiding curves influences the property of the grazing surface. Thus, the degree and the knot vector of the guiding curves can initially be used in the design of the approximate NUBS surface in the parameter u direction (or the guiding curve direction). Of course, the degree and the knot vector of guiding curves must be the same. If they are different from each other, knot insertion [25, 26] can be used to make them equal. To demonstrate the proposed surface design method, each of grazing curves is composed of

three control points and has a degree of two. Consequently the number of control points and the degree of the approximate NUBS surface along the u direction (the guiding curve direction) can initially be assumed to be three and two, respectively.

At each tool position, the grazing curve can be approximated by a cubic NUBS curve with four control points. Thus the number of control points and the degree of the approximate surface along the v direction (the tool axis direction) can be primarily set to four and three, respectively.

A three by four approximate NUBS surface can be constructed. This surface is defined [25, 26] as

$$S(u,v) = \sum_{i=0}^{3}\sum_{j=0}^{2} N_{i,2}(v)N_{j,2}(u)P_{i,j}$$

$$= (1-v)^3 B(u) + 3v(1-v)^2 TB_1(u) + 3v^2(1-v)TB_2(u) + v^3 T(u), \qquad (5.5)$$

where

$$T(u) = (1-u)^2 P_{3,0} + 2u(1-u)P_{3,1} + u^2 P_{3,2}, \qquad (5.6)$$

$$TB_2(u) = (1-u)^2 P_{2,0} + 2u(1-u)P_{2,1} + u^2 P_{2,2}, \qquad (5.7)$$

$$TB_1(u) = (1-u)^2 P_{1,0} + 2u(1-u)P_{1,1} + u^2 P_{1,2}, \qquad (5.8)$$

$$B(u) = (1-u)^2 P_{0,0} + 2u(1-u)P_{0,1} + u^2 P_{0,2}, \qquad (5.9)$$

$P_{i,j}s$ are the control points and $TB_2(u)$, $TB_1(u)$ are two interior curves.

The control points of $T(u)$ and $B(u)$ are known. The control points of $TB_1(u)$ and $TB_2(u)$ need to be determined below.

At $u = 0$, equation (5.5) simplifies to the grazing curve at the first tool position. Since the grazing curve at this point has been calculated, using the method given in section 5.1.3, $P_{1,0}$ and $P_{2,0}$ can be obtained.

Similarly, $P_{1,2}$ and $P_{2,2}$ can be calculated at the tool position $u = 1$ and $TB_1(u_0)$ and $TB_2(u_0)$ can be determined at the tool position $u = u_0$. u_0 is selected using the chord length method or the centripetal method (see Appendix A) that reflect the distribution of control points of each guiding curve. Consequently, $P_{1,1}$ and $P_{2,1}$ can also be obtained using equations (5.7) and (5.8).

After all the control points and their weights are decided, the approximate NUBS surface can be built using equation (5.5). The deviation between the approximate NUBS surface and the grazing surface can be measured and if the maximum surface error exceeds a user defined tolerance, more control points can be added to the u or/and the v directions using knot insertion [25, 26]. Under this situation, the surface need be redesigned and the same procedure can be applied. The degree of the surface is unchanged. With an increase in the number of control points, the approximate surface error can be effectively controlled.

If more control points are used to generate the guiding curves, more interior control points are required. The interior points are determined by calculating $TB_1(u)$ and $TB_2(u)$ at

$u = u_1, u_2, \cdots$, etc. in a manner demonstrated above. The method to determine these control points is the same as the method given in Chapter 4.

5.2 Examples

The above method was implemented and tested by using it to design the surface for flank milling. The same example given in the section 3.3 was used. The control points of the guiding curves are given in Table 3-1. The degree of both the grazing curve and the guiding curve is 2. The knot vector for the two curves is $[0,0,0,1,1,1]$. A cylindrical cutter with radius $R = 5$ is used to machine the surface and Bedi et al.'s tool positioning method is applied to determine the tool path.

Since the number of control points along the guiding curve direction is three and the knot vector is $[0,0,0,1,1,1]$, the number of control points of the design surface along the guiding curve direction is initially set to three and the knot vector is the same as the knot vector of the guiding curve. For the number of control points along the tool axis direction, four non-weighted control points are primarily used. The knot vector is selected as $[0,0,0,0,1\,1,1,1]$ in this direction.

5.2.1 Three by Four Approximating NUBS Surface

Given the above data, a 3 by 4 NUBS surface can be constructed. The method given in section 5.1.4 is used to build a NUBS surface that can closely match the grazing surface. As Fig. 5-5 shows, the control points of guiding curves are directly assigned to the corresponding control points of the design surface; the interior control points, $P_{1,0}$, $P_{2,0}$, $P_{1,1}$,

$P_{2,1}$, $P_{1,2}$, $P_{2,2}$ are determined using the method described in section 5.1.4. $P_{1,0}$ and $P_{2,0}$ are decided at $u = 0$ and $P_{1,1}$ and $P_{2,1}$ are calculated at $u = 1$. Similarly, $P_{1,2}$ and $P_{2,2}$ can be determined at another tool position $u = u_0$. In this example, $u_0 = 0.5$. Using the proposed method, $TB_1(u_0)$ and $TB_2(u_0)$ are obtained first, then $P_{1,2}$ and $P_{2,2}$ are solved using equations (5.7) and (5.8).

After the control points are computed, the approximate NUBS surface can be constructed. The difference between the approximate NUBS surface and the grazing surface is calculated and the result is plotted in Fig. 5-6.

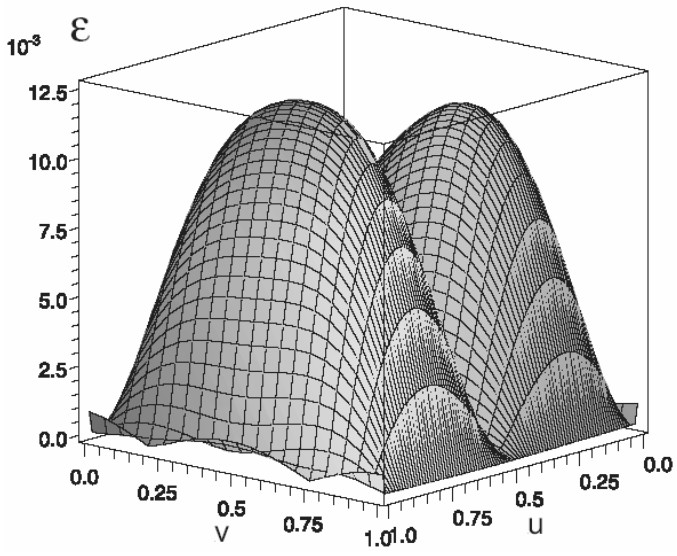

Figure 5-6 Deviation of the 3 by 4 approximating surface

From Fig. 5-6, it can be seen that the deviation for the 3 by 4 approximating surface is in the range [0, 0.0125]. The maximum surface error is less than 0.0125.

The same example was also applied using the method presented in Chapter 4 and results are plotted in section 4.4. Compared to the Fig. 4-13 (a 3 by 3 approximating NURBS surface), the maximum error is around 0.022 which is bigger than the maximum error from the NUBS method, 0.0125. Referred to the Fig. 4-18, the same 3 by 4 approximating NURBS surface (four control points along the tool axis direction), its maximum surface error is around 0.0152 which is close to the result from the NUBS method, but the computation process is more complex than the NUBS method. Mathematically, the maximum surface error for 3 by 4 approximating surface from the Chapter 4 should be smaller than the maximum surface error from the proposed method because an exact arc representation is used in Chapter 4. However, optimization of interior control points over the entire design surface and the average weight employment reduce the accuracy of each approximating NURBS curve at the specified tool positions and result in an increase in the maximum surface error.

As is discussed in section 5.1.1, the weight of each interior control point in the three point circular arc method presented in Chapter 4 can be forced to equal 1 to simplify the computation procedure. If this is done for this example, a 3 by 3 surface (with unit weight) can be constructed and the resulting error is plotted in Fig. 5-7.

From this figure, it can be seen that the maximum surface error is around 0.0223. This is not as good as the three by four unit weight surface generated with the proposed method, but maybe useful in some engineering applications.

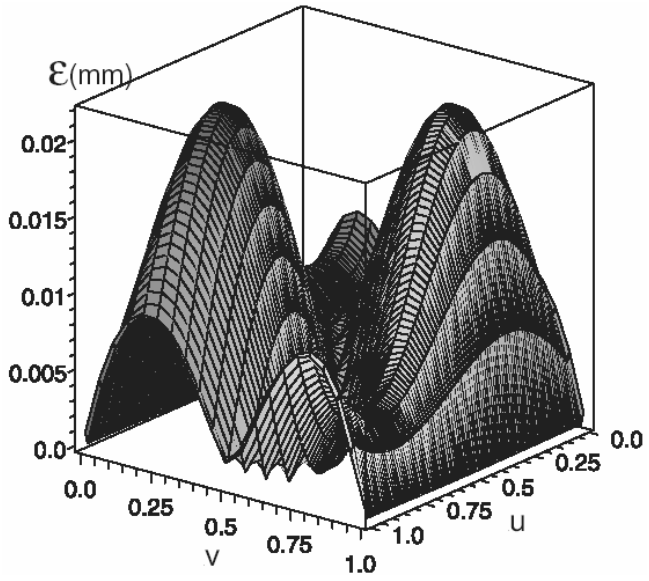

Figure 5-7 Deviation of the 3 by 3 approximating surface ($w = 1$)

5.2.2 Approximate NUBS Surface with More Control Points

If the maximum surface error 0.0125 in Fig. 5-6, obtained from a 3 by 4 approximate NUBS surface, does not fulfill the user's requirement, more control points can be used in the u and/or the v directions to reduce the maximum surface error. The degree in both of u and v directions can be kept the same or be changed to further decrease the designed surface error. For the same example given in the last section, three surfaces, a 4 by 4 NUBS surface, a 5 by 4 NUBS surface and a 6 by 4 NUBS surface, are designed to demonstrate the trend of the maximum surface error.

For the 4 by 4 NUBS surface, the number of control points of the guiding curves is increased from 3 to 4 using the knot insertion technique and the degree of the guiding curves is kept as 2. The knot vector of the guiding curves changes to $[0,0,0,0.5,1,1,1]$. The knot vector and the number of control points along the tool axis direction do not change. Using the

proposed method given above, a 4 by 4 NUBS surface can be constructed. The surface error is measured and listed in Table 5-3.

Similarly, the 5 by 4 and the 6 by 4 NUBS surfaces can also be designed. The knot vector and the number of control points along the tool axis direction are kept the same for both of them and the numbers of control points along the guiding curve direction are changed to 5 for 5 by 4 surface and 6 for 6 by 4 surface. The knot vector in this direction is changed to [0,0,0,0.33,0.67,1,1,1] and [0,0,0,0.25,0.5,0.75,1,1,1]. The degrees in both the guiding curve direction and tool axis direction are not changed, i.e. 2 and 3, for both surfaces. The designed surface errors are also measured and are tabulated in Table 5-3.

C.Ps($u \times v$)	3×4	4×4	5×4	6×4
ε_{max}	0.0125	0.0175	0.005	0.00215

Table 5-3 Errors for different NURBS surface. C.Ps: Control Points.

From Table 5-3, it can be seen that the maximum surface error of the 4 by 4 surface is around 0.0175, close to, but a little bit bigger than, the maximum surface error of the 3 by 4 surface. Although both the surfaces are generated from the same guiding curves (the knot vector in the tool axis direction for the two surfaces is the same; the knot vector in the guiding curve direction for the two surfaces is different), the different knot vectors along the guiding curve direction make both the generated surfaces be different in the areas between the guiding curves. If more control points are used, the maximum surface error is expected to reduce. As Table 5-3 shows, the maximum surface error for the 5 by 4 surface is around

0.005 and for the 6 by 4 surface is around 0.00215, which are smaller than the maximum surface error from 3 by 4 and 4 by 4 approximating surfaces. Thus, with the increase in the number of control points, the designed surface error can be effectively controlled.

5.3 Discussion

Surface design for flank milling is a novel topic in today's manufacture engineering. Using it, an engineer can generate surfaces that exactly match the machined surface and the machining process is also simplified. In designing this type of surface, an error plot is a useful tool that can help designers to inspect the surface error during design. Sometimes, adding one or two control points does not significantly improve the surface; more control points may need be added to develop the quality of the design surface as shown in the last example.

For NURBS guiding curves, the proposed method can still be used to determine the interior unit weight control points and the surface. However, more control points need be added in the u or/and the v directions to control the surface error. Alternatively, the NURBS guiding curves can first be changed to NUBS guiding curves (also requiring more control points) and then the equations given above can be used to design the approximate NUBS surface.

For the grazing curve approximation, both the three weighted control point method and the four non-weighted control point method can give a good NURBS representation. It is up to designer to decide which method is best for their application. But from the perspective of designing the complete surface, the non-weighted control point method will give the designer

an easier way to handle the surface design, especially when the guiding curves are NUBS curves.

All the methods presented in the Chapters 4 and 5 used the cylindrical tools. The advantage of the proposed flank millable surface design methods still need to be extended to conical tools, barrel tools and other tools of revolution to generalize these application. Thus, in the following chapter, these extensions are probed and developed.

Chapter 6
Flank Millable Surface Design with Tools of Revolution

In Chapters 4 and 5, the flank millable surface is generated by lofting the grazing curves along the guiding curves. Each grazing curve lies on the cylindrical tool surface and is represented by a NURBS (or NUBS) curve. This NURBS or NUBS curve is produced by stretching a 2D arc, which is the projection of the grazing curve on the plane perpendicular to the cylindrical tool axis. The 2D arc can be exactly represented by a 2D NURBS curve or closely approximated by a 2D NUBS curve. To extend the method developed in previous chapters to design a larger variety of curved surfaces, it is essential to extend the method to other tool shapes such as conical tools and barrel tools. For tools, like conical shape or barrel shape, the projection of each grazing curve on the plane perpendicular to the tool axis is not a 2D arc; it is a freeform 2D curve. Thus, it can not be simply represented by a three-weighted-control point B-Spline curve or a four-control point polynomial curve. To generalize the methods developed in Chapters 4 and 5 to these shaped tools, the key is to find a NURBS or NUBS representation of the grazing curve on the tool surface (or close to the tool surface), and then to build the flank millable surface with the lofting technique.

In an earlier paper [30], a method using a polynomial composition to design the flank millable surface with any tool of revolution was developed. In this method, each grazing curve is represented with a high degree Bézier curve or B-spline curve, which is based on the theorem developed by DeRose et al. [29], and is used to generate the flank millable surface.

Each generating curve exactly lies on the surface of the cutting tool and the resulting surface is a high degree polynomial. In general, the high degree will make the generated surface complex and not practical, especially in engineering applications.

Since each grazing curve exactly lies on the cutting tool surface, it is possible to accurately define the grazing curve itself. In actual application, the exact definition of the grazing curve is unnecessary. Approximating the grazing curve to within a certain tolerance will satisfy most engineering requirements. Retaining this requirement results in an easy to use surface design method. In this chapter, an approximation method to define grazing curves on the tool of revolution, and subsequently to generate the flank millable surface is presented.

6.1 Flank Millable Surface Design with Conical tools

In the Chapters 4 and 5, the grazing curve at each tool position is approximated by a NURBS curve. Looking at the curve generation procedure, it is seen that the track of the movement of each interior control point is a straight line, and this line is parallel to the cylindrical tool axis. In fact, this line is an aggregate of the central control point of the 2D arc on the different planes that are perpendicular to the cylindrical tool axis, as shown in Fig. 6-1.

A three control point Bézier curve (dash lines in this figure) is used to approximate the given grazing curve. T_1 is the top contact point between the cylindrical tool and the guiding curve $T(u)$, and B_2 is the bottom contact point between the cylindrical tool and the guiding curve $B(u)$. We need to find the interior control point P, which is done as follows.

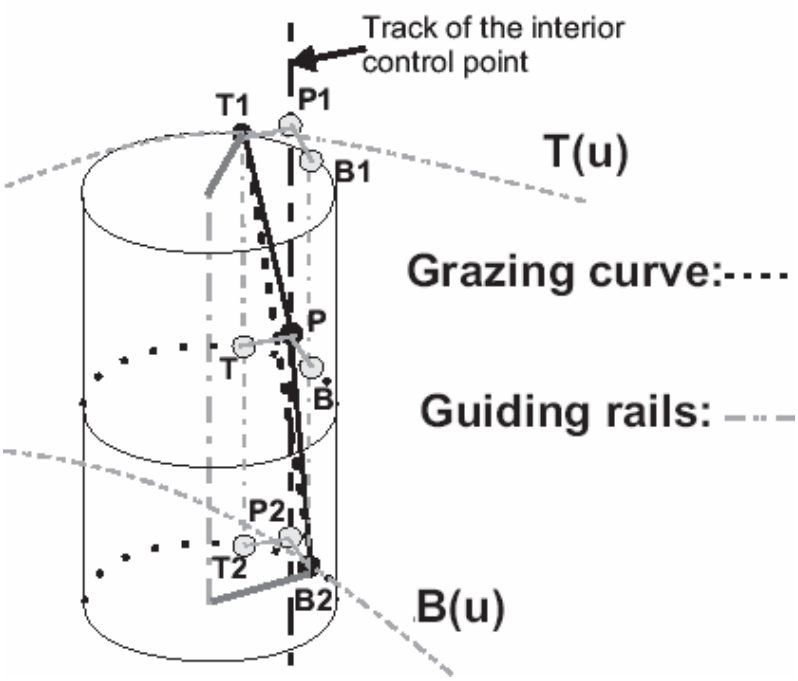

Figure 6-1A grazing curve and its control points on a cylindrical tool

The grazing curve is projected to the top plane and is a 2D arc $\overset{\frown}{T_1B_1}$. This arc can be defined with a three weighted control point Bézier curve. The middle control point of this 2D arc is P_1. The grazing curve can also be projected to the bottom plane to form another 2D arc $\overset{\frown}{T_2B_2}$. Consequently, the other Bézier curve can be constructed and the middle control point of this arc is P_2. Similarly, the grazing curve can be projected to any plane that is perpendicular to the cylindrical tool axis between the top and the bottom plane to form a different 2D arc, say $\overset{\frown}{TB}$. The middle control point of the Bézier curve $\overset{\frown}{TB}$ is P. As we move the plane of the projection, the point P is always on the line segment $\overline{P_1P_2}$. When the point P is moved along the segment $\overline{P_1P_2}$, the optimized Bézier curve with the smallest error

between the given grazing curve and the approximated Bézier curve (the dash line) can be decided. Accordingly, the middle control point of the Bézier curve, P, is placed at certain position on the segment $\overline{P_1P_2}$.

From this point, we can say that, for cylindrical cutting tools, the movement of the interior control point of the 3D Bézier curve is always along the locus of the interior control points of the 2D Bézier curves. The locus is a line segment, $\overline{P_1P_2}$ in Fig. 6-1, that is parallel to the cylindrical tool axis. If more interior control points are used, different tracks of each interior control point can be found, and they are lines and parallel to the tool axis. By moving each interior control point along its own track, a 3D Bézier curve can be defined and one with the smallest approximate error selected for use in surface design.

For a conical tool, a similar concept can be used to find the NURBS representation of each grazing curve.

6.1.1 Approximating a Grazing Curve

When a conical tool is used, the grazing curve at each tool position lies on the conical tool surface (Fig. 6-2(a)) and it is possible to represent it with a NURBS curve. If the grazing curve is projected along the conical tool axis direction into a plane perpendicular to the tool axis, a 2D curve results (Fig. 6-2(b)), but it is not a circular arc as it was for cylindrical tools. Thus, the techniques developed in Chapters 4 and 5 can not be used to find the NURBS representation of the 2D arc and consequently to find the NURBS representation of the grazing curve.

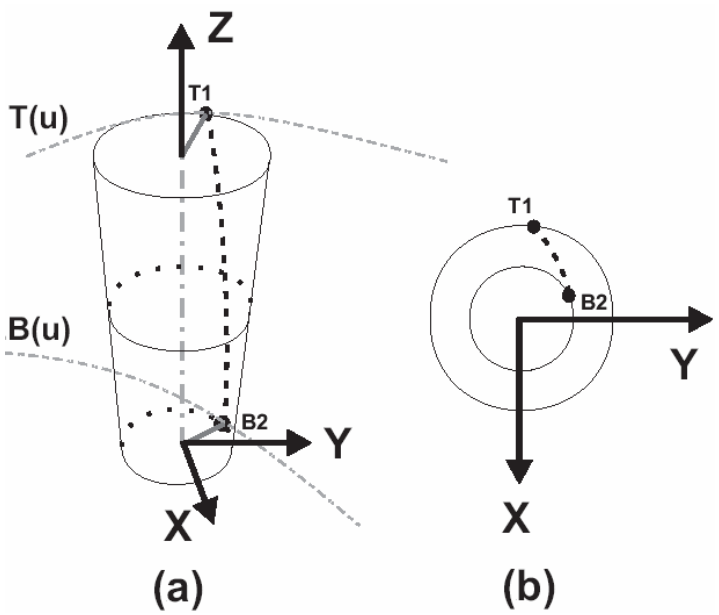

Figure 6-2 A conical tool with the grazing curve

The reason behind using the 2D NURBS representation of the grazing curve is that it is easy to define the 3D NURBS representation of the grazing curve with it. We now present a method to find the 3D NURBS representation of the grazing curve directly based on the properties of the conical tool. Since a three control point Bézier curve is generally used to model the grazing curve for the cylindrical tools, initially a quadratic Bézier curve will be used to represent the grazing curve on the conical tool surface. More control points can be added based on the subsequent surface error analysis.

For cylindrical tools, the NURBS grazing curve can be defined by stretching the three 2D control points along the tool axis direction as described in section 4.1.1. Only one interior control point is defined by moving it along a straight line (see Fig. 6-1). If a quadratic Bézier curve is used to define the grazing curve on a conical tool surface, then based on the characteristic of a NURBS, these the top and the bottom contact points, T_1 and B_2 (see Fig.

6-2(a)), can be used as two boundary control points and only one interior control point is left undecided.

To determine the interior control point, the characteristics of the conical tool are considered. As the generatrix of the cone (the curve that is revolve around the cone axis to construct the surface of the cone) is not parallel to the cone axis, we can project each point of the grazing curve on the cone surface along its generatrix direction to a plane that is perpendicular to the conical tool axis. A circular arc is obtained on this plane. Projection onto different intersection planes between the top and the bottom planes of the cone can result in different circular arcs. Each 2D arc can be represented by a quadratic rational Bézier curve, as Fig. 6-3 shows.

The projection of the grazing curve (the dash line) on the top plane is $\overset{\frown}{T_1B_1}$. It is an arc and can be defined with a three control point Bézier curve. The middle control point is P_1. The projection of the grazing curve in the generatrix direction on the bottom plane is $\overset{\frown}{T_2B_2}$ and the middle control point of its quadratic Bézier representation is P_2. The projection of the grazing curve on the any plane perpendicular to the conical tool axis between the top and the bottom planes is $\overset{\frown}{T_xB_x}$. The middle control point of its Bézier representation is P_x. P_x is on the segment $\overline{P_1P_2}$.

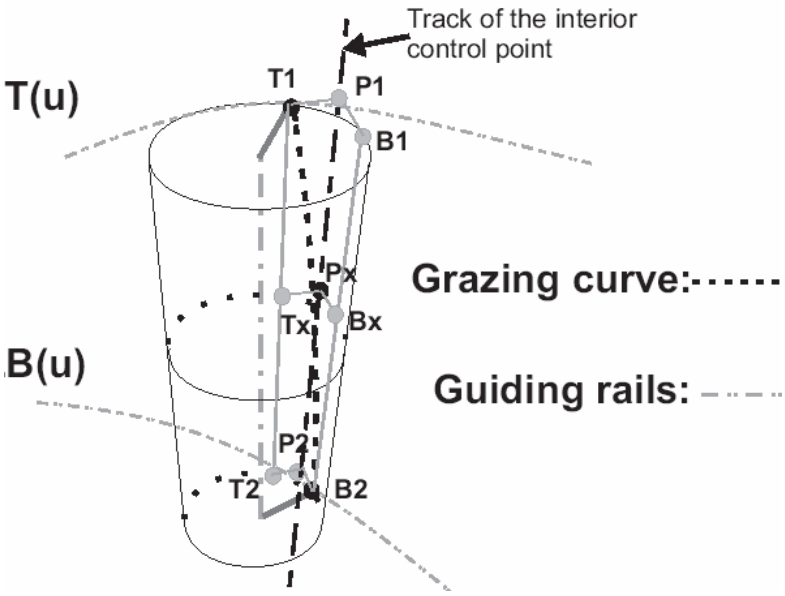

Figure 6-3 The projection of the grazing curve and its control points

Based on this solution, the interior control point of the Bézier representation of the grazing curve should lie on the line P_1P_2. As for cylindrical tools, $\overline{P_1P_2}$ is a track of the interior control point. By moving this point along the line $\overline{P_1P_2}$, an acceptable NURBS curve that approximates the grazing curve can be generated (as Fig. 6-4 shows). As the angles of the 2D grazing arcs ($\overset{\frown}{T_xB_x}$) on different planes (perpendicular to the cone axis) are the same, the weight of the interior control point is fixed and equals the cosine of the half of this angle.

In actual application, the interior control point can first be set to the middle of the segment $\overline{P_1P_2}$, then the best position of the interior control point can be defined by moving it along $\overline{P_1P_2}$ and minimizing the deviation between the given grazing curve and its NURBS approximation.

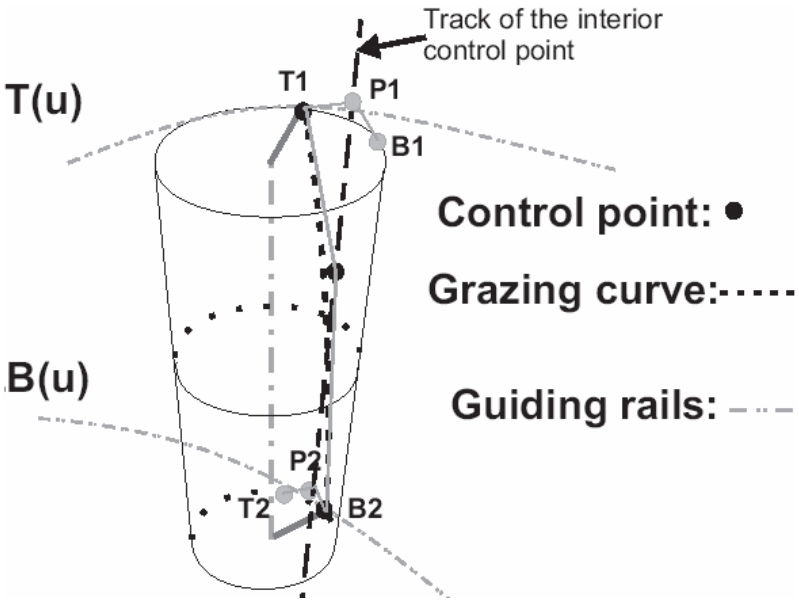

Figure 6-4 The grazing curve on the cone surface and its control points

This method is a generalization of the method used for cylindrical tools in Chapters 4 and 5.

An example is given to test the proposed method. The interior control point is initially set to the middle of $\overline{P_1P_2}$ and the parameters of the conical cutter and the control points are

$$B_2[R_b\cos(\pi/6), R_b\sin(\pi/6), 0],\quad T_1[R_t\cos(\pi/3), R_t\sin(\pi/3), h]$$

$$V_b[-R_b\sin(\pi/6), R_b\cos(\pi/6), 0],\ V_t[-R_t\sin(\pi/3), R_t\cos(\pi/3), 0]$$

$$w_t = 1,\ w_x = \cos(\pi/12),\ w_b = 1,\ R_t = 6,\ R_b = 4,\ h = 45,$$

where R_t and R_b are the top and bottom radius of the cone; w_t, w_x and w_b are the weights of the control points B_2, P_x and T_1; h is the effective contact length along the axis of the

conical cutter; V_b and V_t are velocities at points B_2 and T_1, the directions are along line directions of each circle and their magnitudes are velocities.

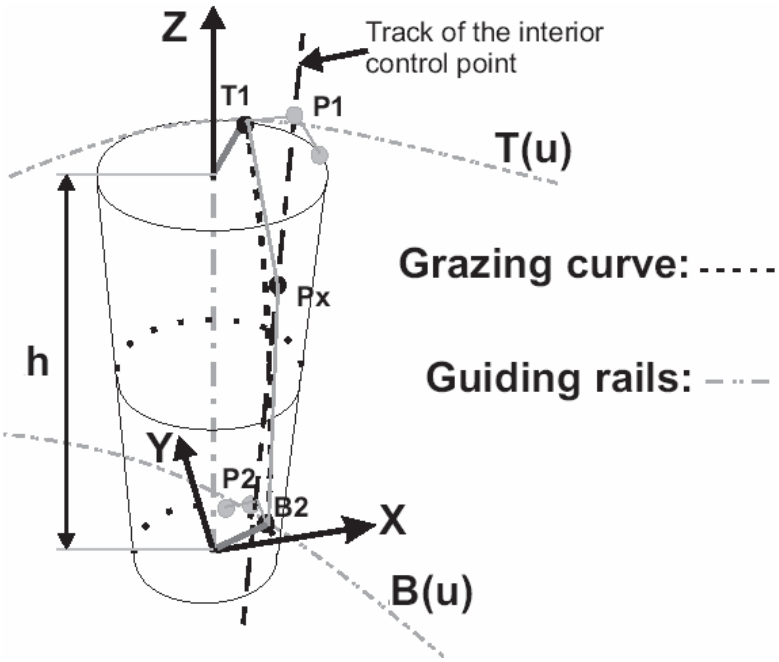

Figure 6-5 The grazing curve and its control points

Bedi et al.'s tool positioning method is used to position this conical tool. The grazing curve can be calculated by equations (2.6) and (2.7). The projection of this grazing curve on the top plane of the cone is a 2D arc. The middle control point of the arc is P_1 and decided by the intersection of two tangent lines at the end of the arc on the top plane. The projection of the grazing curve on the bottom plane of the cone is another 2D arc. The middle control point of the arc is P_2 and can be decided using the same method. The segment $\overline{P_1P_2}$ can be built. The interior control point of the grazing curve, P_x, is on this line and initially set to the middle of $\overline{P_1P_2}$.

After the three control points, B_2, P_x, T_1, and their weights are defined, a quadratic rational Bézier curve can be obtained. The deviation between the given grazing curve and the approximate Bézier curve is calculated and is shown in Fig. 6-6. The errors at T_1 and B_2 are zeros. The shape of the error curve is not symmetric. The maximum error is around $v = 0.6$ and is smaller than 0.135.

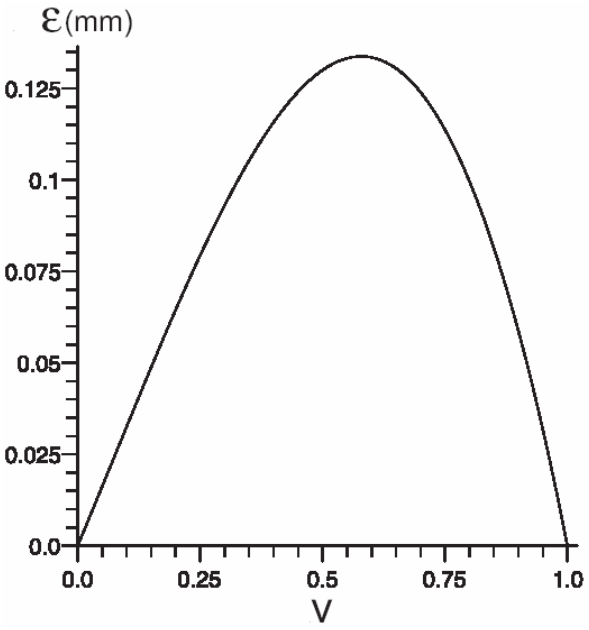

Figure 6-6 Deviation along the grazing curve (P_x in the middle)

To reduce the maximum error, the interior control point P_x should be moved along the segment $\overline{P_1P_2}$. The value of P_x that results in the smallest curve error is used to define the grazing curve. The smallest curve error is found and the distribution of the error along the grazing curve is plotted in the Fig. 6-7. Compared to Fig. 6-6, the maximum curve error is reduced and is around 0.038.

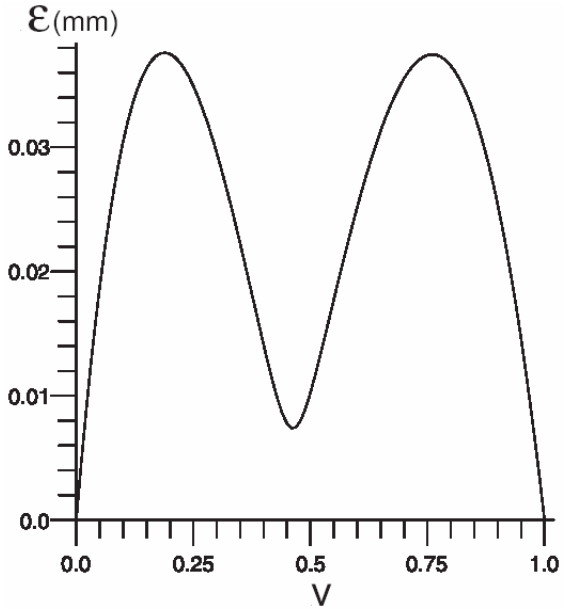

Figure 6-7 Deviation along the grazing curve (P_x is not in the middle)

If the maximum error shown in Fig. 6-7 is still beyond the requirements defined by the user, more control points can be used to approximate the grazing curve. Knot insertion or degree elevation [25, 26] can be used to add the interior control points. (From the perspective of designing the complete surface, knot insertion is recommended.) With an increase in the number of control points, the maximum curve error can be effectively controlled.

If more control points are used to define a NURBS curve to approximate the given grazing curve, the method to decide each control point is the same as before. As Fig. 6-8 shows, a four control point rational quadratic B-spline curve is used to approximate the grazing curve. The projection of the grazing curve on the top plane of cone is an arc and is represented by a three control point rational quadratic Bézier curve (see Fig. 6-3). A four control point rational quadratic B-spline curve can be found to define this arc through knot insertion. (More control

points can be inserted if needed.) The four control points, namely T_1, P_1, P_3 and B_1, with their weights can be decided. Similarly, the control points of the projection of the grazing curve on the bottom plane of the cone (T_2, P_2, P_4 and B_2) can also be defined.

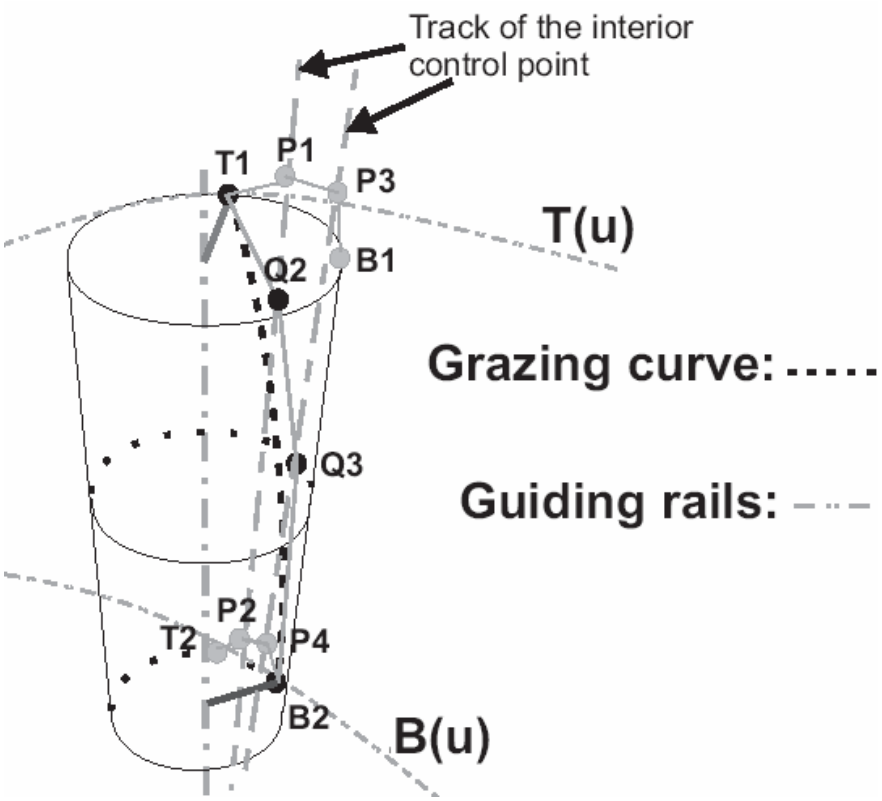

Figure 6-8 A grazing curve with its four control points

$\overline{P_1P_2}$ and $\overline{P_3P_4}$ define two tracks for the interior control points, Q_2 and Q_3. T_1 and B_2 are two contact points and are used directly as boundary control points of the approximate B-spline. Q_2 and Q_3 can initially be set to $|P_4Q_3| = |P_3P_4|/3$ and $|P_2Q_2| = 2|P_2P_1|/3$, then by moving them along the tracks $\overline{P_1P_2}$ and $\overline{P_3P_4}$ to decide their positions and assessing the maximum deviation. Their positions are decided based on minimizing the deviation.

After the four control points are decided, the B-spline curve can be constructed.

So far, a NURBS curve has been used to approximate the grazing curve. A polynomial curve can also be used to approximate the grazing curve. As discussed in Chapter 5, a four control point cubic Bézier curve can be used to represent a 2D arc [28]. Thus, instead of the rational B-spline curves in Fig. 6-8, a cubic polynomial curve is used to define the projection of the grazing curve on the top and the bottom planes of the cone. As a result, the generated approximating curve is a polynomial curve or a NUBS curve. As before, more control points can be added (using the knot insertion) to increase the accuracy of the NUBS approximating curve.

For the advantages of using a NUBS approximating curve, please refer to Chapter 5.

6.1.2 Approximating a Grazing Surface

After a few grazing curves are defined, a NURBS surface can be constructed. This NURBS surface is used to approximate the given grazing surface. The details to generate the NURBS surface (or the flank millable surface) are described in sections 5.1.1 and 4.2.

6.1.3 Examples

An example is given in this section to demonstrate the proposed flank millable surface design method with conical tools. The same control points presented in section 3.3 are used. The design starts with two guiding curves. The degrees for the two guiding curves are two. The control points for these guiding curves are listed in Table 3-1. The knot vector for both of them is [0,0,0,1,1,1].

The geometry of the conical tool is given in Fig. 6-9(a), with $R_t = 7$, $R_b = 4$ and $h = 50$. Bedi et al.'s tool positioning method [9, 11] is used to position the conical tool and generate the tool path. The machined surface is expressed by the grazing surface and is calculated using equations (2.5), (2.6) and (2.7). The proposed method given in section 6.1.2 is used to build the flank millable surface. Each grazing curve is defined with a rational Bézier curve. The control points of the guiding curves are directly adopted by the designed surface. Three tool positions, $u = 0$, $u = 0.48$ and $u = 1$, are used to find the interior control points and their weights of the flank millable surface (see Fig. 4-6). A bi-quadratic rational Bézier surface that can be flank milled is constructed. The deviation between the grazing surface and the flank millable surface is computed and the result is plotted in Fig. 6-10 below.

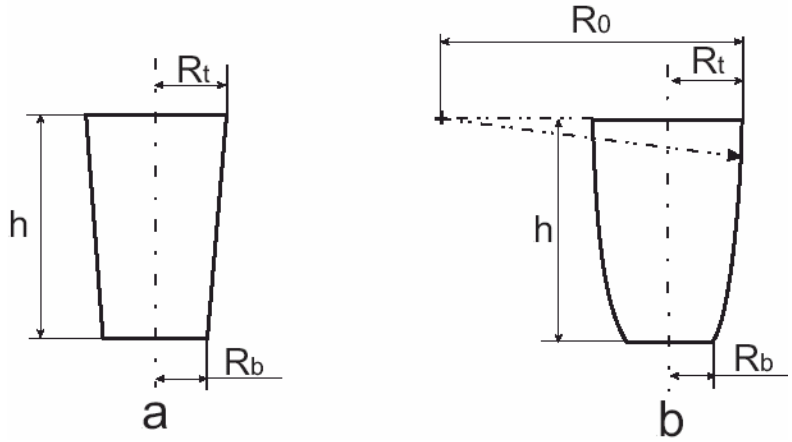

Figure 6-9. a). a conical tool. b). a barrel tool.

From this figure, it can be seen the surface error for the three by three approximate surface is in the range [0, 0.048]. The maximum error is around 0.048. If this error exceeds the user defined tolerance, more control points can be added in u or v or both of u and v directions to control the surface error.

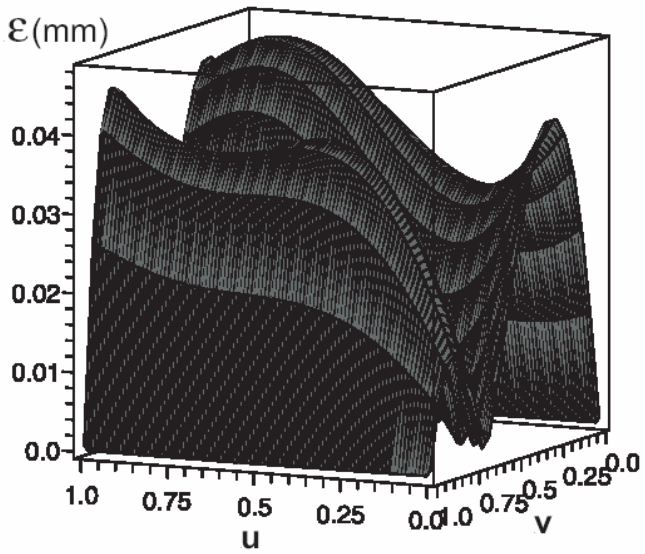

Figure 6-10 Deviation of the 3 by 3 NURBS approximate surface

To display the process of the surface error control, the number of control points is increased from three by three to various values up to four by five and the corresponding NURBS surfaces are created. The maximum surface errors are checked and are tabulated in Table 6-1.

From the table, it can be seen that the surface error is reduced when the number of control points are increased. The reduction of the error from three by three to three by four and then to three by five is small. However, the reduction from three by three to four by three, three by four to four by four and three by five to four by five is significantly. Even the changing from four by three to four by four and then to four by five is notably. This phenomenon illustrates that both of u and v parametric directions need to be considered when the control points are added to the control net of the surface. Sometimes, only changing control points in one

parametric direction can not significantly reduce the maximum surface error. However, this table also confirms that with increasing in the number of control points, the surface error can be effectively controlled.

C.Ps($v \times u$)	K.Vs ($v \times u$)	ε_{max}
3×3	[0,0,0,1,1,1] × [0,0,0,1,1,1]	0.048
3×4	[0,0,0,1,1,1] × [0,0,0,0.5,1,1,1]	0.046
3×5	[0,0,0,1,1,1] ×[0,0,0,0.33,0.67,1,1,1]	0.044
4×3	[0,0,0,0.5,1,1,1] ×[0,0,0,1,1,1]	0.0185
4×4	[0,0,0,0.5,1,1,1] × [0,0,0,0.5,1,1,1]	0.0155
4×5	[0,0,0,0.5,1,1,1] × [0,0,0,0.33,0.67,1,1,1]	0.011

Table 6-1 Errors for different NURBS surface. C.Ps: Control Points. N.Vs: Knot Vectors.

In the sections 6.1.1 and 6.1.2, the NUBS curve and surface were developed. They are used to generate a flank millable surface with the same example given above. Since the given guiding curves are NUBS curves, the NUBS approximate surface can be designed easily.

In the NUBS approximation, each grazing curve is approximated with a NUBS curve. In this case study, a cubic polynomial curve is used to define each grazing curve (see Fig. 5-5). Three cubic polynomial curves at three tool positions, $u = 0$, $u = 0.48$ and $u = 1$, are used to decide the six interior control points. The control points of the two guiding curves are directly used by the designed surface as the boundary control points. A four by three cubic-quadratic NUBS surface can be constructed. The error between the designed flank millable surface and the grazing surface is checked and is plotted in Fig. 6-11.

The surface error of this four by three polynomial surface is in the range [0, 0.0125]. The maximum surface error is smaller than 0.0125. Compared to the NURBS surface with the same numbers of control points shown in Table 6-1, the maximum surface error is similar but smaller. The reason for this phenomenon is discussed in Chapter 5.

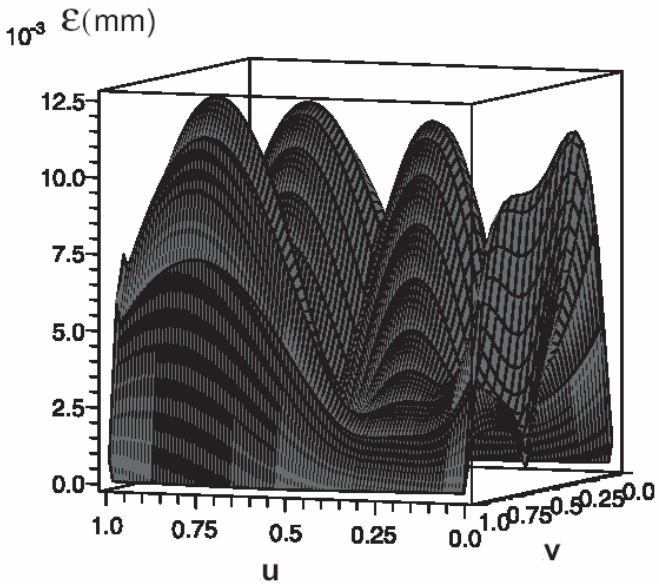

Figure 6-11 Deviation of the 4 by 3 NUBS approximate surface

If the maximum surface error does not satisfy the user defined tolerance, more control points can be added to the u direction or the v direction or both u and v directions to reduce the surface error. In this example, the control points in the v direction are the same, i.e., four. The control points in the u direction are increased to four and then to five. The knot vector in this direction is also changed to $[0,0,0,0.5,1,1,1]$ and $[0,0,0,0.33,0.67,1,1,1]$. Two

cubic-quadratic NUBS surfaces, a four by four surface and a four by five surface, are designed. The surface errors are checked and are listed in Table 6-2.

C.Ps($v \times u$)	ε_{max}
4×3	0.0125
4×4	0.0115
4×5	0.008

Table 6-2 Errors for different NUBS surface. C.Ps: Control Points.

From this table, it can be seen that the maximum surface error is reduced when the number of control points are increased. With increase in the number of control points, the error of the designed flank millable NUBS surface can be effectively controlled.

All examples given in this section focus on the conical tool and the proposed method is used to design the flank millable surface. From these examples, it can be seen that the designed flank millable surface can closely match the grazing surface. We also compare these surfaces to the surface obtained in [30] for the same conical tool and the same guiding curves. It can be seen that the proposed method can easily be used and resulted flank millable surface can be machined to a high degree of accuracy. For example, Table 6-2 shows the error of the four by three polynomial surface. The degree of this surface is three by two and the maximum surface error is 0.0125. For the similar flank millable polynomial surface given in [30], the control points are nine by three and the degrees are eight by two. The maximum surface error is 0.0244. The proposed method gives a better result.

6.2 Flank Millable Surface Design with Tools of Revolution

In the previous section, a method to design a flank millable surface with a conical tool was developed. This method still needs to be generalized to tools defined by surfaces of revolution. The key for the generalization is to model the grazing curve on the tool surface of revolution. If each grazing curve on the tool can be expressed as a NURBS curve, the flank millable surface can be built using the techniques developed in Chapter 4 and section 6.1.

6.2.1 Modeling of the Grazing Curve

In the conical tool, when the grazing curve on the surface of tool is projected along the generatrix to planes perpendicular to the tool axis, 2D arcs are obtained. The interior control points of 2D arcs are composed of a line that is the track of the middle control point of the grazing curve (Fig. 6-3). The ends of grazing curve and the middle control points can be used to define the approximate NURBS curve.

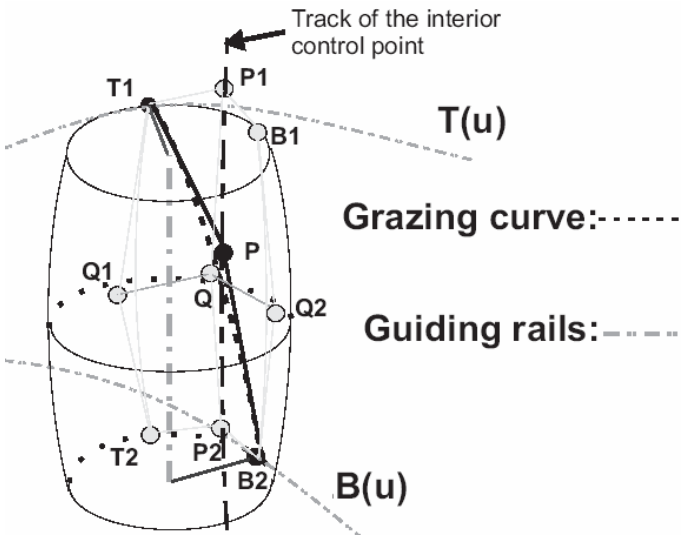

Figure 6-12 Grazing curve and its control points on a tool of revolution

For a tool with a generalized NURBS profile of revolution, the same technique can be applied to find the interior control points of the grazing curve. Based on the character of the tools of revolution, this technique is generalized and is shown in Fig. 6-12. (A non-NURBS profile can be approximated to a high tolerance with a NURBS profile.)

The goal of this method is first to use a quadratic NURBS segment to approximate the grazing curve, then more control points can be added based on the curve error analysis. T_1 and B_2 are two contact points between the cutting tool and the given guiding curves. There are used directly as control points of the quadratic NURBS segment. Only the interior control point P and its weight need to be decided.

To find the interior control point and its weight, a patch is built for a region of interest on tool based on contact points. The control points of the patch are decided by the control points of the profiles, the control points of the top, the middle and the bottom circular arcs. The interior control point of the approximate grazing curve is on curve given by a column of patch control points. Moving the interior control point along this curve, a best fitting quadratic Bézier curve can be defined. The details to find the interior control point and its weight are given below.

The contact points, T_1 and B_2, are located on the surface of the tool. The curves from T_1 to T_2 and from B_1 to B_2 are two profiles of the cutting tool passing through the contact points. These curves can be represented with NURBS curves. The control points of these profiles come from the rotation around tool axis of the NURBS representation of the profile curve. In this study, three control points (T_1, Q_1, T_2 and B_1, Q_2, B_2) are used for each of the profiles.

Of course, more control points can be used for each of the profiles if they are needed. The grazing curve, passing through T_1 and B_2, lies on the patch $T_1T_2B_2B_1$. This patch is also a part of the surface of the cutting tool. This patch can be defined with a NURBS representation. The two boundary columns control points of this patch, T_1, Q_1, T_2, B_1, Q_2 and B_2, are known. Because each intersection of the patch with a plane normal to the tool axis is a circular arc, three interior control points are used for this patch. They are P_1, Q and P_2. P_1 is determined by the top circular arc $\overset{\frown}{T_1B_1}$, and Q and P_2 are decided by the middle and the bottom circular arcs ($\overset{\frown}{Q_1Q_2}$ and $\overset{\frown}{T_2B_2}$). After all control points and their weight are decided, the NURBS representation of this patch can be obtained. The three interior control points, P_1, Q and P_2, are used to define a NURBS curve from P_1 to P_2 (see Fig. 6-12). The weights of control points P_1 and P_2 are set to the cosine of the half angle $\angle T_1P_1B_1$ (or $\angle T_2P_2B_2$), and the weight of the control point Q equals to the product of cosine of the half angle $\angle P_1QP_2$ and the cosine of the half angle $\angle T_1P_1B_1$ (or $\angle T_2P_2B_2$). This NURBS curve (with control points P_1, Q and P_2) is the track $\overset{\frown}{P_1P_2}$ of the interior control point P, which is used to define a NURBS curve to approximate the given grazing curve.

To build the NURBS representation of the grazing curve, the contact points, T_1 and B_2, are used directly. The interior control point P is moved along the track $\overset{\frown}{P_1P_2}$ to find a proper position so that the maximum error between the grazing curve and the approximate NURBS

curve is optimized. A three control point approximate NURBS curve is constructed. The weight of the interior point P equals the cosine of the half angle $\angle T_1P_1B_1$ (or $\angle T_2P_2B_2$).

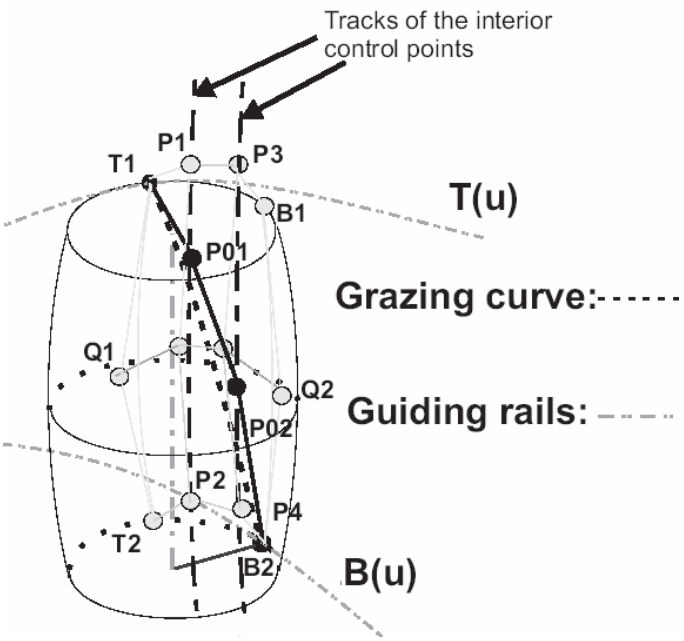

Figure 6-13 Grazing curve and its control points on a tool of revolution

If the three control point NURBS curve does not satisfy the tolerance defined by the user, more control points can be added. As shown in Fig. 6-13, four control points can be used to define the approximate NURBS curve. The control points of the patch along the T_1B_1 direction is increased from three to four using knot insertion, then two tracks of the interior control points can be defined with the method described above. In sequence, two interior control points of the approximate NURBS curve, P_{01} and P_{02}, can be decided. With an increased number of control points, the NURBS curve can accurately match the given grazing curve.

If the generatrix of the tool is a line, the cutting tool will be a cylindrical tool or a conical tool. The solution obtained above will be the same as the solutions obtained for the cylindrical and conical tools. The methods described in Chapter 4, Chapter 5 and section 6.1 are special cases of the general solution for the tools of revolution.

A simple case is given to exhibit the generalized curve design method. A barrel tool is used to test the proposed method. The geometry of the barrel tool is shown in Fig. 6-9(b) and the parameters for this example and cutting tool are given below (see Fig. 6-12).

$$B_2[R_b\cos(\pi/6), R_b\sin(\pi/6), 0],\quad T_1[R_t\cos(\pi/3), R_t\sin(\pi/3), h]$$

$$V_b[-R_b\sin(\pi/6), R_b\cos(\pi/6), 0],\ V_t[-R_t\sin(\pi/3), R_t\cos(\pi/3), 0]$$

$$w_t = 1,\ w_x = \cos(\pi/12),\ w_b = 1,\ R_t = 5,\ R_b = 8,\ R_0 = 339,\ h = 45,$$

where R_t and R_b are radius of the top and the bottom of the tool; R_0 is the radius of the generatrix; w_t, w_x and w_b are the weights of the control points B_2, P and T_1; h is the effective contact length along the axis of the barrel cutter; V_b and V_t are velocities at points B_2 and T_1, the directions are along line directions of each circle and their magnitudes are velocities.

Bedi et al.'s tool positioning method is used to position this tool. The grazing curve can be calculated by equations (2.6) and (2.7), where the radius R varies and is the function of the tool geometries. The projection of this grazing curve along the generatrix of the tool onto the top and the bottom planes of the barrel are 2D arcs. These arcs and the generatrixes between them compose a patch on the surface of the barrel, i.e., $T_1T_2B_2B_1$ (see Fig. 6-19). The control

net of this patch with weights can be calculated using [25, 26] and the interior control points P_1, Q and P_2 are defined. These interior control points are used to construct a B-spline curve P_1P_2, which is the track of the middle control point of the approximate grazing curve. In this example, the middle control point is P. We can initially set it in the half way of the P_1P_2.

Using B_2, P and T_1, a NURBS curve is built to approximate the grazing curve. The error between the grazing curve and its approximate NURBS curve is calculated and is controlled by moving the control point P along the curve P_1P_2. The optimized position of the point P can be found and the error of the curve is plotted in Fig. 6-14 below.

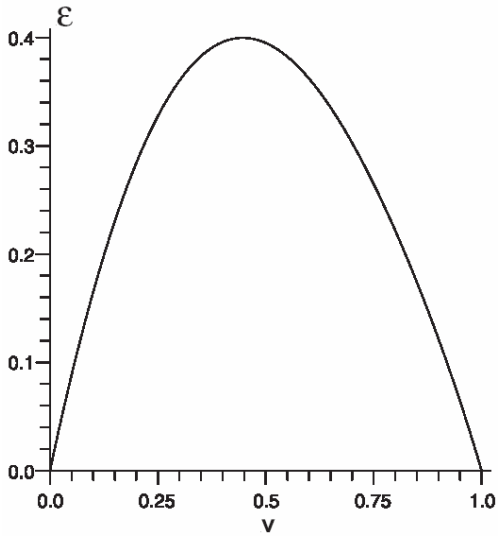

Figure 6-14 Deviation along the grazing curve (three control points)

From Fig. 6-14, it can be seen that the maximum curve error is around 0.4, which is too large for general engineering applications. To reduce the maximum curve error, more control points are needed. In this study, we increased the control points from three to four, and then

to five to control the curve error. The degrees for both of them are the same, i.e., two. The knot vectors were changed to [0,0,0,0.5,1,1,1] for the four control point curve and to [0,0,0,0.33,0.67,1,1,1] for the five control point curve. With the same technique as before, a four control point quadratic NURBS curve and a five control point quadratic NURBS curve are constructed to approximate the grazing curve. The errors are calculated using the parametric error measurement method and the results are plotted in Fig. 6-15 and Fig. 6-16.

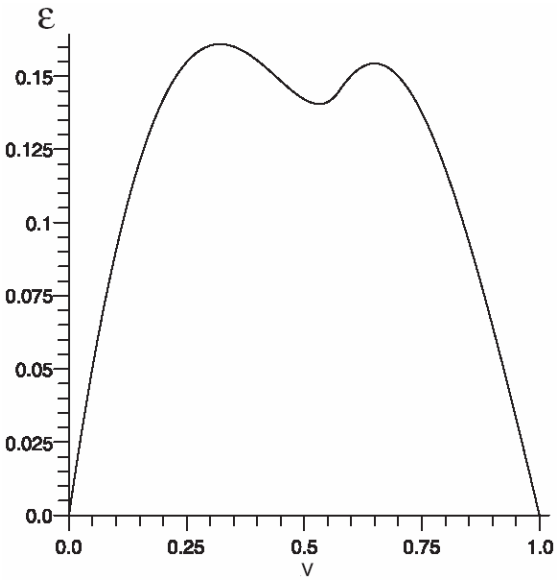

Figure 6-15 Deviation along the grazing curve (four control points)

The maximum error of the approximate curve is significantly reduced from 0.4 (for the three control point NURBS curve) to 0.17 (for the four control point NURBS curve) and 0.09 (for the five control point NURBS curve). With the increase in the number of control points, the approximate curve error can be effectively controlled.

So far a NURBS curve is used to approximate the grazing curve. A NUBS curve can also be used to approximate the grazing curve. As discussed in Chapter 5, a four control point polynomial curve can be used to approximate a 2D arc. Instead of using the NURBS curve, the NUBS curves are used to represent the arcs $\overset{\frown}{T_1T_2}$, $\overset{\frown}{B_1B_2}$, $\overset{\frown}{T_1B_1}$ and $\overset{\frown}{T_2B_2}$ in the Fig. 6-13. As a result, two polynomial curves are generated as the tracks of the interior control points of the approximate curve. Next, a NUBS curve can be built to approximate the grazing curve that minimizing the deviation from the grazing curve.

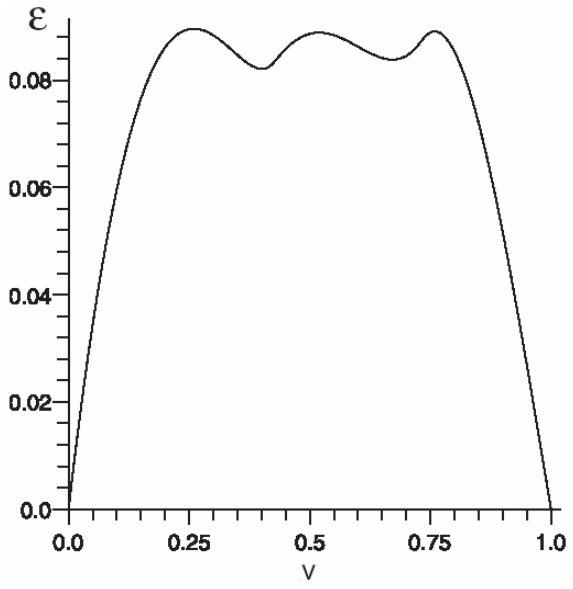

Figure 6-16 Deviation along the grazing curve (five control points)

6.2.2 Modeling of the Grazing Surface

After the grazing curve is defined, it can be used to generate a NURBS surface to approximate the grazing surface. The approximate grazing curves at a few tool positions,

namely the start, end and interior positions, are used to skin a NURBS surface. For the details, please refer to sections 5.1.4 and 4.2.

6.2.3 Examples

Examples are given in this section to demonstrate the proposed flank millable surface design method. The same example presented in the section 6.1 is used. The surface design starts with two guiding curves. The control points of the guiding curves are tabulated in Table 3-1. The degrees of the guiding curves are two and the knot vectors of both of them are $[0,0,0,1,1,1]$.

A barrel tool is used to machine the designed surface. The geometry of the tool is shown in Fig. 6-9(b) and has $R_t = 7$, $R_b = 4$, $R_0 = 418.17$ and $h = 50$. Bedi et al.'s tool positioning method is used to position the tool and generate the tool path. Equations (2.5), (2.6) and (2.7) are used to calculate the grazing surface. Grazing curves at three tool positions, $u = 0$, $u = 0.48$ and $u = 1$, are used to generate each four control point quadratic approximate NURBS curve (see Fig. 6-13, the knot vector is $[0,0,0,0.5,1,1,1]$) with the method developed in section 6.2.1, and consequently to design a four by three bi-quadratic NURBS surface using the method given in section 6.2.2 (see Fig. 5-5). The boundary control points of the guiding curves, the start and the end approximate NURBS grazing curves are used directly in the surface, and only interior control points, $P_{1,1}$ and $P_{2,1}$, need to be determined. Methods presented in Chapters 4 and 5 can be applied to find these points. After all the control points and their weights are decided, the flank millable surface can be constructed. The surface error is calculated and is plotted in Fig. 6-17.

The surface error is in the range [0, 0.145]. The maximum surface error is around 0.145, which is too large for general engineering application. To reduce the maximum error, more control points need to be added to the control net of the surface. Knot insertion can be used to increase the number of control points and the procedure for knot insertion is the same as before. After the number of control points is increased, the flank millable surface can be redesigned and the surface error can also be re-evaluated.

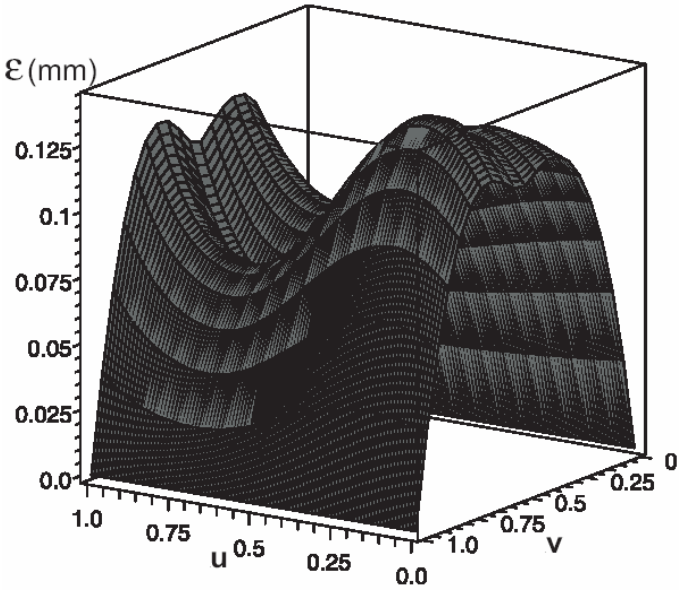

Figure 6-17 Deviation for four by three surface

Two NURBS surfaces, a five by three and a six by three, are developed to reduce the maximum surface error. The control points in the guiding curve direction (the u direction) are kept the same, i.e., three, but the control points in the v direction are increased from four to five and then to six using knot insertion. The degree for both of surfaces is not changed.

The knot vector in the v direction is $[0,0,0,0.33,0.67,1,1,1]$ for the five by three surface and is $[0,0,0,0.25,0.5,0.75,1,1,1]$ for the six by three surface.

Using the proposed surface design method, two NURBS surfaces are designed. The deviation between the grazing surface and the flank millable surface are computed and are listed in Table 6-3.

C.Ps($u \times v$)	ε_{max}
4×3	0.145
4×4	0.079
4×5	0.048

Table 6-3 Errors for different NURBS surface. C.Ps: Control Points.

The maximum surface error is significantly reduced when the numbers of control points are increased from four by three to five by three and six by three. With increase in the number of control points, the surface error can be effectively controlled.

The NURBS curve is used to approximate each grazing curve and subsequently to generate the NURBS surface. In the same example, a polynomial curve can also be used to approximate the grazing curve and consequently to build a NUBS surface. The detail steps to generate the NUBS curve and surface can refer to section 6.2.1, Chapter 4 and Chapter 5.

6.3 Discussion

In this chapter, the method to design the flank millable surface has been developed. The proposed method can effectively control the designed surface error.

If the generatrix of the tool is a curve, more control points are needed to achieve a good NURBS approximation of the grazing curve. However, if the generatrix of the tool is a line, a few control points can fulfill general engineering requirements.

Compared to the method presented in an earlier paper [30], the proposed method has a slightly different process to approximate the grazing surface. A high degree flank millable surface is needed in [30], and the approximate polynomial curves exactly lie on the tools of revolution. For the proposed method, the approximate curve is not on the tools of revolution, lower degree and less control points are needed to define each grazing curve. For general engineering applications, the proposed method gives a better surface approximation.

We can also compare the proposed general flank millable surface design method with the least squares method presented in Chapter 3. As it was discussed before, there is no the amount of sample points problem for the proposed method, but for a non straight line profile cutting tool, the mathematical models of the proposed method is more complex and the time to implement codes is longer than the least squares method. The run time depends on how complexity of the cutting tool profile and the design surface. However, the proposed method offers an easier way to control the properties of the design surface than the least squares method and provides an alternative approach in flank millable surface design. Both of the proposed methods and the least squares method can achieve a quality flank millable surface.

Chapter 7
Experimental Verification and Application

Several methods to design surfaces for flank milling have been developed in this dissertation. The designed flank millable surfaces still need to be experimentally verified. A machine test was done on a Deckel Maho 80p Hi-Dyn five axis machine. A flank millable surface was machined with a conical tool, and the resulting machined surface was measured on a Coordinate Measuring Machine (CMM) BHN 305. The measurement results are compared in this chapter. At the end of this chapter, an example of designing an impeller is also given to display the application of flank millable surface design methods in today's engineering design.

7.1 The Flank Millable Surface

The design of the flank millable surface starts with two quadratic Bézier guiding curves. The control points of each guiding curves are given in Table 7-1.

	T_0	T_1	T_2	B_0	B_1	B_2
x	65	30	0	60	30	15
y	15	30	60	9	30	75
z	-5	-5	-5	-35	-35	-35
w **(weight)**	1	1	1	1	1	1

Table 7-1 Control points for the guiding curves [mm]

A conical tool is used to machine the designed surface. The geometry of the conical tool is shown in Fig. 7-7(b). $R_t = 20.0558$, $R_b = 3.9788$ and $h = 60$. The cutting tool rolls along the two guiding curves to machine the surface. Bedi et al.'s tool positioning method [11] is used to position the tool and the machined surface is accurately approximated by a grazing surface (or a swept surface) computed with equations (2.5), (2.6) and (2.7).

Based on this grazing surface and the conical tool, the method developed in section 6.1 is used to design the flank millable surface. A four by four cubic-quadratic flank millable NUBS surface was defined. The knot vectors in the two parametrical direction are $[0,0,0,0,1,1,1,1]$ and $[0,0,0,0.5,1,1,1]$. The deviation between the grazing surface and the design surface is calculated and plotted in Fig. 7-1.

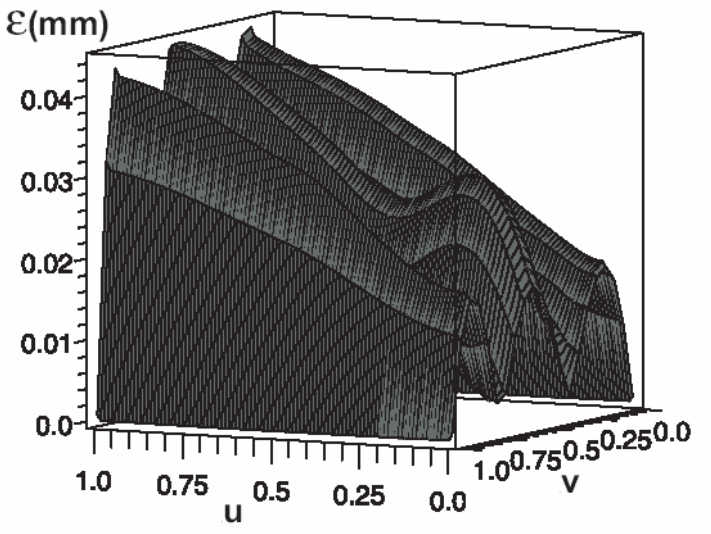

Figure 7-1 Deviation of the flank millable surface

The deviation between the design surface and the grazing surface is the range [0, 0.045]. The maximum surface error is around 0.045. The designed flank millable surface is acceptably close to the grazing surface.

Using the generated tool path, the surface was machined on a pre-cut aluminum stock. The machined surface is shown in Fig. 7-2.

Figure 7-2 Machined part

7.2 Surface Measurement

To verify the accuracy of the surface, a CMM machine was used to measure the machined surface. This CMM uses a probe with a spherical tip to touch the surface and digitizes the coordinate of the central point on the sphere. Since the exact coordinate of the touching point can not be directly obtained, we offset the designed surface by a distance of the radius of the spherical tip along the surface normal toward to the center of the spherical tip. The

comparison of the offset design surface and the center of the spherical tip accurately reflects the match between the machined surface and the design surface [31].

For simplicity, we selected a plane as the scan plane. The axis of the probe was moved in the scan plane (see Fig. 7-3). The scan plane intersects the offset design surface with a curve. The points on this curve correspond to the points on the design surface. The distance between the curve and the center of the spherical tip is studied. This distance closely reflects the deviation between the machined surface and the designed flank millable surface at certain points on the design surface.

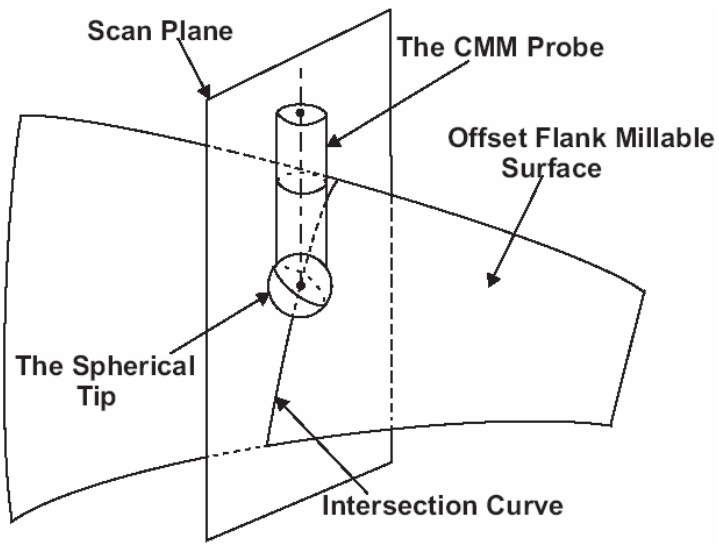

Figure 7-3 the offset surface, the scan plane and the CMM probe

7.3 Results and Discussion

Four scan planes parallel to $X-Y$ plane were set up. There are planes of $Z=-32.021$, $Z=-23.031$, $Z=-15.508$ and $Z=-7.995$. The BHN 305 CMM was used to measure the

machined surface and the axis of the CMM coincides with each of the scan plane. The diameter of the spherical tip is 0.998 and the resolution of the CMM is 10^{-3}. The measurement results with their corresponding intersection curves are plotted and shown in Fig. 7-4 to Fig. 7-7.

The maximum deviation between the scan data and the design surface is smaller than 0.04. The machined surface accurately matches the flank millable surface. Even though only the conical tool is checked in this chapter, surfaces designed with the other developed methods should also closely reflect the actual machined surface.

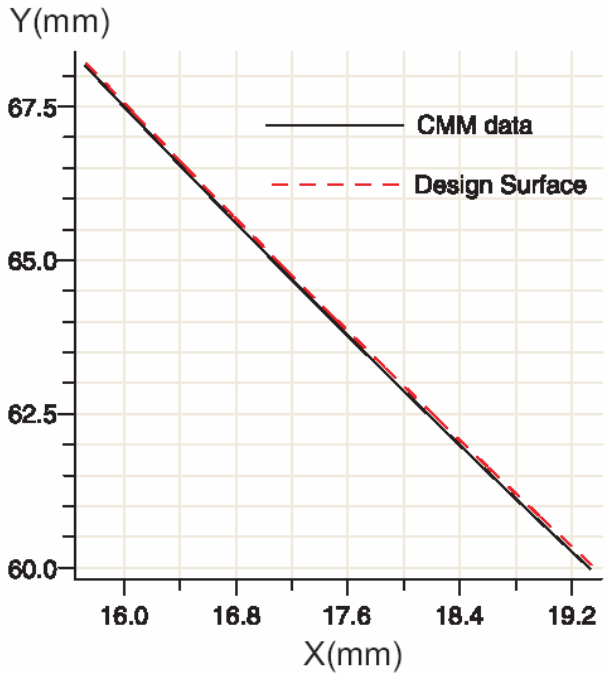

Figure 7-4 CMM scan and surface model at $Z = -32.021$

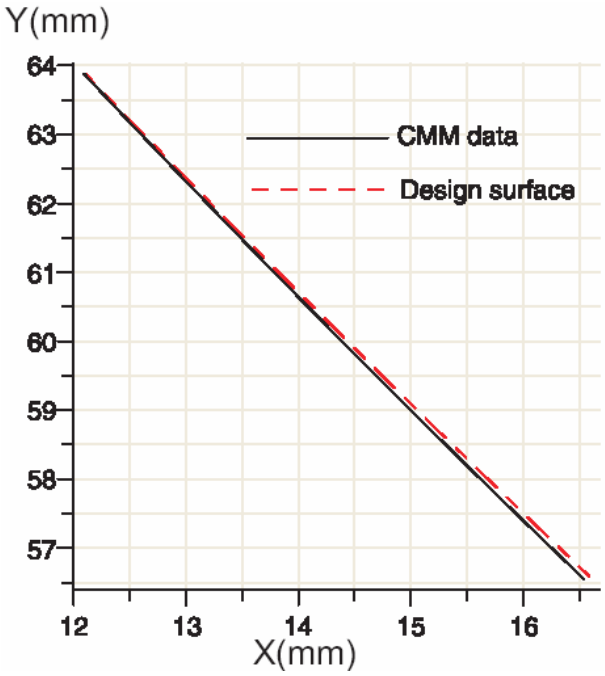

Figure 7-5 CMM scan and surface model at $Z = -23.031$

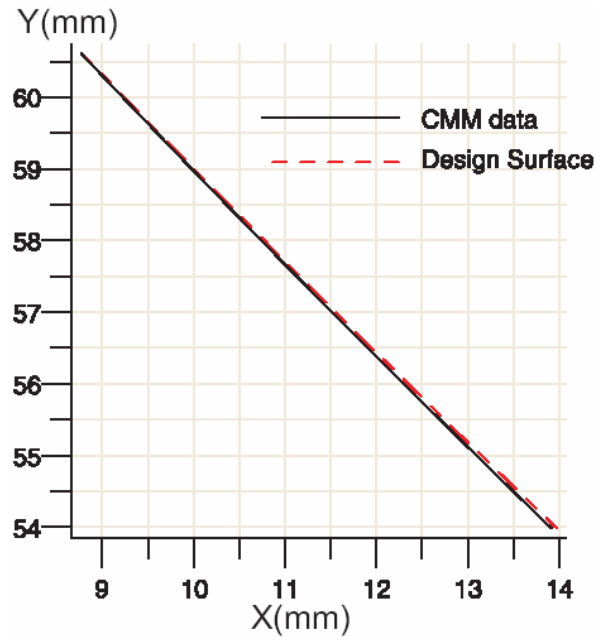

Figure 7-6 CMM scan and surface model at $Z = -15.508$

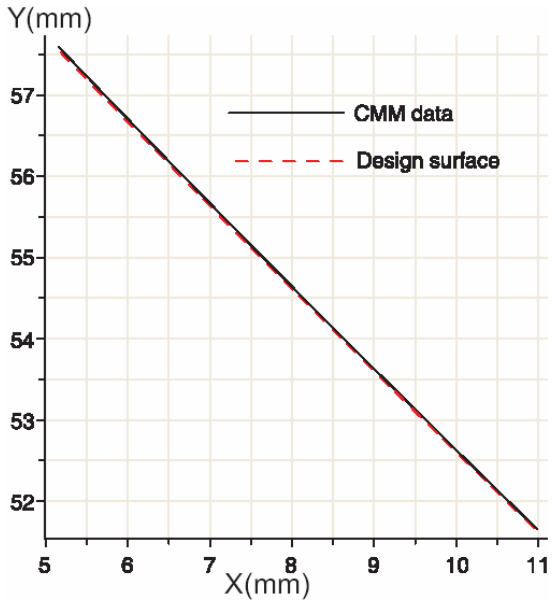

Figure 7-7 CMM scan and surface model at $Z = -7.995$

If the maximum surface error shown in Fig. 7-1 exceeds user defined tolerance, more control points can be used to design the flank millable surface. With an increase in the number of control points, the surface error will be decreased. In this study, we add control point in the tool axis direction (the v direction). The control net of the surface is changed from four by four to six by four. The knot vectors in the two parametrical directions are [0,0,0,0,0.33,0.67,1,1,1,1] and [0,0,0,0.5,1,1,1]. The degrees in both parametrical directions keep the same, i.e., three and two. A six by four NUBS surface can be constructed. The deviation of the surface is calculated and plotted in Fig. 7-8.

The surface error is in the range [0, 0.0124]. The maximum surface error is less than 0.0124. Compared to Fig. 7-1, the maximum surface error is significantly reduced. With the increase in the number of control points, the maximum surface error can be controlled.

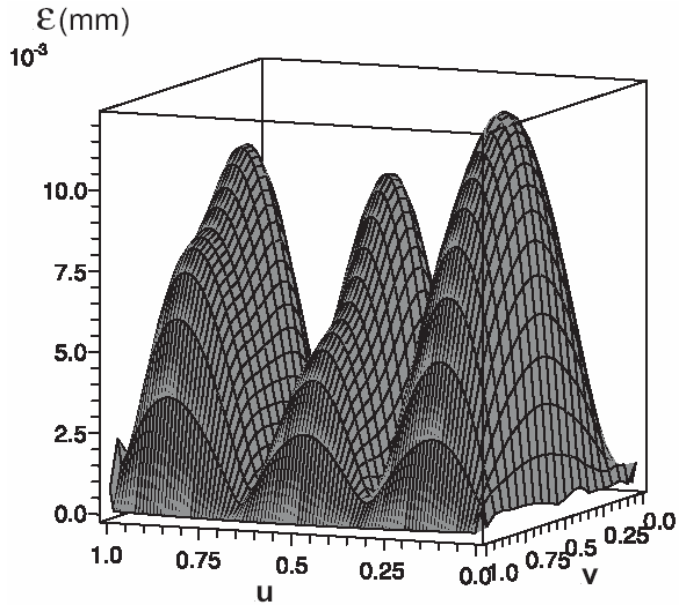

Figure 7-8 Deviation of the flank millable surface

We also compare the simulation results with the results from our earlier research [11, 33]. The example taken in this chapter and the conical cutting tool are the same as the example used in [11, 33]. In the earlier research, the two guiding curves tabulated in Table 7-1 were used to design a ruled surface, which is a widely applied surface design method in today's surface design of impellers and turbine blades, and the conical tool was used to machine this ruled surface. Bedi et al.'s tool positioning method is used to generate the tool path. With this tool path, the surface is flank milled. A simulation showed that the deviation between the machined surface and the ruled surface was in the range [0, -0.225], which is an unacceptably large surface error. To reduce the error [32], the cutting tool has to be lifted or twisted to better match the ruled surface. An optimal tool path can be generated, which is used to machine the target ruled surface. The machined surface is reexamined and shows that its error is in the range [0.046, -0.053]. This error is still bigger than the surface error generated

with the weighted control point method given in section 6.1, and displayed in Fig. 7-8, even Fig. 7-1. Therefore the flank millable surface can match the machined surface better than the ruled surface.

7.4 Design of an Impeller

To demonstrate the usability of the developed surface design methods, the design of an impeller, one of the main applications in the flank millable surface design, is exhibited in this section. The method described in Chapter 5 is used in the design of the flank millable surfaces. The other methods presented before would achieve the similar results and are not displayed in this section.

The design starts with the specification of guiding curves by the designer. A cylindrical cutter with the radius $R = 5$ is rolled along the guiding curves to machine the surface. The control points of the guiding curves for pressure surface and suction surface are given in Table 7-2. The degree of these guiding curves is two. The knot vector of the curves is $[0,0,0,1,1,1]$.

	T0	**T1**	**T2**	**B0**	**B1**	**B2**
Suction surface	(72,14,45)	(20,24,41)	(0,64,37)	(75,15,5)	(20,20,5)	(0,60,5)
Pressure surface	(72,17,45)	(20,28,41)	(1,71,37)	(75,18,5)	(20,24,5)	(1,67,5)
w **(weight)**	1	1	1	1	1	1

Table 7-2 Control points for guiding curves [mm]

Bedi et al.'s tool positioning method is used to generate tool paths. The exact surfaces that will be machined with the generated tool paths are calculated using the swept surface technique presented in section 2.3. The grazing surfaces and the guiding curves for the suction surface and the pressure surface are plotted in Fig. 7-9.

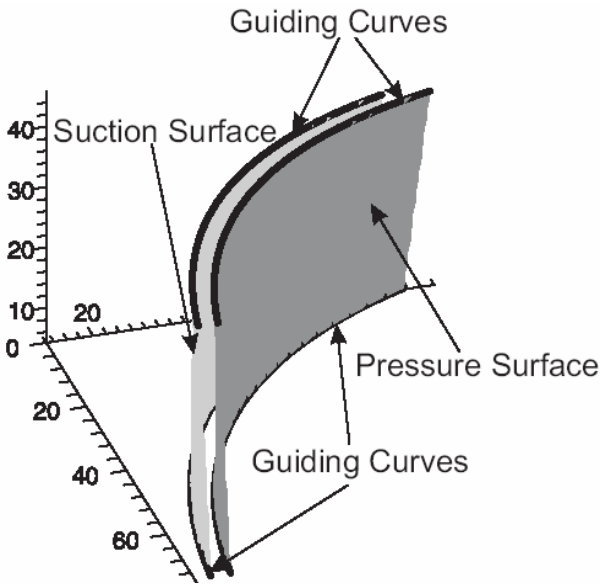

Figure 7-9The grazing surfaces and the guiding curves

Two quadratic NURBS surfaces, each with a 3 by 3 control polygon, are developed to approximate the grazing surfaces. The knot vectors along the grazing curve and the guiding curve directions are [0,0,0,1,1,1] for both surfaces. The reparameterized parametric method is used to measure the error between the machined surface (the grazing surface) and the flank millable surface (the designed surface). Plots of these surface errors are shown in Fig. 7-10 and Fig. 7-11.

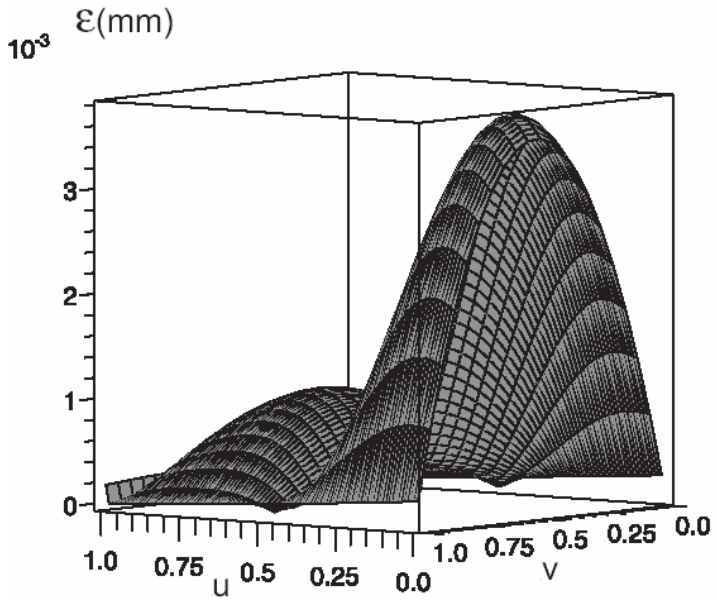

Figure 7-10 Deviation of the NURBS surface for the suction surface

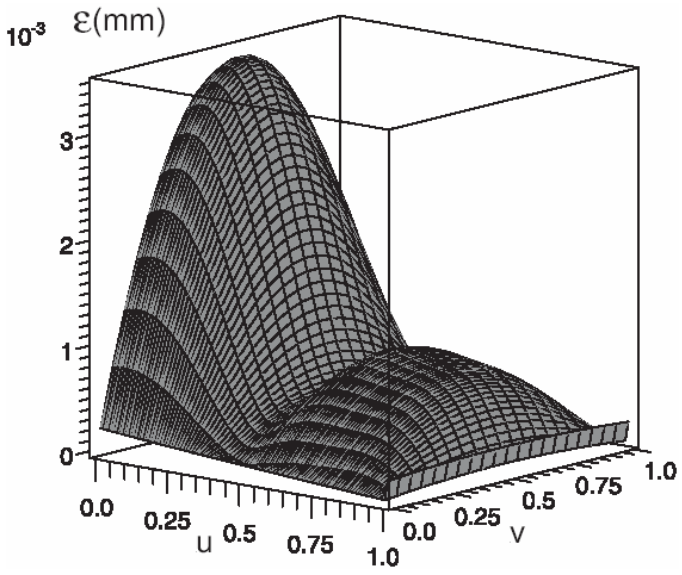

Figure 7-11 Deviation of the NURBS surface for the pressure surface

The deviation between the grazing surface and the approximate surface for the suction surface is in the range [0, 0.0037]. The maximum surface error is less then 0.0037. The deviation between the grazing surface and the approximate surface for the pressure surface is in the range [0, 0.0035]. The maximum surface error is less then 0.0035. If the maximum error still exceeds the user defined tolerance, more control points can be added to the control polygon of the designed NURBS surfaces.

After the flank millable surfaces are defined with NURBS, the geometry of the surfaces can be read into a CAD system to design the impeller. In this case, the control polygons and the knot vectors of the suction surface and the pressure surface were transferred to SolidWorks using IGES files. The IGES files were generated with Rhinoceros, a software package for NURBS modeling. The suction surface and the pressure surface were built by SolidWorks as shown in Fig. 7-12. Consequently, the solid part of the blade is constructed with these surfaces (Fig. 7-13). Using this solid part, one blade of the impeller can be designed (Fig. 7-14). The designer can fillet or chamfer the edge of the part to make it more suitable for design and manufacturing requirements (Fig. 7-15).

An entire impeller is designed and shown in Fig 7-16.

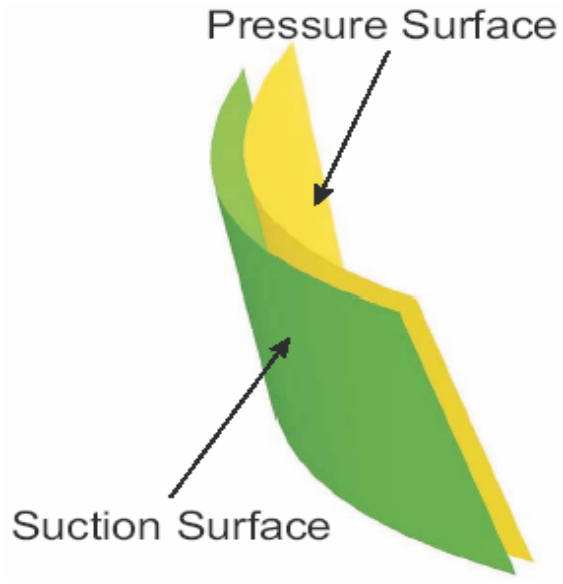

Figure 7-12 Two surfaces of the blade

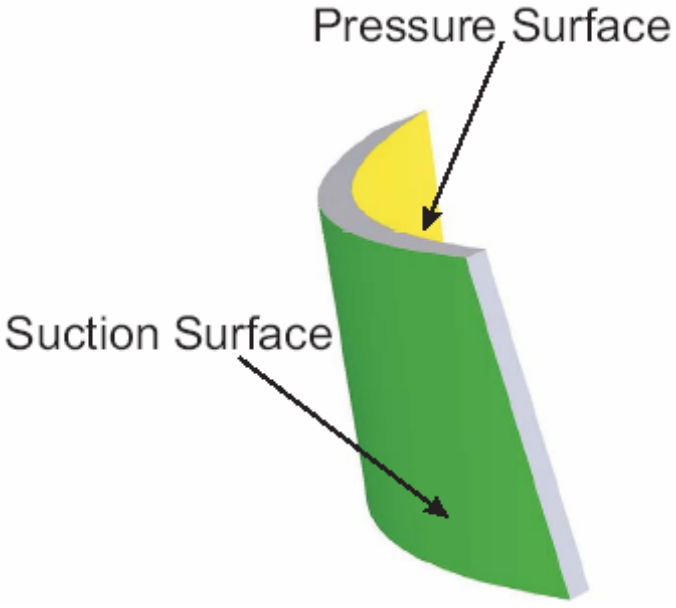

Figure 7-13 Solid part of the blade

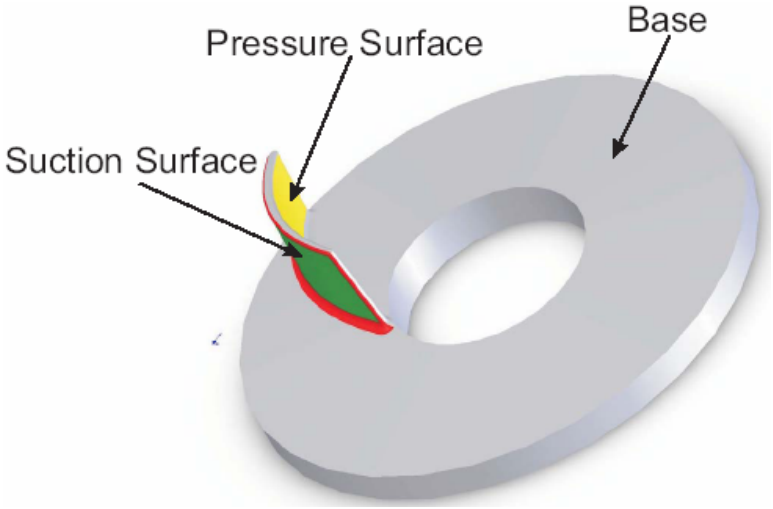

Figure 7-14 An impeller with one blade

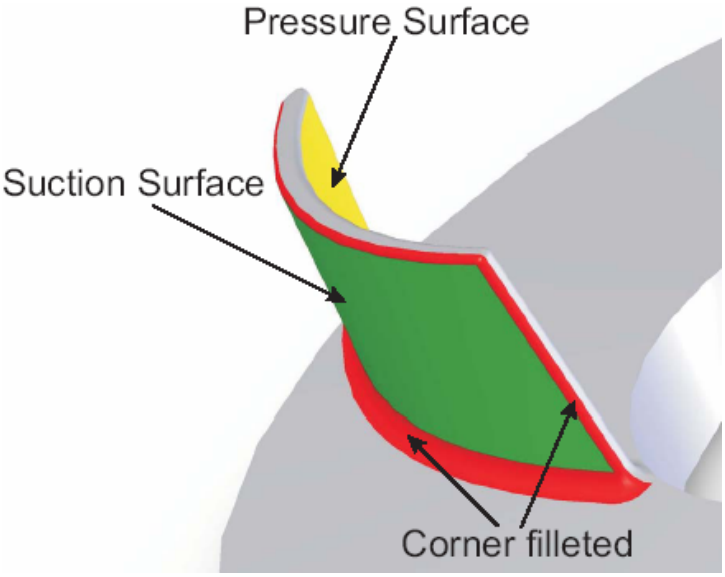

Figure 7-15 Details for one blade

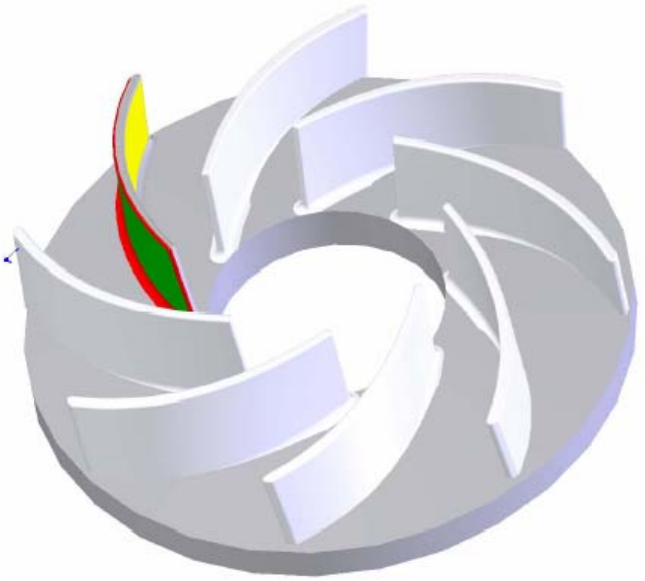

Figure 7-16 An impeller with its blades

The design of the impeller has been finished. Only surface design is considered in the entire design process. In actual impeller design, interference, the size of cutting tool, tolerance requirements, the shape of the surface, etc., all need to be considered. One of these factors will possibly cause the design of the impeller to change. In the mean time, the design of NURBS surfaces is not an easy thing for engineers in firms. It requires engineers to know more about the modeling of the curved surfaces. The surface design tool will become an extra 'burden' to engineers in their design applications. To release the 'burden' from the application engineers, easy ways to handle the flank millable surface design in engineering application still needs to be developed. One of the possible methods will be discussed in the future work (see section 8.2 of this dissertation).

Chapter 8
Conclusion and Future Work

8.1 Conclusion

In this thesis, the NURBS definition of the machined surface generated by the flank milling techniques has been developed. This technique provides a powerful tool to design engineers to effectively control the specification of the surface in design of impellers and turbine blades.

In current engineering design, most surfaces of impellers or turbine blades are designed with ruled surfaces. The main reason to use a ruled surface is that the impellers or the blades can be manufactured inexpensively and the traditional flank milling technique can be used to machine this type of surface. The development of the five-axis machining proves that the machined surface is still a curved surface. Even though different techniques have been developed to make the machined surface closer to the designed ruled surface, it makes the computation steps more complex and expensive. It somehow loses the initial purpose of using ruled surfaces. Further more, the machined surface is still an approximation of the ruled surface, and this will result in the efficiency of impellers or turbine machines being less than the designed efficiency. Some designers insist on using the original curved surface as the design surface, but the surface is still machined using ruled surface techniques with multiple tool paths.

The developed flank millable surface methods overcome these problems. The grazing surface (the machined surface) is directly used in the surface design and guarantees the

machined surface matches the designed surface under a controlled tolerance. The flank milling technique can be used without further concern for the match between the machined surface and the designed surface. The design surface and its specification can be easily controlled by the designer. The efficiency of the impellers or the turbine blades could also be improved.

Only a one pass tool path was considered in the flank millable surface design methods developed in this dissertation. If needed, multiple tool paths can be applied to further satisfy the design requirement. Compared to multiple tool paths in the ruled surface design, the proposed method should provide a better fit to the specification of the design part.

Among the different developed surface design methods with cylindrical and conical tools developed in this thesis, the least squares method can guarantee a high degree of the accuracy of the designed surface. But it is computationally expensive. The other two methods, namely the NURBS and the NUBS methods, are easy to use and computationally inexpensive, but are slightly lower in accuracy. It is up to users to decide which method can be best fit their design requirement. All these methods can offer a high accuracy of design surface.

The general surface design method presented in Chapter 6 provides a flexible way to design flank millable surfaces. Even though each NURBS representation grazing curve is just an approximation of the exact grazing curve, the generated flank millable surface is still guaranteed the accuracy of the design requirement. Compared to the least squares method, the mathematical model of this method is more complex, but it offers a powerful tool to control the properties of the design surface and provide an alternative way to design the flank

millable surface. The method opens the door for engineers to use different types of cutting tools to generate the different surfaces in their design applications.

From the experimental results, it can be seen that the flank millable surface better fits the machined surface than the ruled surface. It is further proved that the flank millable surface can exactly reflect the machined surface condition and satisfy engineering application requirements.

The application of these developed surface design methods should broaden the scope of engineers. Doubly curved surfaces can now be used in the surface design of impellers, turbine blades and other critical engineering parts. Furthermore, it is also possible to design freeform surfaces with these methods for flank milling. The NURBS definition of the designed surface makes it easy be transferred to a CAD system. Within a CAD system, it is convenient to connect it to surrounding surfaces to fulfill the performance requirements of the designed part.

8.2 Future Work

The flank millable surface design methods have been developed and verified. However, there are still some areas that need to be covered in future.

In the stretching of the 2D control points along the tool axis direction to generate the 3D NURBS grazing curve, the interior control points are determined by moving them along the tool axis direction to maximum reduce the deviation between the grazing curve and its NURBS approximate curve. During this process, moving one or two interior control points are probably not a big issue. But if more then two interior control points are moved, there

will be difficulties to find each of these positions. To overcome this problem, the interior control point optimization process and formulas need to be studied.

So far, defining the flank millable surface with a single tool path and a uniform shape tool have been studied. For machining a freeform curved surface, multiple tool paths are generally needed. The techniques to generate the multiple tool paths and build a smooth connection between conjunctive flank millable surfaces need to be developed.

Another interesting way to machine the freeform surface is to use a custom cutting tool to cut the given surface. A cutter with non-uniform profile can be designed to flank mill the given free form surface. Probably the technique developed in this thesis can be used to find a flank millable surface with this non-uniform cutting tool and the profile of the cutter is determined by the shape of the free form surface. This is another attractive topic to be studied.

All the studies in this thesis focused on the flank milling techniques. The advantages of flank milling possibly can be used in the point milling techniques. I am confident that there is a connection between flank milling and point milling. For example, the tip of the ball nose tool is like a small barrel tool, the bull nose tool is more like a flexible cylindrical tool, etc. If mature flank milling techniques are used in point milling, the efficiency of point milling should be greatly increased. I believe that this increased efficiency will be greater than any developed multiple point milling techniques. On the other hand, the combination of the point milling and the flank milling techniques can also improve the limitation of the flank milling applications, especially when multiple tool paths are needed in flank milling applications.

Thus, applying flank milling techniques to point milling applications needs to be investigated.

The development of the internet provides another new area for application of five axis machining. Today, WEB CAD (the Computer Aided Design through WEB application) and WEB CAM (the Computer Aided Manufacture through WEB application) [33, 34, 35] are being developed and will be possibly used in the not far future. These will make the design procedure, like the design of impellers or turbine blades, easier through WEB modeling. To achieve this target, the primary things are to build a server and store the implemented codes for surface design in it. Users can access the server through a Graphic User Interface (GUI) on the web and perform the surface design, analysis and tool path generation, as shown in Fig. 8-1.

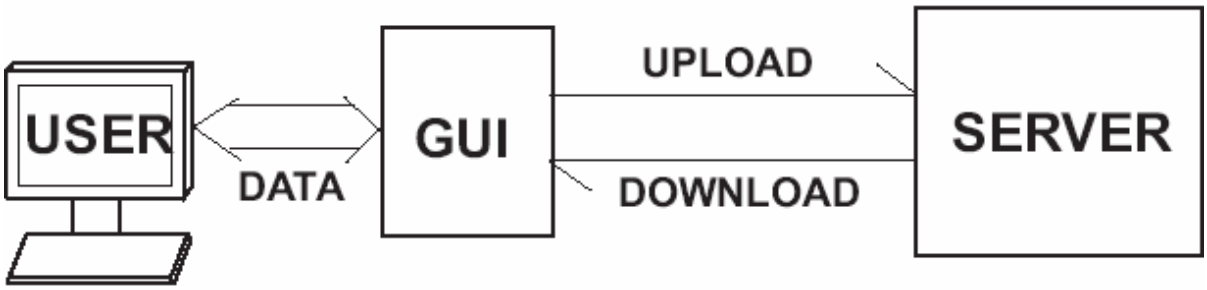

Figure 8-1Data transfer between the user and the server

The implemented codes and GUI are stored in the server and have their own web address. When the user needs to use the implemented codes to design the flank millable surface and generate the tool path, he/she can log on the flank millable surface design web site and download the GUI to his/her local computer. The user can reach the server through the GUI

and upload the data to the server. The server uses these data to generate the flank millable surface, calculate the surface error and determine the tool path. The results are displayed on the user's computer through the GUI. If the results need to be modified, the user can change the input data through the GUI and get refreshed results from the server. This procedure is repeated until the output data satisfy user's design requirement.

A web based flank millable surface design is primarily being set up in the 5-axis machining lab at the University of Waterloo. Users can reach the server through a web address, input the data that users specify to the GUI. The tool path, flank millable surface and the surface analysis report can be shown on the GUI in minutes. Users can use these results to design and machine the flank millable surface.

Only tool path and flank millable surfaces are presented in this web site. The flank millable surface is created using the NUBS grazing curve approximation method and is limited to cylindrical tools. The implemented codes still need to be refined, especially in multiple interior control point optimization. In future, these developed codes need further improve. General shape cutting tools must be involved in surface design and tool path generation. Other design criteria, like force analysis, interference detection, tolerance evaluation, etc., also need to be included in the GUI. With these additions made to the system, the design engineers will be able to design impellers, turbine blades and other critical engineering parts without caring the millability, design details and the accuracy of the target surface, it is no doubt that WEB CAD/CAM will be an important topic needs to be deeply studied in future.

Appendix A

Suppose that the top guiding curve has a set of control points $\{T_k\}$ $k = 0,...,n$; the bottom guiding curve has a set of control points $\{B_k\}$, $k = 0,...,n$. The grazing curves at $u = u_i$ ($i = 1,...,n-1$) are required.

A.1. The Unique Step Method

The u_i used for each grazing curve is given by:

$$u_i = \frac{i}{n}, \qquad i = 1,...,n-1.$$

A.2. The Chord Length Method

For the top guiding curve:

$$d1 = \sum_{k=1}^{n} |T_k - T_{k-1}|,$$

$$\overline{u}_0 = 0, \qquad \overline{u}_n = 1,$$

$$\overline{u}_k = \overline{u}_{k-1} + \frac{|T_k - T_{k-1}|}{d1}, \qquad k = 1,...,n-1 \ .$$

For the bottom guiding curve:

$$d2 = \sum_{k=1}^{n} |B_k - B_{k-1}|,$$

$$\bar{v}_0 = 0, \qquad \bar{v}_n = 1,$$

$$\bar{v}_k = \bar{v}_{k-1} + \frac{|B_k - B_{k-1}|}{d2}, \qquad k = 1,...,n-1.$$

The u_i used for each grazing curve is given by:

$$u_i = \frac{\bar{u}_i + \bar{v}_i}{2}, \qquad i = 1,...,n-1.$$

A.3. **The Centripetal Method**

For the top guiding curve:

$$d1 = \sum_{k=1}^{n} \sqrt{|T_k - T_{k-1}|},$$

$$\bar{u}_0 = 0, \qquad \bar{u}_n = 1,$$

$$\bar{u}_k = \bar{u}_{k-1} + \frac{\sqrt{|T_k - T_{k-1}|}}{d1}, \qquad k = 1,...,n-1.$$

For the bottom guiding curve:

$$d2 = \sum_{k=1}^{n} \sqrt{|B_k - B_{k-1}|},$$

$$\bar{v}_0 = 0, \qquad \bar{v}_n = 1,$$

$$\bar{v}_k = \bar{v}_{k-1} + \frac{\sqrt{|B_k - B_{k-1}|}}{d2}, \qquad k = 1,...,n-1.$$

The u_i used for each grazing curve is given by:

$$u_i = \frac{\overline{u}_i + \overline{v}_i}{2}, \qquad i = 1,\ldots,n-1.$$

Bibliography

[1] Stute, G.,Storr, A. and Sielaff, W. NC programming of ruled surface for five axis machining. *Ann CIRP*, 28(1):267-271, 1979.

[2] X. Liu. Five-axis NC cylindrical milling of sculptured surfaces. *Computer Aided Design.* Vol.27, No12, pp.887-894, 1995.

[3] E.L.J.Bohez, S.D.R.Senadhera, K.Pole, J.R.Duflou and T.Tar. A Geometric Modelling and Five-Axis Machining Algorithm for Centrifugal Impellers. *Journal of Manufacturing systems*, 16(6):422-463, 1997.

[4] D.M.Tsay and M.J.Her. Accurate 5-axis Machining of Twisted Ruled Surfaces. *Journal of Manufacturing Science and Engineering*, 123:734-738, 2001.

[5] J.-M. Redonnet, W. Rubio and G. Dessein, Side Milling of Ruled Surfaces: Optimum Positioning of the Milling Cutter and Calculation of Interference. *Advanced Manufacturing Technology*, Vol.14, No.7, pp.459-465, 1998.

[6] F Monies, J-M Redonnet, W Rubio and P Lagarrigue. Improved Position of a conical mill for machining ruled surfaces: application to turbine blades. *Journal of Engineering Manufacture*. Vol.214, Part B, pp.625-634, 2000.

[7]F Monies, W Rubio, J-M Redonnet and P Lagarrigue. Comparative study of interference caused by different position settings of a conical milling cutter on a ruled surface. *Proceedings of the Institution of Mechanical Engineers-B- JNL of Engineering Manufacture*. Vol.215, No.9, pp1305, 2001.

[8] F Monies, J.N.Felices, W Rubio, J-M Redonnet and P Lagarrigue. Five-axis NC milling of ruled surface: optimal geometry of a conical tool. *International Journal of Production Research*. Vol.40, No.12, pp.2901-2922, 2002.

[9] S. Bedi, S. Mann, and C. Menzel. Flank milling with flat end cutters. *Computer Aided Design*, 35:293-300, 2003.

[10] C. Menzel, S. Bedi, S. Mann. Triple Tangent Flank Milling of Ruled Surfaces. *Computer Aided Design*, 36, 2004.

[11] C G. Li, S. Bedi, S.Mann. Flank milling of ruled surface with conical tools-an optimization approach. *The International Journal of Advanced Manufacturing Technology*. Volume 29, Issue:11-12, 1115-1124, 2006.

[12] W. Rubio, P. Lagarrigue, G. Dessein and F. Pastor. Calculation of Tool Paths for a Torus Mill on Free-Form Surfaces on Five-Axis Machines with detection and Elimination of Interference. *The International Journal of Advanced Manufacturing Technology*. Vo.l 14, No.l, pp13-20, 1998.

[13] K. Marciniak. Geometric Modelling for Numerically Controlled Machining. *Oxford University Press*. 1991.

[14] F.Rehsteiner and H.J.Renker. Collision-Free Five-Axis Milling of Twisted Ruled Surfaces. *CIRP ANNALS*, Vol.42, No.1, pp457-461, 1993.

[15] J. C.J. Chiou. Accurate tool position for 5-axis rule surface machining by swept envelope approach. *Computer Aided Design*. 36(10): 967-974, 2004.

[16] H. Gong, L X. Cao, J. Liu. Improved positioning of cylindrical cutter for flank milling ruled surfaces. *Computer Aided Design*. 37: 1205-1213, 2005.

[17] C H. Chu, J T. Chen. Tool path planning for five-axis flank milling with developable surface approximation. *The International Journal of Advanced Manufacturing Technology*. Vol. 29 (7-8), pp 707-713, 2006.

[18] G. Elber and R. Fish. 5-Axis Freeform Surface Milling using Piecewise Ruled Surface Approximation. *ASME, Journal of Engineering for industry*. 119, 383-387, 1997.

[19] C.Y. Wu. Arbitrary Surface Flank Milling of Fan, Compressor and Impeller Blades. *Transactions of the ASME , Journal of Engineering for Gas Turbines and Power*. 117, 534-539, 1995.

[20] S. Mann, S. Bedi. Generalization of the imprint method to general surfaces of revolution for NC machining. *Computer Aided Design*. 34:373-378, 2001.

[21] C G. Li, S. Mann, S. Bedi. Error Measurements for Flank Milling. *Computer Aided Design*. 37:1459-1468, 2005.

[22] C. Lartigue, E. Duc, A. Affouard. Tool path deformation in 5-axis flank milling using envelope surface. *Computer Aided Design*. 35:375-382, 2003.

[23] J. Senatore, F. Monies, J-M Redonnet, W. Rubio. Analysis of improved positioning in five-axis ruled surface milling using envelope surface. *Computer Aided Design*. 37:989-998, 2005.

[24] K. Marciniak. Geometric Modelling for Numerically Controlled Machining. *Oxford University Press*. 1991.

[25] G. Farin. Curves and Surfaces for Computer-Aided Geometric Design: A Practical Guide. *Academic Press*. 2002.

[26] L. Piegl, W. Tiller. The NURBS Book. *Springer*, 1997.

[27] Jin J Chou. Higher order Bézier circles. *Computer Aided Design*. 27(4): 303-309. 1995.

[28] T. Dokken, M. Daehlen, T. Lyche, K. Morken. Good approximation of circles by curvature-continuous Bézier curves. *Computer Aided Geometric Design*. 7: 33-41. 1990.

[29] T. DeRose, R. Goldman, H. Hagen, S. Mann. Functional Composition Algorithms via Blossoming. *ACM Trans. Graph*. 12(2):113-135. 1993.

[30] C G. Li, S. Mann, S. Bedi. Flank Mill able Surfaces Generated via Polynomial Composition. *Computer Aided Design and Applications*. June, 2007. Accepted for publication.

[31] P. J. Gray. Tool Positioning for 3 ½ ½ - Axis and 5-axis Surface Machining. *Ph.D Thesis. University of Waterloo.*

[32] C G. Li. Flank Milling of Ruled Surface with Conical Tools. *MASc Thesis. University of Waterloo.*

[33] C. Jian, C. Lin, H K. Jiang, Y F. Yi. Integrated technology of products' design and manufacture and its application based on web. *Modular Machine Tool & Automatic Manufacturing technique*. 9: 15-17. 2006 (Chinese).

[34] M. Pappas, V. Karabatsou, D. Mavrikios, G. Chryssolouris. Development of a Web-based collaboration platform for manufacturing product and process design evaluation using virtual reality techniques. *International Journal of Computer Integrated Manufacturing*. 19(8):805-814. 2006.

[35] J S. Liang, P W. Wei. Conceptual design system in a Web-based virtual interactive environment for product development. *International journal of Advanced Manufacturing Technology*. 30(11-12): 1010-1020. 2006.